Ministry of Higher Education
and Scientific Research
University of Kerbala
College of Education for Pure Sciences

Pure Sciences International Journal of Kerbala

PSIJK

Year:2024
Volume : 1
Issue : 3

ISSN: 6188-2789 Print
3005 -2394 Online

Pure Sciences International Journal of Kerbala

(PSIJK) is published in four issues annually

A quarterly peer-reviewed scientific journal issued by the College of Education for Pure Sciences at the University of Kerbala, specializing in pure sciences, accredited for the purposes of scientific promotion Pursuant to Ministerial Resolution No. **B.T 7575** Dated **14 /9 /2023**

Licensed by

Ministry of Higher Education
and Scientific Research and Scientific Research

Issued by

University of Kerbala
College of Education for Pure Sciences

First year ,Volume 1 , Issues 3
30 September 2024

Ministry of Higher Education and Scientific Research

College of Education for Pure Sciences

University of Kerbala

Print ISSN: 6188-2789

Online ISSN: 3005 -2394

Consignment Number in the Housebook and Iraqi

Documents: 2515, 2021

Postal Code: 56001

Mailbox: 232

Mobile: +964 7769920165

https://journals.uokerbala.edu.iq

Iraq - Holy Karbala

Workflow by OJS/PKP

About the Journal

The "Pure Sciences International Journal of Kerbala", published quarterly and distributed internationally by the College of Education for Pure Sciences provides a forum for publication of significant science advancements and developments in chemistry, biology, computer, physics, mathematics and interdisciplinary areas of science. All prospective authors are invited to submit their original contributions on new theoretical and applied aspects of growing research. All manuscripts submitted, including symposium papers, will be peer reviewed by qualified scholars assigned by the editorial board.

You are cordially encouraged to use this journal as a means of dissemination of information on the various facets of science and technical problems; and to impart specialized knowledge, quality and excellence to strengthen the perception of technological resources and needs of the world. The PSIJK is looking forward to receiving your assistance to working together to develop a worthwhile, high quality journal.

Aims and Scope

The objective of the Pure Sciences International Journal of Kerbala is to provide a forum for communication of information among the world›s scientific and technological community and Iraqi scientists. This journal intends to be of interest and utility to researchers and practitioners in the academic, industrial and governmental sectors. All original research contributions of significant value in all areas of science discipline are welcome.

This journal will publish authoritative papers on theoretical and experimental research and advanced applications embodying the results of extensive field, plant, laboratory or theoretical investigation or new interpretations of existing problems. It may also feature - when appropriate - research notes, technical notes, state-of-the-art survey type papers, short communications, letters to the editor, meeting schedules and conference announcements. The language of publication is English. Each paper should contain an abstract both in English and Arabic. However, for the authors who are not familiar with Arabic language, the publisher will prepare the translations. The abstracts should not exceed 250 words.

All manuscripts will be initially checked for plagiarism and then peer-reviewed by qualified reviewers. The material should be presented clearly and concisely:

-Full papers Authors are urged to be succinct; long papers with many tables and figures may require reductions prior to being processed or accepted for publication. Although there is not an absolute length restriction for original papers, authors are encouraged to limit the text to =5,000 words (including references) and references up to 40.

-Review papers are only considered from highly qualified well-known authors generally assigned by the editorial board or editor-in-chief. Author of review papers should have high qualifications with distinct developed research area, an outstanding scholar with an extensive publications.

-Short communications and letters to the editor should contain a text of about 3000 words and whatever figures and tables that may be required to support the text. They include discussion of full papers and short items and should contribute to the original article by providing confirmation or additional interpretation. Discussion of papers will be referred to author(s) for reply and will concurrently be published with reply of author(s).

Instructions for Authors

Submission of a manuscript represents that it has neither been published nor submitted for publication elsewhere and is result of research carried out by author(s). Presentation in a conference and appearance in a symposium proceeding is not considered prior publication.

Authors are required to include a list describing all the symbols and abbreviations in the paper. Use of the international system of measurement units is mandatory.

-On-line submission of manuscripts results in faster publication process and is recommended. Instructions are given in the PSIJK web sites https://journals.uokerbala.edu.iq/

-Hardcopy submissions must include MS Word and jpg files.

-Manuscripts should be typewritten on one side of A4 paper, double-spaced, with adequate margins.

-References should be numbered in brackets and appear in sequence through the text. List of references should be given at the end of the paper.

-Figure captions are to be indicated under the illustrations. They should sufficiently explain the figures.

-Illustrations should appear in their appropriate places in the text.

-Tables and diagrams should be submitted in a form suitable for reproduction.

-Photographs should be of high quality saved as jpg files.

-Tables, Illustrations, Figures and Diagrams will be normally printed in single column width (8cm). Exceptionally large ones may be printed across two columns (17cm).

This journal makes articles available online as soon as possible after acceptance. This concerns the accepted article (both in HTML and PDF format), which has not yet been copyedited, typeset or proofread. A Digital Object Identifier (DOI) is allocated, thereby making it fully citable and searchable by title, author name(s) and the full text. The article›s PDF also carries a disclaimer stating that it is an unedited article. Subsequent production stages will simply replace this version.

The Pure Sciences International Journal of Kerbala is an open access journal: all articles will be immediately and permanently free for everyone to read and download. To provide open access, this journal has an open access fee of USD 100 excluding taxes (also known as an article publishing charge APC) which needs to be paid by the authors or on their behalf e.g. by their research funder or institution. If accepted for publication in the Journal following peer review, authors will be notified of this decision and at the same time requested to pay the article processing charge. A CC user license manages the reuse of the article.

-Author(s)' bio-data including affiliation(s) and mail and e-mail address(es).

-Manuscript including abstracts, key words, illustrations, tables, figures with figure captions and list of references.

-MS Word file of the paper.

The following list will be useful during the final checking of an article prior to sending it to the journal for review. Please consult this Guide for Authors for further details of any item.

Publication Ethics

1. Author responsibility

The authors are exclusively responsible for the contents of their submissions, the validity of the experimental results and must make sure that they have permission from all involved parties to make the data public.

It is the responsibility of each author to ensure that papers submitted to PSIJK are written with ethical standards in mind, concerning plagiarism.

Please note that all submissions are thoroughly checked for plagiarism. If an attempt at plagiarism is found in a published paper, the authors will be asked to issue a written apology to the authors of the original material. Any paper which shows obvious signs of plagiarism will be automatically rejected and its authors will be banned for duration of three years from publishing in PSIJK. The authors will receive proper notification if such a situation arises.

Information on what constitutes plagiarism is provided below.

2.Plagiarism: Definition and Context

Plagiarism, where someone assumes another›s ideas, words, or other creative expression as one›s own, is a clear violation of scientific ethics. Plagiarism may also involve a violation of copyright law, punishable by legal action.

Plagiarism may constitute the following:

Word for word, or almost word for word copying, or purposely paraphrasing portions of another author›s work without clearly indicating the source or marking the copied fragment (for example, using quotation marks);

Copying equations, figures or tables from someone else›s paper without properly citing the source and/or without permission from the original author or the copyright holder.

Self-plagiarism, as a related issue, is the word for word or almost word for word reproduction of portions of one›s own copyrighted work without proper citation of the original material. Self-plagiarism does not apply to publications based on the author›s own previously copyrighted work (for example from conference proceedings) where proper reference was given for the original text.

International Journal of Engineering editorial board will place any plagiarism-related investigation at high priority and will take appropriate action as needed.

Editorial board

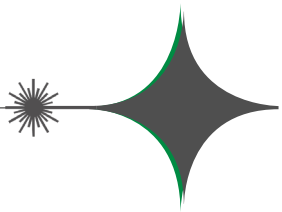

Pure Sciences International Journal of kerbala

Year:2024 Volume : 1 Issue : 3 ISSN: 6188-2789 Print 3005 -2394 Online

Sahar Hashim Khudhair , Sajid Hassan Guzar, Flow Injection Spectrophotometric Measurement of Ni (II) Nickel Using a Novel Reagent, MTMTCH, in an Analytical Sample, Pure Sciences International Journal of Kerbala, Vol. 1, No. 3, (2024) 11-16

Pure Sciences International Journal of Kerbala

Journal Homepage:https://journals.uokerbala.edu.iq/index.php/psijk

Flow Injection Spectrophotometric Measurement of Ni (II) Nickel Using a Novel Reagent, MTMTCH, in an Analytical Sample

Sahar Hashim Khudhair [1*], Sajid Hassan Guzar [2]

[1]*Chemistry Department, College of Education for Pure Science, University of Kerbala, Kerbala, Iraq*
[2]*Chemistry Department, College of Science, University of Kerbala, Kerbala, Iraq*

P A P E R I N F O

Received: 31 March 2024
Accepted: 27 June 2024
Published: 30 September 2024

Keywords:
Flow injection, Spectrophotometric, Ni, MTMTCH

A B S T R A C T

This study describes flow-injection spectrophotometric methods for the determination of Ni (ll) Nickel in analytical sample by a new reagent MTDTCH.
An accurate and sensitive flow injection (FI) Spectrophotometric methods have been developed for the determination of ion Nickel (ll) in aqueous solution by preparing the new organic -Schiff base- reagent was prepared by reaction 3-methylthiophene-2-carbaldehyde with hydrazinecarbothiohydrazide. This reagent was worked as a ligand by reacting with the Nickel (II) ion to form a Nickel complex and determination trace amounts of it. The absorbance of the reaction was measured in the injection system which gave the wavelength of 357nm. With a limit of detection of 0.050 µg.mL^{-1} and a limit of quantitation of 0. 169 µg.mL^{-1} Relative standard deviation 0.495 and Recovery is 99.50, the metal concentration obeys Beer's law within the range0.5-9.mL^{-1} with a correlation coefficient value of 0.9997 . The complex composition was specific to the UV-visible spectra. the molar ratio of the metal to the reagent was (1:2).

1. INTRODUCTION

MTMTCH**(**N"-[(3-methylthiophen-2-yl) methyl-idene] thiocarbonohydrazide) is a Schiff bases are compounds containing an azomethine group, (-CH=N), can be formed by a condensation reaction of carbonyl compounds, (Aldehyde or ketone) with a primary amine in which the carbonyl group is replaced by a group (C = N-R)[1] ,[2] To measure Ni(ll) and other materials Such as: alloys [3], water [4] and soil [5] techniques have been devised [6]. They consist of the following: indirect flameless atomic absorption spectrophotometry [7]. Flow injection technique [8] Schiff's base creation, spectrophotometric [9]and colorimetric [10]In the field of pharmacological analysis, the flow injection technique has gained popularity [11]. Such methyldopa[11]. The present study describes new FIA-spectrophotometric methods [12]. To determination of Ni(ll) via reaction with (MTMTCH) forming yellow colored product that has absorption at λmax at 357 nm [2]. Definitions state that the flow-injection technique is a flow-through technology that applies particular thermodynamic conditions to the model region in a current stream. According to (Ruzicka and Hansen), the technique entails injecting a liquid into a suitable liquid stream that is continuously separated as the injected sample moves toward a detector that continuously records absorptivity or any other physical variable that results from the sample material passing through the transient flow cell. The injected sample forms the moving region of the model.

2. APPARATUS

Shimadzu 120 UV-VIS spectrophotometer equipped with a Cecil 10 uL flow cell was used. A Shimadzu 1650 PC UV-VIS double beam spectrophotometer was used for λmax determination**.** The carrier fluid was transported using a peristaltic pump (Gilsason minipuls (2)) fitted with flexible polyvinyl chloride tubes with an internal diameter of 0.8 mm.Using a tow-channel manifold (Figure 1), the FIA-spectrophotometer was used to determine Ni(ll). using FIA spectrophotometer. The Rheodyne -USA injection valve was utilized to administer standard solutions and samples at the proper injection volumes. The (MTMTCH) solution was transported via the Manifold's Channel A. While the alkaline oxalate solution stream was being transported via injection of ion Ni (II) via channel B, buffer solution (pH=6), which acted as an oxidizing agent**,** The reaction coil R.C as used to

*Corresponding Author Institutional Email: *e03153471@s.uokerbala.edu.iq* (Sahar Hashim Khudhair)

combine the product with a stream of buffer solution. The final product was mixed with the stream of alkaline oxalate at point (y), following the the mixing of coil RC.

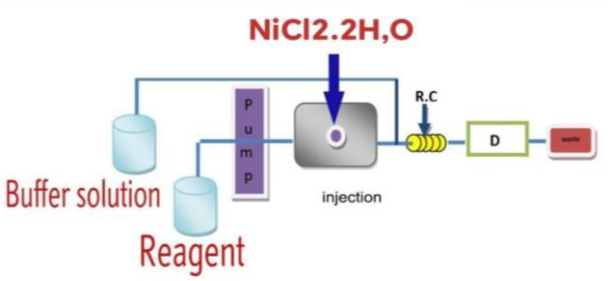

Figure 1. Manifold Used to Measure Ni (II) Using FIA Spectrophotometric Analysis

3. EXPERMINTAL

3.1 Materials

The B.D.H., Fluka, and Merck firms provided all of the high-purity solvents and chemical reagents utilized in this investigation; no further purification procedures were required.

3.1.1 Synthesis of the Ligand

Firstly, 1.06 g of thiocarbohydrazide (0.01mmoles) was dissolved in 58 mL of 95% EtOH and 20 mL of H2O. Next, 1.26g of 3-methylthiophene-2-carbaldehyde (0.01mmoles) was added, and last, three drops of 6N HCl were added. After three hours of stirring at 80 °C, the reaction mixture was allowed to crystallize at room temperature for twenty-four hours After filtering and a 1:1 EtOH/H2O wash, the solid was produced. and recrystallized from EtOH 95% to give N"-[(3-methylthiophen-2-yl)methylidene] thiocarbono-hydrazide in the form of a slightly ochre solid in 72.52% yield (0.7 1 g) [13] Scheme 1, and measure the degree of its fusion is.(233-235) °C, and Table 1 shows the chemical composition of ligand and some physical properties.

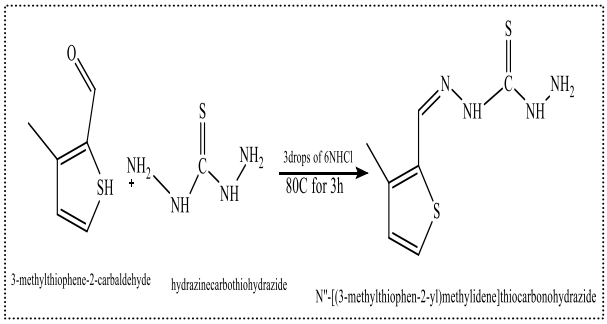

Scheme 1: Describes the steps for preparing the ligand (MTMTCH)

TABLE 1. The Physical Properties and Molecular Formulas of The Prepared Ligands

Color	Proportion of product	M.P (C^0)	M.W g / mol	M.F	Name
Yellow	72.52%	233-235	214.12	C_7S_2 N_4H_{10}	N"[(3methylthiophen2yl)methylidene] thiocarboenohydrazid

3.1.2 Preparation of Buffer Solutions and Ni (II) Nickel

The buffer solutions were prepared by dissolving 0.778 g of ammonium acetate at a concentration of 0.01M in 1000 mL of distilled water in a one-liter capacity tank.

This solution was used to create a number of solutions with a variety of acidic functions, ranging from (pH =3–10). by incorporating concentrated acetic acid or ammonia solution into the ammonium acetate that has been made[14]. and the Nickel (II) di Nickel compound (0.00134 g) was dissolved in distilled water to create the solution, and the volume was then increased to 100 mL using the same solvent. By gradually diluting this standard solution with distilled water, other standard solutions were created.

4. PRODUCT DESCRIPTION

UV-VIS was used to characterize the synthesized reagent and complex products that were recovered from the process, and FT-IR and $_1$HNMR spectra were obtained for the novel reagent.

5. METHODS

5.1 Procedure for the FIA Method

A 100.00µl sample is injected into a stream of 1×10^{-4} M MTMTCH reagent solution at a rate of 0.60 ml/min. The stream is allowed to combine with another stream of (pH=6) solution in a 50 cm reaction coil. Next, a valve was injected with salt ($NiCl_2.2H_2O$). Mixture is passed while sustaining the reaction, and absorbance is gauged at 375.nm [15].

6. RESULTS AND DISCUSSION

6.1. Study of Ultra Violet – Visble Spectra

A spectroscopic of the Nickel complex was carried out in the 190-1100nm range and in the ultraviolet–visible portion of the spectrum. At a concentration of 1×10^{-5}M, the electronic absorption spectra of the novel reagent and complex were examined in an absolute ethanol solution. Within the reagent spectrum, the electronic spectrum of the reagent showed three bands at (λ=280) nm, (λ=354) nm and

(λ=213) nm. In complex spectrum, the Ni(II) complex, showed three absorption bands at (λ=375) nm, (λ=276) nm, (λ=290) nm, (λ=250) nm, as show in Figure 2, 3.

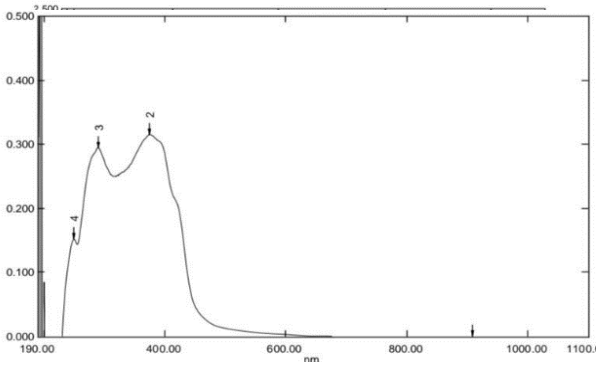

Figure 2. Absorption Spectrum of Ligand (MTMTCH)

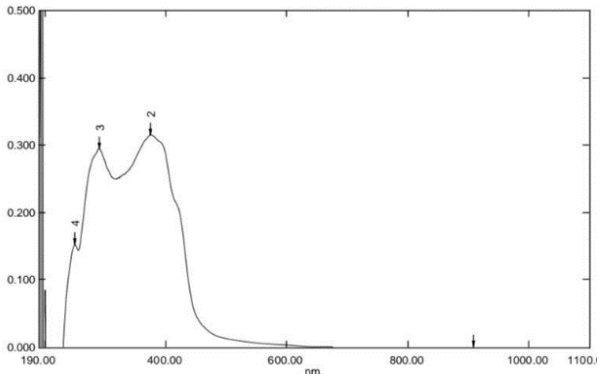

Figure 3. Absorption Spectrum of Nickel Complex (II) with Ligand MTMTCH

6.2. Study FT-IR Spectra for Reagent

The FT-IR spectrum of the prepared new reagent shows a peak belonging to (NH) at 3271 cm^{-1}, a peak at 1593 cm^{-1} belonging to (C=N), and the (C=C) peak at 1647 cm^{-1}. (NH_2)at 3151,and(C=s)1200-1100 cm^{-1}, a peak at700 cm^{-1} belonging to (C-S), as show in Figure 4.

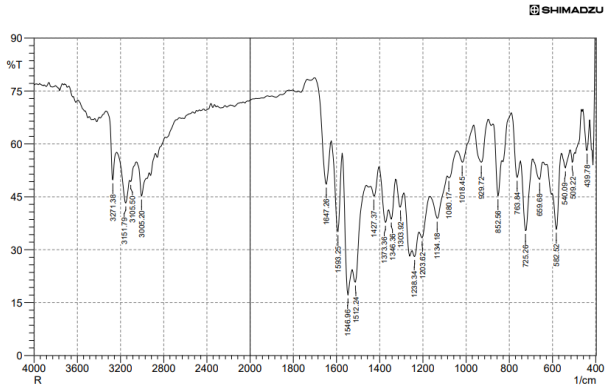

Figure 4. FT-IR Spectrum of Reagent

6.3. Proton NMR Spectrum for Reagent

From the signals appearing in the spectrum ^{1}H-NMR, the singlet signal at (δ=6.97 ppm,2H) refers to the proton of the NH_2 group, , the singlet signal at (δ=8.47 ppm,1H) refers to the proton of the (CH=N) group, the singlet signal at (δ=11.27 ppm,1H) refers to the proton of the NH group, , the signal at (2.32 ppm,3H) refers to the proton of the CH_3, the signal at 3.39 ppm indicates the presence of moisture H_2O and the signal at 2.5 ppm indicates the solvent DMSO, as show in Figure 5.

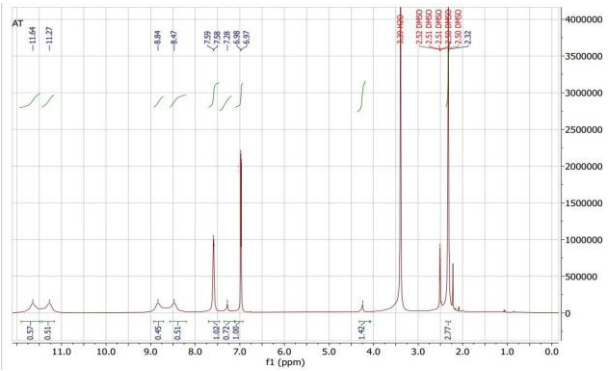

Figure 5. ^{1}H-NMR Spectrum for Reagent.

6.4. Study of the Variables of the Flow Injection System for the Determination of the Nickel (II) Ion.

The following system conditions have been investigated in relation to the effect of changing the reaction coil length range (25-125)cm: and the system conditions are: $NiCl_2.2H_2O$ concentration is 1×10^{-5} M and the concentration of MTMTCH reagent is 1×10^{-4}M, Figure 6 show the results obtained.. The regulator buffer solution is 6, the cell size is 10 µL loaded in the standard model loading link, the first and second carrier currents flow at 2.1 ml min-1, and the impact of changing total flow-rate within the range of (0.4-2.8) ml/min was investigated. concentration of $NiCl_2.2H2O$ (1×10^{-5}) M, while the reagent has a concentration of(1×10^{-4}) M. buffer solution has an (pH=6) and a cell size of 10 µL. model link, the maximum wavelength for Ni is 375 nm, and the flow velocities of the first and second load currents are 2.1 ml.min-1. Figure 7 shows the results obtained. A loop has been used in a pump with steel metal of various lengths and sizes (50 ml to 250 ml), as demonstrated by the results in Figure 8. The loop passes the current carrier detector and the buffer solution, which has a pH equivalent of (6) at a fixed concentration of $1 * 10^{-5}$, and absorbs readings for each length using a 10 ML spectrometer [16]

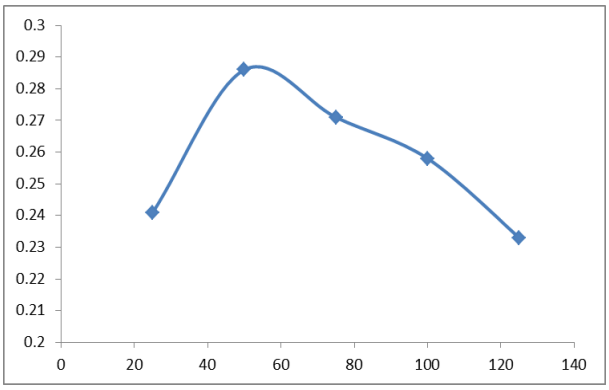

Figure 6. Effect of Reaction Coil Length.

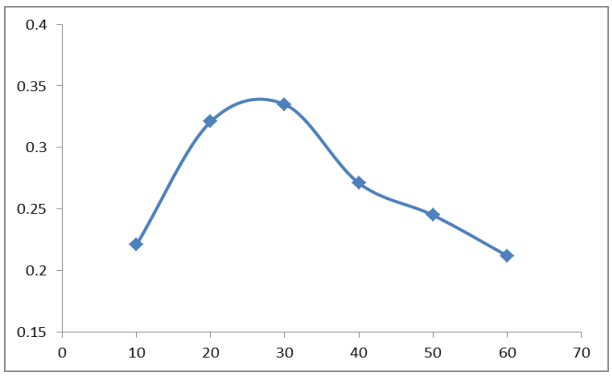

Figure 7. Effect of Total Flow-Rate.

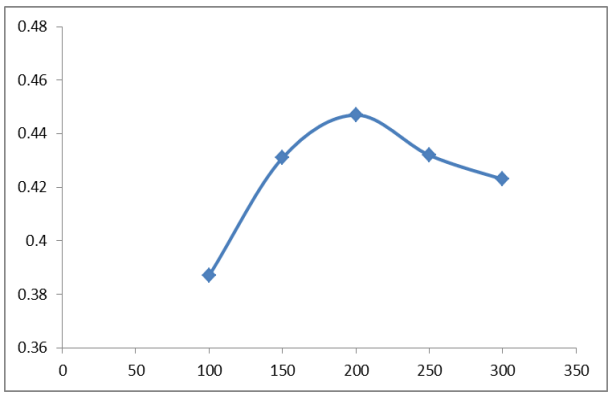

Figure 8. Effect of Loop Volume Injected.

By creating a calibration curve, the concentrations of the nickel complex that follow the Beer-Lambert law were found. Due to their departure from the Beer-Lambert law and the emergence of absorption peaks outside the measurement limits, many concentrations were eliminated. Consequently, (0.5–9) µg/mL are the concentrations that follow the Beer-Lambert law. Figure (9) shows the calibration curve for cobalt complex.

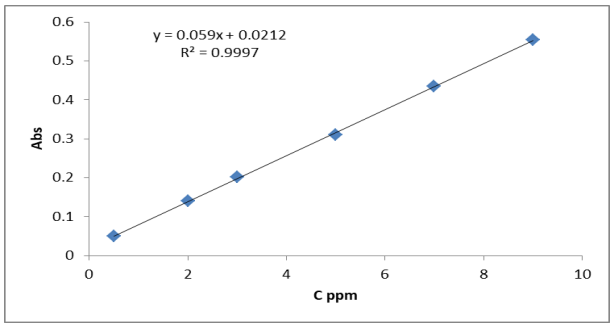

Figure 9. Calibration Curve for Ni (II) Complex

$$S.D = \frac{\sqrt{\sum(xi - x')^2}}{(N-1)}$$

$$R.S.D\% = \frac{(S.D)}{(x')} \times 100$$

$$L.O.Q = 10\ \frac{S.D}{Slope}$$

$$L.O.D = 3\ \frac{S.D}{Slop}$$

7. CONCLUSION

A spectrophotometer detector was employed in tandem with an accurate and sensitive F1A system during its design, construction, and operation. Flow-injection spectrophotometric methods were created for the determination of ion Ni(II) in a new simple reagent. This proposed approach can be carried out without the requirement for additional stages such as solvent extraction or pH control and other conditions.

8. REFERENCES

1. V. Bhatt, *Essentials of coordination chemistry: A simplified approach with 3D visuals*. Academic Press, 2015.
2. M. D. Azeez, S. H. Guzar, and A. H. Mekky, "Synthesis, Characterization and Spectrophotometric Studies of New Hydrazone Derived from Ethyl benzoate," 2009.
3. W. Al-Gethami, D. Alhashmialameer, N. Al-Qasmi, S. H. Ismail, and A. H. Sadek, "Design of a novel nanosensors based on green synthesized CoFe2O4/Ca-alginate nanocomposite-coated QCM for rapid detection of Pb (II) ions," *Nanomaterials*, vol. 12, no. 20, p. 3620, 2022.
4. M. Blanco-Meneses, "Molecular identification of microorganisms in agricultural, ornamental and forest crops in Costa Rica, 2009-2018. Part 1," *Agronomía Mesoamericana*, vol. 33, no. 2, 2022.
5. S. Rafi, D. V. Rao, and T. S. Reddy, "Spectrophotometric Determination of Gold (III) using Tolterodine Tartrate (TLD)(R)-N, N-Diisopropyl-3-(2-Hydroxy-5-Ethylphenyl)-3-Phenylpropanamine L-Hydrogen Tartrate Reagent," *International Research Journal of Pure and Applied Chemistry*, vol. 3, no. 4, pp. 276-285, 2013.
6. E. Raafid, M. A. Al-Da'amy, and S. H. Kadhim, "Determination and Identification of Nickel (II) Spectroscopy in Alloy Samples Using Chromogenic

Reagent (HPEDN)," in *IOP Conference Series: Materials Science and Engineering*, 2020, vol. 871, no. 1: IOP Publishing, p. 012025.
7. B. Saritha and T. S. Reddy, "Direct spectrophotometric determination of Ni (II) using 5-bromo-2-hydroxyl-3-metoxybenzaldehide-4-hydroxy benzoic hydrazine, IOSR J," *App. Chem*, vol. 7, no. 3, pp. 22-26, 2014.
8. D. Beauchemin, "Flow injection," *Sample Introduction Systems in ICPMS and ICPOES*, pp. 143-211, 2020.
9. L. A. Mohammed, N. I. Mahdi, and R. A. B. Aldujaili, "Preparation, characterization and the biological activity study of a new heterocyclic (Azo-Schiff base) ligand and their complexation with {Co, Ni, Cu, Zn (II)} ions," *Egyptian Journal of Chemistry*, vol. 63, no. 1, pp. 289-300, 2020.
10. V. Wamorkar, S. Manjunath, and M. M. Varma, "Development and validation of UV spectroscopic method for determination of metoclopramide hydrochloride in bulk and tablet formulation," *Int J Pharm Pharm Sci*, vol. 3, no. 3, pp. 171-4, 2011.
11. H. A. Al-Azzawi, F. M. Al-Obadi, and N. Theia'a, "Spectrophotometric assay of metoclopramide hydrochloride in bulk and in dosage form," *Iraqi National Journal Of Chemistry*, vol. 15, no. 1, 2015.
12. S. D. Kolev and I. D. McKelvie, "Advances in flow injection analysis and related techniques," 2008.
13. [13] A. J. KADHIM, D. S. R. RASOOL, and R. A. GHAFIL, "Formation, Identification, Microbial Studying of Series Compounds from Chalcone," *International Journal of Pharmaceutical Research*, vol. 12, no. 1, 2020.
14. A. A. Green, "The preparation of acetate and phosphate buffer solutions of known pH and ionic strength," *Journal of the American Chemical Society*, vol. 55, no. 6, pp. 2331-2336, 1933.
15. M. R. Siddiqui, Z. A. AlOthman, and N. Rahman, "Analytical techniques in pharmaceutical analysis: A review," *Arabian Journal of chemistry*, vol. 10, pp. S1409-S1421, 2017.
16. M. Trojanowicz and M. Pyszynska, "Flow-injection methods in water analysis—recent developments," *Molecules*, vol. 27, no. 4, p. 1410, 2022.

Arabic Abstract

توصف هذا الدراسة الطرق الطيفية للحقن الجرياني لتقدير النيكل الثنائي في عينة تحليلية بواسطة كاشف MTMTCH الجديد طريقة القياس الطيفية طريقة دقيقة وحساسة لحقن الجرياني التي تم تطويرها لتقدير النيكل ايون النيكل في محلول مائي من خلال تحضير كاشف جديد ناتج من تفاعل 3-ميثيلثوفين-2-كربلديهايد مع الهيدرازين كاربوتيو هيدرازيد. كان هذا الكاشف بمثابة ليكند من خلال تفاعله مع ايون النيكل لتكوين معقد النيكل وتحديد كميات قليلة منه. تم قياس امتصاص التفاعل في نظام الحقن الذي اعطى طول موجي ٤٠٠ نانومتر. مع حد كشف قدره ٠.٠٥٠ميكرو جرام مل-١ وحد كشف كمي ٠.٠١٦٩ميكروغرام.مل-١.ويخضع تركيز المعدن لقانون بير لامبرت ضمن النطاق ٠.٥-٩مل مع قيمة معامل ارتباط تبلغ. ٠.٩٩٩٧كان تركيب المعقد خاصا بالأطياف المرئية فوق البنفسجية. وكانت النسبة المولية المعدن للكاشف ١:٢).

Pure Sciences International Journal of kerbala

Year:2024 Volume : 1 Issue : 3 ISSN: 6188-2789 Print 3005 -2394 Online

Jihan Hameed Abdulameer, Nada Habeeb Obaid, Maha Jassim Manshad, The Impact of Environmental Heavy Metal Contamination on Human Health, Pure Sciences International Journal of Kerbala, Vol.1 No. 3, (2024) 17-25

First year 2024 ,Volume 1 , Issue 3 PSIJK 17-25

Pure Sciences International Journal of Kerbala

Journal Homepage:https://journals.uokerbala.edu.iq/index.php/psijk

A review: The Impact of Environmental Heavy Metal Contamination on Human Health

Jihan Hameed Abdulameer[1*], Nada Habeeb Obaid[2], Maha Jassim Manshad[3]

[1, 2,3]*Department of Chemistry, Collage of Education for Pure Science, University of Kerbala, Kerbala, Iraq.*

P A P E R I N F O

Received: 31 March 2024
Accepted: 9 July 2024
Published: 30 September 2024

Keywords:
Heavy metals, Environmental health, Toxicity, Nanotechnological approaches, Nanomedicin

A B S T R A C T

Heavy metals are a popular threat to the environment because of their toxic effects, tendency to linger in the Earth's atmosphere, as well as capacity to bioaccumulate within the body of an individual. Heavy metal poisoning of ecosystems that are both terrestrial and aquatic is a serious environmental issue that has an impact on human health. The bulk of metallic elements are found in nature, despite the fact that humans produce some of them. Two of the most distinctive features of heavy metals are their atomic mass and the danger they pose to living organisms. Furthermore, despite differences in technology, research on innovative medical diagnostics is still being conducted. The rapidly developing field of nanotechnology is enabling significant advancements in the investigation of mineral material regeneration from complex matrices. Numerous carbon nanomaterials have been employed for the removal of metal, including magnetic nanoparticles, metal oxide nanoparticles, nanotubes, graphene and its derivatives, and nanotubes. Applying nanotechnology to the removal and analysis of heavy metals from food and water sources has many benefits over traditional methods. Among these benefits are high sensitivity, excellent selectivity, minimum limits on detection and measurement, and a wide linear range. Therefore, the goal of the review was to investigate how heavy metals affect the ecosystem, the harm they cause to human health, and the potential for using natural resources to create novel medications. This review also emphasises the application of nanotechnology and non-medical applications to the problem of heavy metal toxicity.

1. INTRODUCTION

The surrounding environment in which people, animals, plants, or microbes live is referred to as the "environment." It is made up of the land, seas, and atmosphere of Earth. The four domains that comprise the Earth system are the lithosphere (earth), hydrosphere (water), atmosphere (air), and biosphere (organisms), and they are all interdependent. Pollutants and contaminants found in the environment are chemicals which are more frequent there than elsewhere. [1].

Metallic elements with densities higher than water's are referred to as heavy metals [2]. Metalloids like arsenic that show toxicity even at low exposure levels are categorised as heavy metals, assuming a correlation between toxicity and heaviness [3]. In recent years, environmental poisoning caused by toxic metals has grown in importance as a global environmental and public health concern. Moreover, human exposure has increased dramatically [4] due to the exponential growth of its numerous industrial, agricultural, domestic, and technical applications. The presence of heavy metals in the environment is widely acknowledged to originate from various sources, including geological, industrial, pharmaceutical, agricultural, residential, and atmospheric processes. Businesses having point sources, such as foundries, smelters, and mining, among other metal-based industrial activity operations, are primarily responsible for environmental pollution [5]. Although heavy metals belong to naturally occurring substances found in the crust of the Earth, people activity—such as metal extraction, the smelting industrial production, and use of metals and metal-containing compounds in residential and agricultural settings is the main source of environmental pollution and human exposure to Heavy metals. Environmental contamination can also be caused by corrosion of metallic materials, air pollution, soil erosion, heavy metal leaching, sedimentation resuspension, and the evaporation of metals from water resources into soil and groundwater [6]. Additionally, it has been observed that two instances of natural occurrences that

*Corresponding Author Institutional Email:
Jihan.hameed@uokerbala.edu.iq (Jihan Hameed Abdulameer)

significantly contribute to heavy metal contamination are weathering and volcanic eruptions [7]. Examples of industrial sources include paper mills, plastics, textiles, microelectronics, wood preservation, nuclear power plants, burning coal in power plants, refining metal in refineries, and high tension lines [8].

1.1. Sources of pollution with heavy metals

These metallic substances have naturally been in the Earth's crust since the dawn of time. The remarkable rise in the use of toxic metals will soon lead to an increase in metallic compounds in both terrestrial and aquatic environments [9]. The primary contributor to pollution, human activity, is the reason behind the increase in heavy metal contamination. This is largely because of the foundry, smelting, mining, and other metal-based industries. It is also caused by the leaching of metals from a range of sources, such as water runoff, landfills, rubbish dumps, secretions, and livestock and poultry manure [10]. The usage of heavy metals in fertilisers, herbicides, and other agricultural goods has been the secondary reason of heavy metal contamination in agriculture. Furthermore, a rise in heavy metal pollution can result from a number of natural processes, including geological weathering, sediment re-suspension, soil erosion, evaporated metals from soil and water, and eruptions of volcanoes [11].

1.2. Heavy metals' impact on human health

Even though human nature needs some heavy metals, over exposure to them can have negative unexpected effects on several bodily systems and general health. Among the 35 metals of concern due to exposure at home or work, 33 are heavy metals, including antimony, arsenic, bismuth, cadmium, cerium, chromium, cobalt, copper, gallium, gold, iron, lead, manganese, mercury, nickel, platinum, silver, tellurium, thallium, tin, uranium, vanadium, and zinc. These heavy metals are frequently found in food and the environment. In little amounts, they are essential for maintaining health, but in larger quantities, they may be toxic or dangerous [12]. High levels of dangerous heavy metals can damage key organs like the kidney, liver, brain, lungs, and blood components in addition to causing energy depletion. Long-term Expose may cause degenerative processes to progress that mimic multiple sclerosis, Parkinson's disease, Alzheimer's disease, and muscular dystrophy in the neurological system, musculoskeletal system, and body. Long-term exposure to some metals and their compounds on a regular basis have even been connected to cancer [13]. Some heavy metals have toxicity levels that are somewhat greater than the ambient levels seen in the natural world. Therefore, in order to be able to take the necessary measures against excessive exposure to heavy metals, having a thorough awareness of them is essential [14].

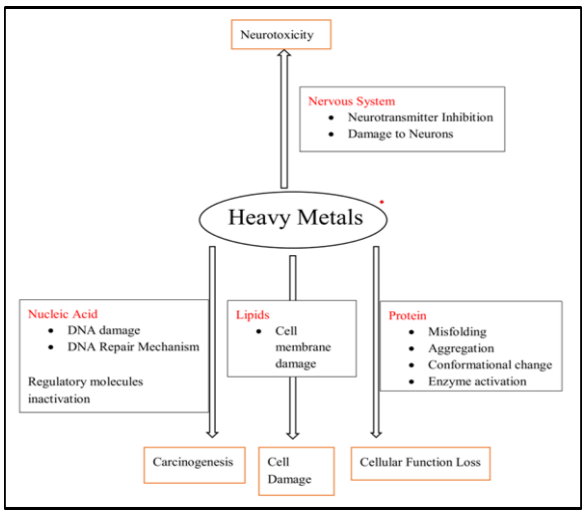

Figure 1. Heavy Metal Source Pathway and Human Exposure

1. Carcinogenicity

Histone modifications, DNA methylation, altered p53 protein expression, epigenetic changes, and decreased p21 expression are all brought on by arsenic. Arsenic raises the risk of cancer because it binds to proteins that bind to DNA and slows down the process of DNA repair [15].

2. Hepatotoxicity

The liver and the renal cortex are the two human target tissues for cadmium. It builds up in the liver after an acute exposure and is linked to certain hepatic dysfunctions. Hepatocellular injury and oxidative stress are the outcomes of cadmium's alteration of the cellular redox equilibrium. Acute and chronic liver failure are possible outcomes of cadmium-induced hepatotoxicity, which increases the risk of cancer [16]. Numerous studies have connected Cr (VI) to liver injury, and histological changes such as hepatocyte steatosis, parenchymatous degeneration, and necrosis have already been reported. Reduced antioxidant enzyme activity, DNA damage, and mitochondrial dysfunction—including apoptosis, halted cell growth, and decreased bioenergetic activity—are associated with elevated levels of the production of reactive oxygen species (ROS), lipid peroxidation, inhibitions of RNA, DNA, and protein synthesis. Cr(VI) for mitochondria as well. injury to the liver [17].

3. Neurotoxicity

Manganese is a necessary element that the body needs for several physiological processes. Acute exposure

to it reduces apoptotic cell death, which may have a neuroprotective effect. However, prolonged exposure can cause adverse diseases such as neurological conditions such as Alzheimer's and Parkinson's, which affect homeostasis and cause apoptotic cell death. The cellular Mn's homeostasis depends on adequate intake, storage, and excretion through several cell receptors and ion channels [18].

4. Immunological toxicity

Both short- and long-term exposure to lead can impact the immune system negatively and result in a variety of immunological reactions, including an increase in allergies, infectious illnesses, cancer, and autoimmune disorders. In some population groups, lead exposure has been connected to an increased risk of stomach, lung, and bladder cancer. Exposure to lead raises MHC activation , B and T cell production. It might alter T-cell function and make people more vulnerable to developing autoimmunity and hypersensitivity, which could have an impact on humoral and cellular responses [19].

5. Cardiovascular toxicity

Numerous issues can arise in the body as a result of acute or chronic lead exposure. By altering the renin-angiotensin system, reducing vasodilation prostaglandins, raising constrictors vessels prostaglandins, reducing NO the availability, and interfering with vascular smooth muscle cells Chronic lead exposure may result in artery disease and high blood pressure, blood clots atherosclerosis, and heart illness by altering the vascular response to vasoactive agonists, triggering inflammation and endothelium-dependent vasorelaxation, and affecting Ca (II) signaling [20]. Prolonged exposure also causes an increase in arterial pressure. Cadmium is a toxic and carcinogenic element. Besides tumors, cadmium also causes problems with the kidneys, bone harm, and heart disease [21].

6. Skin toxicity

Prolonged arsenic exposure increases the risk of developing several significant skin conditions, such as excessive pigmentation, hyperkeratosis, and multiple kinds of cancers of the skin. The pigmentation is one of the most prevalent skin conditions caused by prolonged exposure to arsenic. An early form of skin cancer known as Bowen's disease may result from exposure to arsenic [22]. The soles and palms of the hands are typically affected by arsenic hyperkeratosis, while the dorsum, fingers, arms, legs, and toes of the hands may also be affected. Some lesions associated with Bowen's illness & hyperkeratotic illnesses may develop into invasive malignancies [23].

7. Genotoxicity

Genetic factors have been identified as the primary reason of the significant interindividual variation in sensitivity to arsenic poisoning that has been shown by numerous investigations. The chromosome anomalies mutations, creation of micronuclei, deletion, and sister chromatid exchange are examples of deoxyribonucleic acid modification brought on by the arsenic DNA damage [24].

1.3. Natural resource-based treatment alternatives

1. Treatment for neurotoxicity

To assess the effectiveness of various therapeutic techniques and neuroprotective drugs in mitigating Mn-induced neurotoxicity, a multitude of studies have been conducted, Taking Mn-related toxicity causes and pharmacokinetic into consideration [25]. Anti-inflammation drugs, synthetic and naturally occurring antioxidants, glutamine protection, and ATP/ADP ratio protectors have all been tested to reduce Mn-induced neurotoxicity. Moreover, the effectiveness of a number of therapeutic approaches, including levodopa, para-aminosalicylic acid [PAS], and [EDTA] called ethylene-diamine-tetra acetic acid, as well as the underlying processes of these approaches, have been demonstrated. [PPEES] called the polyphenolic extract Euphorbia suppina of a Korean prostrate spurge had been shown to dramatically reduce Mn-induced neurotoxicity by antioxidants through regulating endoplasmic reticulum (ER) shock and ER shock-mediated death . Lipid peroxidation results in the production of malondialdehyde (MDA) and ROS, both of which were dramatically decreased. Simultaneously, the antioxidant activity of catalase (CAT), GSH and SOD. PPEES was also observed in vivo to ameliorate Mn-induced histological changes in the cerebral cortex and striatum [26].

2. Treatment for Nephrotoxicity

When oral cadmium poisoning occurs over an extended period of time, the kidneys are severely harmed. Curcumin pretreatment has improved the histologic alterations brought on by CD. Urine excretion from the Kidney Damage Molecules (KIM-1) was greatly decreased. The use of osteopontin (OPN), netrin-1, lipocaline-associated neutrophil gelatinase (NGAL), tissue inhibitor of metalloproteinase 1 (TIMP-1), and curcumin lowers the risk of nephrotoxicity caused by Cd exposure considerably [27]. Lipids oxidation, kidney injury molecules-1 (KIM-1), metallothionein, interleukin-1b, tumour necrosis factor-i, nitric oxide, and the apoptosis regulators Bax and caspases-3 were significantly elevated in the tissues of the kidneys of mice given royal jelly therapy. Glutathione levels, antioxidant enzyme activity, and the apoptotic inhibitor Bcl-2 were also shown to differ significantly. Histopathological investigations reveal

vacuolation and blocked glomeruli in the renal tissue of the animal treated with royal jelly [28]. Additionally, protocatechuic acid treatment improved the cadmium-induced toxicity by lowering the total protein level.

3. Treatment for Carcinogenicity

DMA and sodium arsenite aggravate long-term bladder exposure, per a recent study. Carcinogenesis is associated with both survival and the metallopeptidase 9 matrix (MMP-9) activity. The detection of mediated bladder cancer may be aided by these indicators. The amount of oxidative damage that reduces the risk of cancer is reduced. For blood cancer brought on by systemic arsenic exposure, miADMSA might be helpful. The tissue-arsenic content, ROS, TBARS level, catalases, SOD activity, and GSH level all were significantly higher [29], and these factors can elevate the eighth OHdG while treated with DMA and sodium arsenite. Pro-oncogenic indicators including MMP-9 and serum, bladder tissue, NBT-II, and T-24 cells may have improved as a result of these developments. Increased cell migration and clonogenic potential in arsenic-exposed NBT-II and T-24 cells are signs of significant carcinogens. Following therapy with MiADMSA, there was a notable improvement in these biomarkers [30]. According to a different study, levels of lipid peroxidation and lead-mediated hepatic and renal damage products were much lower before receiving treatment with Rosmarinus officinalis extract.

4. Treatment for Immunological toxicity

The naturally occurring substance pterostilbene (PT) is primarily present in blueberries. Research has demonstrated that PT is a potent anti-inflammatory and anti-oxidant substance. Mice's ear skin became inflamed when epidermal Cr(VI) was administered, according to a live study. The epidermal layer included cytokines that promoted inflammation, such as TNF-a and IL-1, which could mean that the condition deteriorated while receiving Cr(VI) therapy [32]. In the meantime, results from an additional in vitro study demonstrated that treating HaCaT cells with different concentrations of Cr(VI) raised Humans keratinocyte cell endoplasmic reticulum (ER) stresses and cell death. Furthermore, HaCaT cell death and inflammation were decreased by in vitro PT therapy. Moreover, new research has raised the possibility of a link between the inflammasome NLRP3 and Cr (VI)-mediated apoptotic and inflammatory in allergy dermatitis to contact (ADC). Furthermore, nuclear factor (Nrf2) attenuated autoimmunological problems generated by erythroid-derived 2 (Nrf2) [33].

5. Treatment for Cardiovascular toxicity

Cadmium and mercury are extremely dangerous substances that can seriously harm an animal's or human's heart. In a study looking at the preventive benefits of vitamin C in rabbits contrary to these elements, positive findings regarding heart damage were discovered [34]. In a different investigation. injecting 300 mg/kg of C aurantium peel extract dramatically reduced the histologic and biochemical changes found in the rat heart after it was exposed to $K_2Cr_2O_7$. Their results suggest that the antioxidant properties of C. Extraction of aurantium skins may be able to prevent cardiac damage brought on by $K_2Cr_2O_7$ [35]. According to a recent study, sulforaphane (SFN) reduced the effects of $K_2Cr_2O_7$-induced oxidative stress, haematological alterations, structural disorder, cardiomyocyte apoptosis, and cardiac malfunction.

6. Treatment for Toxic The skin

To determine whether peel extract from Solanum melongena could be used to treat Bowen's disease caused by arsenic poisoning, research was done. From the two areas where arsenic is endemic, eight individuals with Bowen's disease caused by arsenic were chosen. Each patient was given instructions to apply an ointment comprising peel extract twice daily to the lesion location for a period of twelve weeks. A discernible improvement was observed in the Bowen's disease lesion [36].

7. Treatment for Genotoxicity

A well-known genotoxicant, arsenic causes harm to cells by triggering an excess of reactive oxygen species (ROS), antioxidant enzyme systems, and activating oxidatively sensitive signalling pathways. Epigallocatechin gallate (EGCG), the main polyphenolic catechin in tea made from green tea, has demonstrated strong in vitro genoprotective, antioxidants, and free radical scavenging properties [37]. The purpose of the study was to ascertain whether EGCG protects against oxidative stress are caused by arsenic in mice and is useful as an antioxidant and genoprotector. The animals were given oral EGCG at therapeutic and preventative dosages of 25 and 50 mg/kg b.wt for a duration of 15 days. Subsequently, they were administered intraperitoneally with 1.5 mg/kg b.wt. (1/10th of LD50) of lead for a ten-day period. reduced hepato-renal antioxidant levels (about 46%) and elevated genome fragmented in hepato-renal tissues; increasing chromosomal mutations (79%) and micronucleation (22%) in the bone marrow cells; and comet tailing (26%) in mouse lymphocytes after lead toxicity [37].

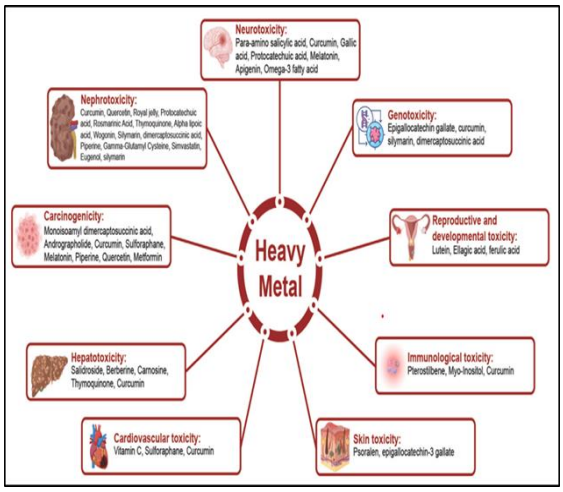

Figure 2. Diagrammatic Description of How Naturally Occurring Bioactive Compounds Alleviate Heavy Metal Toxicity.

1.4. Strategies involving nanotechnology and nanomedicine to address heavy metal toxicity

The investigation and eliminating of toxic substances from food and water through the use of nanotechnology is becoming more popular. Numerous nanomaterials, such as metal oxide nanoparticles, magnetic nanoparticles (MNPs), graphene and its derivatives, and carbon nanotubes (CNTs), have been used to remove heavy metals. There are multiple advantages to adopting nanotechnology for heavy metal analysis and removal from food and water sources rather to more traditional methods. Among the advantages include a large linear range, minimal detection and quantification restrictions, high sensitivity, and excellent selectivity. Nanotechnology-based approaches must be used in the field in a transparent safe way [38]. The next sections will examine the use of carbon nanotubes (CNTs), graphene, its oxides, and derivatives for the removal of heavy metals, as well as metal oxide nanoparticles (MNPs).

1.5. The metallic oxide nanoparticles

Metal oxide nanoparticles, Because of their unique physical and chemical features, have been utilised to remove harmful heavy metal ions from polluted water. Natural biopolymers and biological wastes can be converted into magnetic nano adsorbents thanks to recent advancements in green chemical technology. These approaches were developed because of their high availability, biodegradable properties low prices, and significant affinity for metals encapsulation. [39].

CuO that has undergone various structural modifications during its nanoscale production has exhibited favorable Adsorption characteristics for As(III), As(V), Pb(II), and Cr(VI). In this work, cold finger assisted magnetron sputtering was used to generate CuO nanoparticles having a uniform particle size distribution and a large specific surface area. It was discovered that the production of CuO nanoparticles had a major impact on the adsorption of heavy metal ions. Increasing the surface area and adsorption site of CuO will increase the material's adsorption capacity. The nanoscale modification of CuO structure results in an increase in metal ion active sites, which aids in the elimination of ions of heavy metals from the environmental [40]

The creation of SiO_2 mesoporous nanoparticles using organic surfactants is a novel approach to tackling environmental challenges caused by the Cr (III) ions. Sunflower oil and n-dodecyl amine were utilized as templating agents in a one-pot co-condensation of 2-cyanoethyltriethoxysilane and tetraethoxysilane at 1:4 and 1:9 ratios, respectively, to generate organo-silica mesoporous materials containing cyano functional groups. The cyano group acted as an adsorption site, and the carboxyl surface functional group was formed by hydrolyzing the carboxyl surface functional group. The effectiveness of the removal of the Cr (III) ion can vary between 48 and 83% depending on the function of the groups of the adsorbents utilized and the silicone to silica ratio of the mixture. The substance generated is a powerful adsorbent, according to the results [41].

1. Magnetic nanoparticles

Magnetic Fe_3O_4 nanoparticles with surface coatings are frequently employed to: (1) enhance target selectivity; and (2) inhibit oxidation and aggregation. For instance, a core–shell structure made up of a polythiophene shell, a SiO_2 shell, and a Fe_3O_4 core has been seen. Hg(II) ions can be swiftly enriched and separated using it in a range of matrices. Another example [42], is Fe_3O_4 hybridised with polyaniline and MnO2 (Fe_3O_4/PANI/MnO_2). It may be made in an environmentally and economically acceptable way and has a high capacity for the adsorption of heavy metal ions, such as Pb(II), Zn(II), Cd(II), and Cu(II) [43]. A high concentration of amine and imine functional groups in the amino-conjugated polymer poly-(m-phenylenediamine) (PmPD) leads to improved adsorption, chelation, and redox activity. The organisational structure and functionalities of PANI and PmPD are conforming.Accordingly, mixing MnO_2 and PmPD could work. Heavy metal impurities may be eliminated from the MnO_2/Fe_3O_4/PmPD core-shell hybrid via ion exchange, electrostatic attraction, and coordination interaction because of its high adsorption capacity and intrinsic paramagnetic characteristic [44].

2. Carbon nanotubes

(Nanotubes) As a possible remediation technique for heavy metal-contaminated water, carbon nanotubes are gaining popularity due to their superior physicochemical qualities. Carbon nanomaterials, such as carbon nanotubes, graphene, fullerenes, graphene oxide, and activated carbon, have enormous potential for removing heavy metals from water because of their large surface area, nanoscale size, and availability of a variety of functionalities. Furthermore, it is easier to recycle and modify them chemically. [45]

3. Graphene and its composition

Graphene oxides (GO) have an immense theoretically specific surface area of 2630 m2/g and a complicated layered structure containing a range of hydrophilic polar groups, such as hydroxyl (-OH) groups, epoxy resins, and carboxyl (-COOH) groups. These traits suggest that GO could be able to eliminate organic pollutants and heavy metal ions from their environment [46]. However, because graphene has a small particle size, extracting it from an aqueous solution using the conventional centrifugal filtration method presents challenges [47]. Consequently, graphene-based magnetic adsorbents have found applications in the environmental cleanup industry because they separate readily in the presence of a magnetic field.

3. CONCLUSIONS AND RECOMMENDATIONS FOR THE FUTURE

The majority of heavy metals exist naturally in the environment. Human activity causes the discharge of certain harmful heavy metals into the environment. The human body is exposed to heavy metals through either the environment (where the metal is naturally present) or exogenous sources. Variations in the paths of intake are possible. It is vital to understand how heavy metals enter the body, how hazardous they are, and how often they cause mortality rates. After conducting a comprehensive analysis, we conclude that the most common way to do this is by oral ingestion of heavy metals. Excessive amounts can cause serious injury to all organs of the body and can present as neurological disorders, respiratory ailments, carcinogenicity, GI obstruction, osteoporosis, etc [48]. Many treatments based on natural products and nanotechnology have been developed to counteract the toxicity. From a social perspective, it is also critical to consider certain preventive measures. Moving afflicted persons away from the exposure location is the first step in minimizing the damaging effects of heavy metals. It is also essential to confirm that less heavy metals are used in industrial operations. When hazardous heavy metals are used frequently, chemical products shouldn't be used [49]. Either way, by increasing their self-awareness, everyone could lessen their addiction to heavy metal. Long-term low-dose exposure to diverse elements poses a considerable danger to public health in many metal-polluted places, particularly when metal pollution is hang out. Understanding the fundamental concepts behind heavy metal interactions is crucial for evaluating and minimizing health dangers associated with chemical combinations. Therefore, more research is needed to fully comprehend the molecular process and implications for public health that arise from exposure to combinations of hazardous metals in humans [50].

3. REFERENCES

1. Abdel-Daim, M.M., Abdou, R.H., 2015. Protective effects of diallyl sulfide and curcumin separately against thallium-induced toxicity in rats. Cell J. 17, 379– 388. https://doi.org/10.22074/cellj.2016.3752.
2. Abolaji, A.O., Fasae, K.D., Iwezor, C.E., Aschner, M., Farombi, E.O., 2020. Curcumin attenuates copper-induced oxidative stress and neurotoxicity in Drosophila melanogaster. Toxicol. Reports 7, 261–268. https://doi.org/10.1016/ j.toxrep.2020.01.015.
3. Abolhasani, J., Hosseinzadeh Khanmiri, R., Babazadeh, M., Ghorbani-Kalhor, E., Edjlali, L., Hassanpour, A., 2015. Determination of Hg(II) ions in sea food samples after extraction and preconcentration by novel Fe3O4@SiO2@polythiophene magnetic nanocomposite. Environ. Monit. Assess. 187 (9). https://doi.org/10.1007/s10661-015-4770-5.
4. Adefegha, S.A., Omojokun, O.S., Oboh, G., 2015. Modulatory effect of protocatechuic acid on cadmium induced nephrotoxicity and hepatoxicity in rats in vivo. Springerplus 4 (1). https://doi.org/10.1186/s40064-015-1408-6.
5. Adeyemi, O.S., Aroge, C.S., Akanji, M.A., 2017. Moringa oleifera-based diet protects against nickel-induced hepatotoxicity in rats. J. Biomed. Res. 31, 350–357. https://doi.org/10.7555/JBR.31.20160051.
6. Al Olayan, E.M., Aloufi, A.S., AlAmri, O.D., El-Habit, O.H., Abdel Moneim, A.E., 2020. Protocatechuic acid mitigates cadmium-induced neurotoxicity in rats: Role of oxidative stress, inflammation and apoptosis. Sci. Total Environ. 723, 137969. https://doi.org/10.1016/j.scitotenv.2020.137969.
7. Ali, S., Awan, Z., Mumtaz, S., Shakir, H.A., Ahmad, F., Ulhaq, M., Tahir, H.M., Awan, M. S., Sharif, S., Irfan, M., Khan, M.A., 2020. Cardiac toxicity of heavy metals (cadmium and mercury) and pharmacological intervention by vitamin C in rabbits. Environ. Sci. Pollut. Res. 27 (23), 29266–29279. https://doi.org/10.1007/ s11356-020-09011-9 .
8. Almeer, R.S., AlBasher, G.I., Alarifi, S., Alkahtani, S., Ali, D., Abdel Moneim, A.E., 2019. Royal jelly attenuates cadmium-induced nephrotoxicity in male mice. Sci. Rep. 9 (1). https://doi.org/10.1038/s41598-019-42368-7.
9. Ataei, N., Aghaei, M., Panjehpour, M., 2018. The protective role of melatonin in cadmium-induced proliferation of ovarian cancer cells. Res. Pharm. Sci. 13, 159– 167. https://doi.org/10.4103/1735-5362.223801.
10. Azeh Engwa, G., Udoka Ferdinand, P., Nweke Nwalo, F., Unachukwu, N.M., 2019. Mechanism and health effects of heavy metal toxicity in humans. Poisoning Mod. World - New Tricks an Old Dog? https://doi.org/10.5772/ intechopen.82511 .
11. Baby, R., Saifullah, B., Hussein, M.Z., 2019. Carbon nanomaterials for the treatment of heavy metal-contaminated water and environmental remediation. Nanoscale Res. Lett. 14 (1). https://doi.org/10.1186/s11671-019-3167-8.
12. Banerjee, N., Wang, H., Wang, G., Khan, M.F., 2020. Enhancing the Nrf2 antioxidant signaling provides protection against trichloroethene-mediated inflammation and autoimmune

response. Toxicol. Sci. 175, 64–74. https://doi.org/ 10.1093/toxsci/kfaa022.
13. Batool, Z., Agha, F., Tabassum, S., Batool, T.S., Siddiqui, R.A., Haider, S., 2019. Prevention of cadmium-induced neurotoxicity in rats by essential nutrients present in nuts. Acta Neurobiol. Exp. (Wars) 79, 169–183. https://doi.org/ 10.21307/ane-2019-015.
14. Benvenga, S., Marini, H.R., Micali, A., Freni, J., Pallio, G., Irrera, N., Squadrito, F., Altavilla, D., Antonelli, A., Ferrari, S.M., Fallahi, P., Puzzolo, D., Minutoli, L., 2020. Protective effects of myo-inositol and selenium on cadmium-induced thyroid toxicity in mice. Nutrients 12 (5), 1222. https://doi.org/10.3390/nu12051222.
15. Branca, J.J.V., Morucci, G., Pacini, A., 2018. Cadmium-induced neurotoxicity: Still much ado. Neural Regen. Res. 13, 1879–1882. https://doi.org/10.4103/1673- 5374.239434.
16. Camps, I., Maldonado-Castillo, A., Kesarla, M.K., Godavarthi, S., Casales-Díaz, M., Martínez-Gómez, L., 2020. Zerovalent nickel nanoparticles performance towards Cr(VI) adsorption in polluted water. Nanotechnology 31 (19), 195708. https://doi.org/10.1088/1361-6528/ab70d4.
17. Chen, C., Lin, B., Qi, S., He, J., Zheng, H., 2019. Protective effects of salidroside on lead acetate-induced oxidative stress and hepatotoxicity in sprague-dawley rats. Biol. Trace Elem. Res. 191 (2), 426–434. https://doi.org/10.1007/s12011-019- 1635-8.
18. Chen, S., Liu, G., Long, M., Zou, H., Cui, H., 2018. Alpha lipoic acid attenuates cadmium-induced nephrotoxicity via the mitochondrial apoptotic pathways in rat. J. Inorg. Biochem. 184, 19–26. https://doi.org/10.1016/j. jinorgbio.2018.04.001 .
19. Coetzee, J.J., Bansal, N., Chirwa, E.M.N., 2020. Chromium in environment, its toxic effect from chromite-mining and ferrochrome industries, and its possible bioremediation. Expo. Heal. 12 (1), 51–62. https://doi.org/10.1007/s12403-018- 0284-z.
20. Dourado, N.S., Souza, C.D.S., de Almeida, M.M.A., Bispo da Silva, A., dos Santos, B.L., Silva, V.D.A., De Assis, A.M., da Silva, J.S., Souza, D.O., Costa, M.d.F.D., Butt, A.M., Costa, S.L., 2020. Neuroimmunomodulatory and neuroprotective effects of the flavonoid apigenin in in vitro models of neuroinflammation associated with Alzheimer's disease. Front. Aging Neurosci. 12. https://doi.org/10.3389/ fnagi.2020.00119 .
21. Elblehi, S.S., Hafez, M.H., El-Sayed, Y.S., 2019. L-a-Phosphatidylcholine attenuates mercury-induced hepato-renal damage through suppressing oxidative stress and inflammation. Environ. Sci. Pollut. Res. 26 (9), 9333–9342. https://doi.org/ 10.1007/s11356-019-04395-9.
22. riberg, L., Kjellström, T., Elinder, C.-G., Nordberg, G.F., 2019. Cadmium and health: a toxicological and epidemiological appraisal. Cadmium Heal. A Toxicol. Epidemiol. Apprais. https://doi.org/10.1201/9780429260599 .
23. Gabris, M.A., Jume, B.H., Rezaali, M., Shahabuddin, S., Nodeh, H.R., Saidur, R., 2018. Novel magnetic graphene oxide functionalized cyanopropyl nanocomposite as an adsorbent for the removal of Pb(II) ions from aqueous media: equilibrium and kinetic studies. Environ. Sci. Pollut. Res. 25 (27), 27122–27132. https://doi. org/10.1007/s11356-018-2749-9.
24. Gargouri, M., Soussi, A., Akrouti, A., Magné, C., El Feki, A., 2018. Ameliorative effects of spirulina platensis against lead-induced nephrotoxicity in newborn rats: Modulation of oxidative stress and histopathological changes. EXCLI J. 17, 215– 232. https://doi.org/10.17179/excli2017-1016 .
25. Garza-Lombó, C., Pappa, A., Panayiotidis, M.I., Gonsebatt, M.E., Franco, R., 2019. Arsenic-induced neurotoxicity: a mechanistic appraisal. J. Biol. Inorg. Chem. 24 (8), 1305–1316. https://doi.org/10.1007/s00775-019-01740-8 .
26. Genchi, G., Carocci, A., Lauria, G., Sinicropi, M.S., Catalano, A., 2020. Nickel: Human health and environmental toxicology. Int. J. Environ. Res. Public Health 17 (3), 679. https://doi.org/10.3390/ijerph17030679.
27. Gong, Z., Chan, H.T., Chen, Q., Chen, H., 2021. Application of nanotechnology in analysis and removal of heavy metals in food and water resources. Nanomaterials 11 (7), 1792. https://doi.org/10.3390/nano11071792.
28. Goodarzi, Z., Karami, E., Ahmadizadeh, M., 2017. Simvastatin attenuates chromiuminduced nephrotoxicity in rats. J. Nephropathol. 6, 5–9. https://doi.org/ 10.15171/jnp.2017.02.
29. Gworek, B., Dmuchowski, W., Baczewska-Da˛browska, A.H., 2020. Mercury in the terrestrial environment: a review. Environ. Sci. Eur. 32 (1). https://doi.org/ 10.1186/s12302-020-00401-x.
30. Harischandra, D.S., Ghaisas, S., Zenitsky, G., Jin, H., Kanthasamy, A., Anantharam, V., Kanthasamy, A.G., 2019. Manganese-induced neurotoxicity: New insights into the triad of protein misfolding, mitochondrial impairment, and neuroinflammation. Front. Neurosci. 13. https://doi.org/10.3389/ fnins.2019.00654.
31. Huang, H.-W., Lee, C.-H., Yu, H.-S., 2019. Arsenic-induced carcinogenesis and immune dysregulation. Int. J. Environ. Res. Public Health 16 (15), 2746. https:// doi.org/10.3390/ijerph16152746.
32. Islam, M.N., Rauf, A., Fahad, F.I., Emran, T.B., Mitra, S., Olatunde, A., Shariati, M.A., Rebezov, M., Rengasamy, K.R.R., Mubarak, M.S., 2021. Superoxide dismutase: an updated review on its health benefits and industrial applications. Crit. Rev. Food Sci. Nutr. https://doi.org/10.1080/10408398.2021.1913400.
33. Jiao, D., Jiang, Q., Liu, Y., Ji, L., 2019. Nephroprotective effect of wogonin against cadmium-induced nephrotoxicity via inhibition of oxidative stress–induced MAPK and NF-kB pathway in Sprague Dawley rats. Hum. Exp. Toxicol. 38 (9), 1082–1091. https://doi.org/10.1177/0960327119842635.
34. Joardar, S., Dewanjee, S., Bhowmick, S., Dua, T.K., Das, S., Saha, A., De Feo, V., 2019. Rosmarinic acid attenuates cadmium-induced nephrotoxicity via inhibition of oxidative stress, apoptosis, inflammation and fibrosis. Int. J. Mol. Sci. 20 (8), 2027. https://doi.org/10.3390/ijms20082027.
35. Kaushal, S., Ahsan, A.U., Sharma, V.L., Chopra, M., 2019. Epigallocatechin gallate attenuates arsenic induced genotoxicity via regulation of oxidative stress in balb/C mice. Mol. Biol. Rep. 46 (5), 5355–5369. https://doi.org/10.1007/s11033- 019-04991-5.
36. Zhou, L.i., Zhang, C., Qiang, Y.u., Huang, M., Ren, X., Li, Y., Shao, J., Xu, L., 2021. Anthocyanin from purple sweet potato attenuates lead-induced reproductive toxicity mediated by JNK signaling pathway in male mice. Ecotoxicol. Environ. Saf. 224, 112683. https://doi.org/10.1016/j.ecoenv.2021.112683.
37. Yin, Y., Meng, F., Sui, C., Jiang, Y., Zhang, L., 2019. Arsenic enhances cell death and DNA damage induced by ultraviolet B exposure in mouse epidermal cells through the production of reactive oxygen species. Clin. Exp. Dermatol. 44, 512– 519. https://doi.org/10.1111/ced.13834.
38. Zhou, C., Huang, C., Wang, J., Huang, H., Li, J., Xie, Q., Liu, Y., Zhu, J., Li, Y., Zhang, D., Zhu, Q., Huang, C., 2017. LncRNA MEG3 downregulation mediated by DNMT3b contributes to nickel malignant transformation of human bronchial epithelial cells via modulating PHLPP1 transcription and HIF-1a translation. Oncogene 36 (27), 3878–3889. https://doi.org/10.1038/onc.2017.14.
39. Yang, J.H., Yoon, J.Y., Kwon, H.H., Min, S., Moon, J., Suh, D.H., 2017. Seeking new acne treatment from natural products, devices and synthetic drug discovery. Dermatoendocrinol. 9 (1), e1356520. https://doi.org/10.1080/ 19381980. 2017.1356520.
40. Yang, D., Han, B., Baiyun, R., Lv, Z., Wang, X., Li, S., Lv, Y., Xue, J., Liu, Y., Zhang, Z., 2020. Sulforaphane attenuates hexavalent chromium-induced cardiotoxicity: Via the activation of the Sesn2/AMPK/Nrf2 signaling pathway. Metallomics 12, 2009–2020. https://doi.org/10.1039/d0mt00124d.
41. Zhang, C., Ge, J., Lv, M., Zhang, Q.i., Talukder, M., Li, J.-L., 2020. Selenium prevent cadmium-induced hepatotoxicity through modulation of endoplasmic reticulum-resident selenoproteins and attenuation of endoplasmic reticulum stress.

Environ. Pollut. 260, 113873. https://doi.org/10.1016/j.envpol.2019.113873.
42. Xiong, T., Yuan, X., Cao, X., Wang, H., Jiang, L., Wu, Z., Liu, Y., 2020. Mechanistic insights into heavy metals affinity in magnetic MnO2@Fe3O4/poly(mphenylenediamine) coreshell adsorbent. Ecotoxicol. Environ. Saf. 192, 110326. https://doi.org/10.1016/j.ecoenv.2020.110326.
43. Yumoto, T., Tsukahara, K., Naito, H., Iida, A., Nakao, A., 2017. A successfully treated case of criminal thallium poisoning. J. Clin. Diagnostic Res. 11, OD01–OD02. https://doi.org/10.7860/JCDR/2017/24286.9494.
44. Wang, Y., Mandal, A.K., Son, Y.O.K., Pratheeshkumar, P., Wise, J.T.F., Wang, L., Zhang, Z., Shi, X., Chen, Z., 2018b. Roles of ROS, Nrf2, and autophagy in cadmiumcarcinogenesis and its prevention by sulforaphane. Toxicol. Appl. Pharmacol. 353, 23–30. https://doi.org/10.1016/j.taap.2018.06.003.
45. Yousef, M.I., El-Demerdash, F.M., Radwan, F.M.E., 2008. Sodium arsenite induced biochemical perturbations in rats: ameliorating effect of curcumin. Food Chem. Toxicol. 46 (11), 3506–3511. https://doi.org/10.1016/j.fct.2008.08.031.
46. Zambelli, B., Uversky, V.N., Ciurli, S., 2016. Nickel impact on human health: An intrinsic disorder perspective. Biochim. Biophys. Acta - Proteins Proteomics 1864 (12), 1714–1731. https://doi.org/10.1016/j.bbapap.2016.09.008.
47. Zhao, L., Wang, J.L., Wang, Y.R., Fa, X.Z., 2013. Apigenin attenuates copper-mediated b-amyloid neurotoxicity through antioxidation, mitochondrion protection and MAPK signal inactivation in an AD cell model. Brain Res. 1492, 33–45. https:// doi.org/10.1016/j.brainres.2012.11.019.
48. Zhu, Y., Murali, S., Cai, W., Li, X., Suk, J.W., Potts, J.R., Ruoff, R.S., 2010. Graphene and graphene oxide: synthesis, properties, and applications. Adv. Mater. 22 (35), 3906–3924. https://doi.org/10.1002/adma.201001068.
49. hang, X., Yang, L., Li, Y., Li, H., Wang, W., Ye, B., 2012. Impacts of lead/zinc mining and smelting on the environment and human health in China. Environ. Monit. Assess. 184 (4), 2261–2273. https://doi.org/10.1007/s10661-011-2115-6 .
50. Young, H.A., Geier, D.A., Geier, M.R., 2008. Thimerosal exposure in infants and neurodevelopmental disorders: An assessment of computerized medical records in the Vaccine Safety Datalink. J. Neurol. Sci. 271 (1-2), 110–118. https://doi.org/10.1016/j.jns.2008.04.002.

Arabic Abstract

تشكل المعادن الثقيلة تهديدًا شائعًا للبيئة بسبب آثارها السامة، وميلها إلى البقاء في الغلاف الجوي للأرض، فضلاً عن قدرتها على التراكم الحيوي داخل جسم الفرد. يعد التسمم بالمعادن الثقيلة في النظم البيئية الأرضية والمائية مشكلة بيئية خطيرة لها تأثير على صحة الإنسان. تم العثور على الجزء الأكبر من العناصر المعدنية في الطبيعة، على الرغم من حقيقة أن البشر ينتجون بعضها. من أكثر السمات المميزة للمعادن الثقيلة هي كتلتها الذرية والخطر الذي تشكله على الكائنات الحية. علاوة على ذلك، وعلى الرغم من الاختلافات في التكنولوجيا، لا تزال الأبحاث حول التشخيص الطبي المبتكر جارية. يتيح مجال تكنولوجيا النانو سريع التطور تقدمًا كبيرًا في دراسة تجديد المواد المعدنية من المصفوفات المعقدة. تم استخدام العديد من المواد النانوية الكربونية لإزالة المعادن، بما في ذلك الجسيمات النانوية المغناطيسية، والجسيمات النانوية لأكسيد المعادن، والأنابيب النانوية، والجرافين ومشتقاته، والأنابيب النانوية. إن تطبيق تكنولوجيا النانو على إزالة وتحليل المعادن الثقيلة من مصادر الغذاء والماء له فوائد عديدة مقارنة بالطرق التقليدية. ومن بين هذه الفوائد الحساسية العالية، والانتقائية الممتازة. ولذلك، كان الهدف من المقال هو دراسة كيفية تأثير المعادن الثقيلة على النظام البيئي، والضرر الذي تسببه لصحة الإنسان، وإمكانية استخدام الموارد الطبيعية لتحضير أدوية جديدة، كما تؤكد هذه المقالة أيضًا على تطبيق تكنولوجيا النانو والتطبيقات غير الطبية على مشكلة سمية المعادن الثقيلة.

Pure Sciences International Journal of kerbala

Year:2024 Volume : 1 Issue : 3 ISSN: 6188-2789 Print 3005 -2394 Online

Biadaa Jamel Nama , Kiaser Abdulsajjad Mohmmed Hussain , Preparation and Diagnosis of Green Nanocomposite from Salvia Officinalis and Study of its Inhibitory Effectiveness of Resistant Bacterial Isolated from Different Clinical Cases, Pure Sciences International Journal of Kerbala, Vol. 1 No. 3 (2024) 26-33

First year 2024 ,Volume 1, Issue 3 PSIJK 26-33

Pure Sciences International Journal of Kerbala
Journal Homepage:https://journals.uokerbala.edu.iq/index.php/psijk

Preparation and Diagnosis of Green Nanocomposite from Salvia Officinalis and Study of its Inhibitory Effectiveness on Resistant Bacteria Isolated from Different Clinical Cases

Biadaa Jamel Nama[1*] , Kiaser Abdulsajjad Mohmmed Hussain[2]
[1,2]*Department of Biology, College of Education for Pure, University of Kerbala, Kerbala, Iraq*

P A P E R I N F O

Received: 20 May 2024
Accepted: 27 June 2024
Published: 30 September 2024

Keywords:
Antibacterial activity, Green synthesis, Nanotechnology, Salvia officinalis, Silver nanoparticles.

A B S T R A C T

The current research aims to prepare the aqueous extract and nanocomposite of sage leaves using green synthesis method, and to identify the silver nanoparticles using FTIR and SEM analysis. The antibiotic ciprofloxacin was loaded on the nanocomposite and the inhibitory activity on the studied bacterial isolates G-ve Klebsiella pneumoniae and Pseudomonas aeruginosa was studied. The study groups were divided into two replicates and five groups with three concentrations. The first group was treated with the antibiotic ciprofloxacin, the second group was treated with the aqueous extract of sage, and the nanocomposite was applied to the third group. The extract loaded with the antibiotic was used to treat the fourth group, and the nanocomposite loaded with the antibiotic was used to treat the fifth group. The color change from yellow to dark brown is evidence of the formation of nanoparticles, and the wave shift in the nanocomposite loaded with the antibiotic towards the frequency 2156.93 cm^(-1) is evidence of the success of the antibiotic loading process on the nanocomposite. The resulting compounds were characterized using scanning electron microscopy, and its results showed that the extract particles were in the form of irregular aggregates with the presence of some small particles with a spherical shape and an average particle size of 85.49 nm, while the nanocomposite was cubic in shape and an average particle size of 35.42 nm. The inhibition zones were evident in the fourth treatment T4, the aqueous extract loaded with the antibiotic, and the fifth treatment T5, the nanocomposite loaded with the antibiotic. Silver nanoparticles showed the highest synergistic efficiency with the antibiotic ciprofloxacin against the multidrug-resistant. bacteria strain *K.pneumoniae*, recording a rate of 14.33±1.41, while against *P.auroginosa* bacteria, a rate of 13.44±88 was recorded.

1. INTRODUCTION

The increasing numbers of antibiotic-resistant microorganisms pose a threat to human health, especially among poor populations and in hospitals and intensive care units. This is due to the misuse of antibiotics, poor hygiene in society, unsafe food, inadequate infection control in medical facilities, accumulation of antibiotics in the environment and their use in the food and animal industries [1]. Bacteria rapidly develop new resistance systems that enable them to withstand the effects of antibiotics, through mutations that occur in some bacterial cells that make them resistant to the effects of antibiotics, and then this advantage is passed on to the next generation, which is generation with complete resistance to the antibiotic [2]. *Pseudomonas aeruginosa*, *Klebsiella pneumoniae*, *Escherichia coli*, *and Acinetobacter baumannii* have all been recognized as pathogens with mostly high rates of antibiotic resistance, resulting in a declining range of treatments available for these organisms [3].

To confront the problem of bacterial resistance to multiple drugs, scientists have invented nano-delivery systems that have demonstrated high efficiency in overcoming many anatomical and functional barriers to delivering the drug to the target site. Thus, they have been able to produce highly effective drugs with few side effects [4]. Green nanotechnology is a field that focuses on making products that are environmentally friendly, safer for all living organisms, less expensive and more stable than other manufacturing methods such as bacteria, fungi, yeasts and viruses or using different plant parts such as leaves, stems, fruits, peels, etc. The "green synthesis" of nanoparticles has attracted a lot of attention to the use of metal oxides, such as silver oxides ($Ag\text{-}NO_3$), because of their optical, chemical, electrical and optical properties [5]. It has been found that nanomaterials face the problem of increasing resistance to bacteria because of their unique properties whose dimensions fall within the nanoscale of (1-100) including increased solubility. Biocompatibility, ease of

*Corresponding Author Institutional Email: baidaa.j@s.uokerbala.edu.iq (Biadaa Jamel Nama)

production, and stability. The nanoparticles' tiny size relative to the area of their surface is one of the most important characteristics that distinguishes these materials [6]. Many studies have proven that plants are considered a safe source for the pharmaceutical industry and a preventive source for many diseases, due to the medical effectiveness of plant compounds that contain antioxidant and antimicrobial properties [7]. Among the medicinal plants is the sage plant. It is part of the Lamiaceae family, which is often known as the "salvation plant", derived from the Latin word "salvarem". It means "preservation or treatment An evergreen perennial shrub, one of about 900 species of the genus Salvia, native to the Mediterranean and Middle East, Salvia grows as a subshrub up to 60 cm tall, with opposite and simple leaves, with white hairs on the lower surface of the leaf and a gray-green color on the upper surface of the leaf.".. Stems are erect with an abundance of dark green hairy branches. Leaves are elongated and petiolate with a serrated edge and a serrated surface, sometimes with basal lobes. The flowers are 2 to 4 mm long from their petioles. It is in the form of false upper flowers with 5 to 10 blue-violet colored, colorful flowers that form compound false spines. It blooms from March to July, depending on the habitat and climatic conditions [8]. It has been used for a variety of purposes, including reducing perspiration, treating sore throats (used as a gargle), regulating menstrual cycles, fighting infections, improving lipid status and liver function, improving appetite and digestion, and enhancing mental ability [9]. Thus, the goal of the present investigation was to prepare the aqueous extract and nanocomposite of the Salvia officinalis plant using the green synthesis method

2. MATERIALS AND METHODS

2.1. Isolation and Diagnosis of Bacteria

One hundred samples of both sexes, with ages ranging from (1 day to 70) years, were collected from Burn and wound patients and children in hospital. The number of burn isolates was 35 isolates, surgical isolates were 52 isolates, and children were 13 isolates. The isolates were transferred in swab form and placed in a sterile carrier medium. From hospitals in the Holy Governorate of Karbala, Al-Hussein General Hospital and Children's Teaching Hospital, all isolates were grown on MacConkey agar and Blood agar medium and incubated for 24 hours at 37 ℃ and the bacteria were diagnosed using the VITEK-2 Compact System device.

2.2. Preparation of the Aqueous Extract and Nanocomposite of Salvia Officinalis

Fifteen gram of dried *salvia* powder was weighed and 300 ml of boiled distilled water was added. After 30 minutes, it was left at room temperature. It was filtered using pieces of gauze and subsequently filtered twice utilizing filter papers (Whatman No. 1). The filtrate was then placed in a centrifuge and dried. 45°C was the temperature at which the filtrate was placed in an oven to obtain a dry extract in powder form. The powder was placed in a sealed, opaque tube and stored until it is used. Green Ag-NPs were manufactured by bio absorption of Ag+ in a clean solution of Salvia officinalis extract. By taking 1 mM of silver nitrate, the plant extract (1.5 gm of ready-made dry plant extract into 100 ml of non-ionic distilled water) was dropped onto the alkaline $AgNO_3$ solution with a ratio of (80% silver nitrate solution: 20% plant extract) and was done. Mixing for 30 minutes at 45-55 °C. Then the mixture is monitored for 3 hours. Then, it is observed that the color of the mixture changes from yellow to dark brown and this indicates the formation of Ag-NPs [10].

2.3. Diagnosis of Nanoparticles

FTIR analysis is used to determine the active groups responsible for reducing $AgNO_3$ to AgNPs, in addition to being responsible for the stability and coverage of the Ag NPs. SEM is employed to find out the shape and the nanoparticles' size and that all the prepared compounds are within the nanoscale limits [11].

2.4. Antibacterial Effectiveness

The minimum inhibitory concentration (MIC) was estimated utilizing the well diffusion method [12] for the antibiotic Ciprofloxacin, the aqueous extract of the free sage plant loaded with the antibiotic, and the nanocomposite before and after loading the antibiotic. The MIC for *K. pneumonia* bacteria, and *P. aeruginosa* is equal to 4 µg/ml of the VITEK and the MIC for extract 8 µg/ml and nanocomposite 8 µg/ml [13]. The extract is loaded with the antibody (2+4) µg/ml, and the nanocomposite is loaded with the antibody (2+4) µg/ml. The bacterial suspension was added to dishes containing Muller Hinton agar solid medium and was spread well on the surface of the dish using a diffuser. Figure - L sterile swab. Then, wells were made on the surface of the agar with equal dimensions for five groups. The first group was treated with the antibiotic ciprofloxacin, The Salvia officinalis plant's aqueous extract was used to treat the second group, The nanocomposite was applied to the third group, The antibiotic-loaded aqueous extract was given to the fourth group, and The Salvia officinalis plant's aqueous extract was given to the fifth group. It was treated with the nanocomposite loaded with the antibiotic, at three concentrations greater than the MIC, and at a concentration of MIC and less than the MIC, in a volume of 50 microlitres, using a micropipette. The concentrations were placed on the dishes containing the

bacterial culture, after which the plates were kept in the incubator for a full day at 37 °C.

3. RESULTS AND DISCUSSION

3. 1. Isolation and Diagnosis of Bacteria

The VITEK2 device was used to diagnose the identity of the bacterial isolates and the results were as shown in Figure 1.

klebsiella pneumonia 24%, *pseudomonas aeuroginosa* 21%, *staphylococcus aureus 7%, E. coli* 13% *coagulase negative staphylococcus 8%, Enterobacter aerogenes 5%, Staphylococcus Haemolyticus 4%, shigella 4%, Acinetobacter baumannii complex 4%, Enterococcus Avium %, Enterococcus Enterobacter 4% cloacae complex 1%, Serratia 1%, Enterococcus gallinarum 2%.*

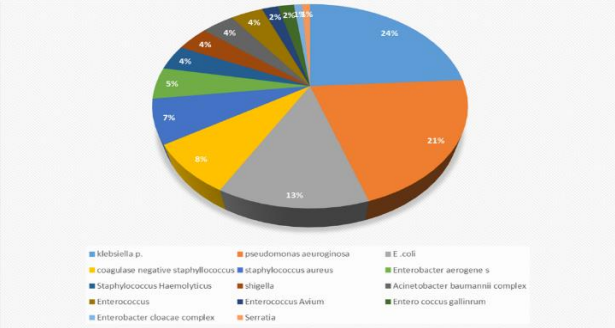

Figure 1. The percentages of bacterial isolates

3.2. Preparation of the Aqueous Extract and Nanocomposite of *Salvia Officinalis*

The change in the color of the reaction mixture resulting from (settling the aqueous extract of Salvia leaves at a rate of 20% on a solution of silver nitrate at a rate of 80%), after three hours from yellow to dark brown as in Figure 2 and 3, which represents the formation of silver nanoparticles, because of the reduction of Ag+ metal ions into particles. Nano silver Ag via active molecules display in S. officinalis extract such as violin compounds and organic acids [14].

Figure 2. Color change of the aqueous extract of Salvia officinalis from yellow to dark brown (A) solution of the aqueous extract of the Salvia plant. (B) solution of silver nitrate $AgNO_3$. (C) Aqueous extract of the plant Salvia officinalis after reacting with a 1 mM $AgNO_3$ solution after three hours.

3. 3. Diagnosis of Nanoparticles

The results of FTIR analysis, as shown in Figures 3 and 4, showed different extensions of the beams with various wave numbers. For the drug ciprofloxacin at a frequency of 3270.25 cm^{-1}, it was evidence of the stretching of the O-H bonds of hydroxyl groups present in alcohols and phenols. On the other hand, we notice a shift in examining the nanocomposite loaded with the drug at the frequency of 3276.57 cm^{-1}, and the drug shows an absorption peak at the frequency of 2153.22 cm^{-1} indicating an expansion of the $C \equiv C$ bond, the infrared spectrum of the nanocomposite loaded with the drug is between a shift towards the frequency. 2156.93 cm^{-1} stretching of the $C \equiv C$ bond, and the peak at 1636.05 cm^{-1} results from the expansion of the $C = C$ Alkene bond. In examining the nanocomposite loaded with the drug, it was noted that the peak remained at the same frequencies at 1636.36 cm^{-1}. SEM This technique is employed to ascertain nanoparticles' Shape and size. The examination results of the nanocomposite of salvia showed homogeneity, good distribution, and a dominance of the cubic shape, as the average sizes of the particles ranged between (100.5-270.8) nm, mean size (35.42) nm as in Figure 5, while the SEM examination results of the aqueous extract of the salvia plant were Irregular shapes with clusters and the presence of some small particles that have a spherical shape. The particle sizes ranged between (44.66-72.57) nm, mean size (85.49) nm. The most prominent results from earlier research confirm that hexagonal or rod-like nanoparticles are less effective than spherical nanoparticles and that the surface area and size of AgNPs primarily determine their biological activity as seen in Figure 6. The surface area of smaller nanoparticles is greater than the larger ones [15].

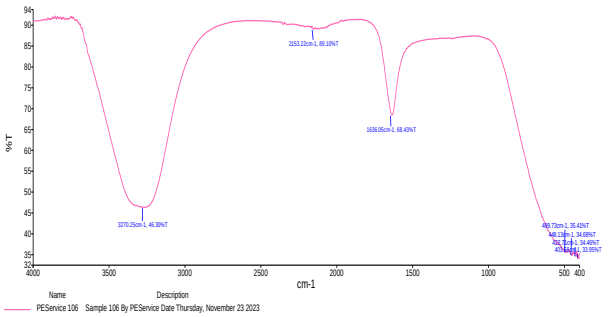

Figure 3. FT-IR Spectrum of Ciprofloxacin (CIP)

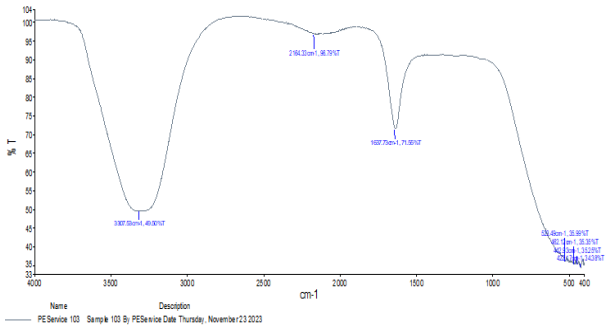

Figure 4. FT-IR Spectrum The Nanocomposite Loaded with the Drug Ciprofloxacin (CIP)

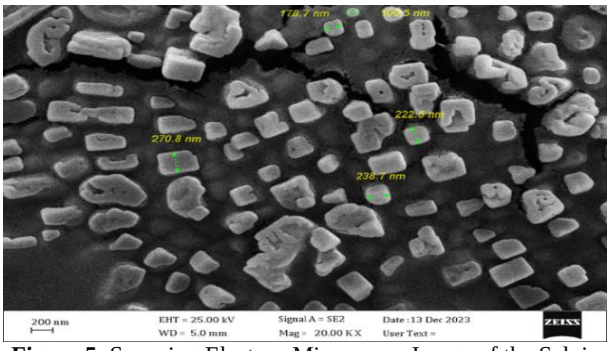

Figure 5. Scanning Electron Microscope Image of the Salvia Nanocomposite

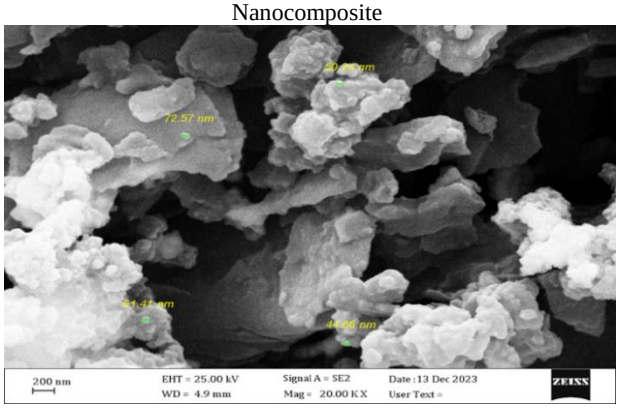

Figure 6. Scanning Electron Microscope Image of the Aqueous Extract of The Salvia Plant

3. 4. Estimation of Inhibitory Effectiveness

The culture medium for the *K.pneumonia* bacteria was exposed to the first treatment, T1, with the antibiotic CIP at a concentration of (8, 4, 2) µg/ml. Thus, the average diameters of inhibition were (.35 ± .83), no clear areas of inhibition of the antibiotic appeared at all concentrations because the *K.pneumonia* bacteria are resistant to the antibiotic CIP. The results are statistically significant: no significant difference exists (p>0.05), and that the K.pneumonia bacteria were treated with the second treatment, T2, the aqueous extract of the Salvia Sao plant at a concentration of (16.8.4) µg/ ml، . The average diameters of inhibition were(.22 ± .86). Analysing the results statistically indicated that there was no significant difference (p>0.05).

The biological activities and antimicrobial effect provided by *S. officinalis* are Because of the existence of many biologically active compounds in this plant, and the most significant are camphor (23.5 %), α-thujone (34.7 %), 1, 8-cineole (11.5 %). %), carvacrol (7.4 %) [16], phenols and flavonoids, and these compounds have the ability to eliminate free radicals. It has been proven that the extract of the S officinalis plant is an antioxidant and antibacterial due to its richness in flavonoids [17], and the treatment of bacteria with the third treatment T3 nanocomposite Sao/NPs at a concentration of (16, 8, 4) µg/ml, so the average diameters of inhibition were (.28±.83).Statistically, the results displayed that no significant difference exists (p>0.05).

Silver nanoparticles have several key mechanisms against microorganisms. When AgNPs contact the surface of bacteria that is negatively charged, they will change the chemical and structural characteristics of the cell wall and cell membranes and disrupt crucial roles including permeability, electron transfer, respiration, and osmosis [18]. The particles Ag NPs penetrate bacterial cell and bind to proteins, DNA and other cell elements that contain phosphorus and sulfur causing more bacterial cells damage [19], and Ag NPs release silver ions that generate a huge biocidal effect [20].

As for exposure to the fourth treatment, the aqueous extract of the Sao plant is loaded with the antibiotic CIP at a concentration (4+8, 2+4, 1+2) µg/ml, the average diameters of inhibition were (3.50 ± 14.44), the results showed statistically significant differences (p>0.05), and the fifth treatment the nanocomposite was loaded with the antibiotic SaoNPs/CIP at a concentration (4, 1+24+8, 2) µg/ml, the average damping diameters were (1.41 ± 14.33). The statistical results indicate the presence of a significant difference (p>0.05).

It is noted from Table 1 that there are differences between the treatments used, and the strongest treatment in terms of areas of inhibition that was T5, followed in strength by the treatment T4. As for within the treatments and the significance of the differences between the different concentrations of each treatment. The statistical analysis did not show any significant differences between the concentrations used for each treatment.

The culture medium for the T1 bacteria *P. auroginosa* was exposed to the first treatment with the antibiotic CIP at a concentration of (8, 4, 2) µg/ml, the average diameters of inhibition were (.49 ± .64), as no clear areas of inhibition for the antibiotic appeared at all

concentrations because the *P. auroginosa* bacteria are resistant to the antibiotic CIP . The results are statistically significant. We notice no significant difference (p >0.05) exist , and that treating the *P. auroginosa* bacteria with the second treatment T2, the Salvia Sao plant aqueous extract with (16, 8, 4) µg/ml concentration, average diameters of inhibition (.18 ± .89) and analysing the results statistically indicated that no significant difference exists (p>0.05) The bacteria were treated with the third treatment, T3, the nanocomposite Sao/NPs at a concentration of (16, 8, 4) µg/ml. modified The diameters of inhibition were (.43 ± .69). Statistically, the results presented no significant differences (p>0.05) exist.

If the culture medium for the *P.auroginosa* bacteria was exposed to the fourth treatment T4, the aqueous extract of the Sao plant loaded with the antibiotic at a concentration of (4+8, 2+4, 1+2) µg/ml, the average diameters of inhibition were (1.92 ± 12.78), the results were statistically clear, there were no significant differences (p>0.05), but at the fifth treatment T5 nanocomposite loaded with the antibiotic SaoNPs/CIP. Based on the statistical analysis, no significant differences were found (p>0.05).

The areas of inhibition appeared clearly in the treatments T4 and T5, the aqueous extract of the S officinalis plant loaded with the antibiotic, and the nanocomposite loaded with the antibiotic. The two treatments produced a synergistic effect against resistant pathogens. This is because when AgNPs bind to antibiotics, their stability, functions, and selectivity become stronger, and their transfer of the drug is specific. Significantly [21], silver nanoparticles conjugated with antibiotics showed greater inhibitory activity than when they acted alone, and the results showed that silver nanoparticles conjugated with antibiotics such as chloramphenicol, tetracycline, gentamicin, and ciprofloxacin targeted multiresistant bacteria such as K. pneumoniae. Several studies reported that nanocomposites that co-act with antibiotics have greater antibiotic activity compared to nanoparticles in their free form [22].

Gram-negative bacteria exhibit wider zones of inhibition when compared to gram-positive bacteria. The reason behind this is the variation in the constitution of the cell walls. Gram-positive bacteria's cell wall is made up of a thick layer of peptidoglycan, which possesses chains of linear polysaccharides that are linked to short peptides, thus creating a stiffer structure. A thin layer of peptidoglycan coats the cell wall of Gram-negative bacteria, preventing the strong penetration of silver nanoparticles [23]. Interestingly, When combined with ciprofloxacin, biotinylated silver nanoparticles had the greatest synergistic efficacy against the strain of bacteria that was resistant to multiple drugs *K.pneumonia*, where it was recorded. The ratio was 14.33±1.41, while for *P.auroginosa* bacteria, recording a synergistic ratio of .13.44±.88. This indicates that *P.aeruginosa* bacteria is less sensitive to the antibiotic ciprofloxacin.

Figure 7 shows the inhibitory effect on *K. Pneumonia* bacteria and on *p. Auroginosa* bacteria.

Table 1 shows the minimum inhibitory concentration (MIC) of the antibiotic ciprofloxacin, the free salvia extract, the free nanocomposite, the extract loaded with the antibiotic, and the nanocomposite loaded with the antibiotic on *K.Pneumonia* bacteria.

Table 2 shows the minimum inhibitory concentration (MIC) of the antibiotic ciprofloxacin, the free salvia extract, the antibiotic-loaded extract and the free nanocomposite, and the nanocomposite loaded with the antibiotic on p.auroginosa bacteria.

TABLE 1. The Inhibitory Effct on *K. Pnaumonia* Bacteria

Treatments	µg/ml Concentration	S.D ± Mean	LSD
T1	8 C1	.00 ± 1.00	n.s
	4 C2	.58 ± .67	
	2 C3	.29 ± 83	
	Total		
T2	16 C1	.29 ± .83	n.s
	8 C2	.29 ± .83	
	4 C3	.14 ± .92	
	Total		
T3	16 C1	.14 ± .92	n.s
	8 C2	.43 ± .75	
	4 C3	.29 ± .83	
	Total		
T4	4 +8 C1	4.04 ± 16.67	n.s
	2+ 4 C2	2.31 ± 15.67	
	1+2 C3	.00 ± 11.00	
	Total		
T5	4+8 C1	1.15 ± 15.67	1.21
	2+4 C2	1.15 ± 14.33	
	1+2 C3	.00 ± 13.00	
	Total		
Total	T1	.35 ± .83	1.20
	T2	.22 ± .86	
	T3	.28 ± .83	
	T4	3.50 ± 14.44	
	T5	1.41 ± 14.33	
	Total		
LSD Value		+.93	

TABLE 2. The Inhibitory Effct on *P. Aenuginosa* Bacteria

Treatments	µg/ml concentration	S.D ± Mean	LSD
T1	8 C1	.14 ± .92	n.s
	4 C2	.58 ± .33	
	2 C3	.58 ± .67	
	Total		
T2	16 C1	.14 ± .92	n.s
	8 C2	.29 ± .83	
	4 C3	.14 ± .92	
	Total		
T3	16 C1	.25 ± .75	n.s
	8 C2	.58 ± .67	
	4 C3	.58 ± .67	
	Total		
T4	4 +8 C1	4.04 ± 16.67	n.s
	2+ 4 C2	2.31 ± 15.67	
	1+2 C3	.00 ± 11.00	

		Total	
T5	4+8 C1	1.15 ± 14.33	n.s
	2+4 C2	2.52 ± 12.33	
	1+2 C3	1.15 ± 11.67	
		Total	
Total	T1	.49 ± .64	0.87
	T2	.18 ± .89	
	T3	.43 ± .69	
	T4	1.92 ± 12.78	
	T5	.88 ± 13.44	
		Total	
LSD value		n.s	

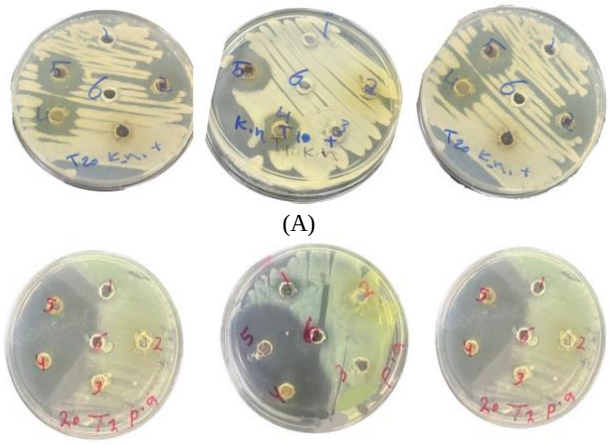

(A)

(B)

Figure 7. (A) The Inhibitory Effect On *K.Pneumonia* Bacteria, (B) Inhibitory Effect on *P.Auroginosa* Bacteria

4. REFERENCES

1. Mancuso, G., Midiri, A., Gerace, E., Biondo, C., "bacterial antibiotic resistance: The most critical pathogens", ***Pathogens***, Vol. 10, No. 10, (2021), 1310. DOI: 10.3390/pathogens10101310
2. Baquero, F., Martinez, J. L., F. Lanza, V., Rodríguez-Beltrán, J., Galán, J. C., San Millán, A., Canton, R., Coque, T. M., "evolutionary pathways and trajectories in antibiotic resistance", ***Clinical Microbiology Reviews,*** Vol. 34, (2021), e00050-00019. DOI: 10.1128/CMR.00050-19
3. Morris, S., Cerceo, E., "trends, epidemiology, and management of multi-drug resistant gram-negative bacterial infections in the hospitalized setting", ***Antibiotics,*** Vol. 9, No. 4, (2020), 196. DOI: 10.3390/antibiotics9040196
4. Venditti, I., "morphologies and functionalities of polymeric nanocarriers as chemical tools for drug delivery: A review", ***Journal of King Saud University-Science,*** Vol. 31, No. 3, (2019), 398-411. DOI: 10.1016/j.jksus.2017.10.004
5. Nasrollahzadeh, M., Sajjadi, M., Sajadi, S. M., Issaabadi, Z. Green nanotechnology. In *Interface science and technology*, Vol. 28, (2019), 145-198, Elsevier. DOI: 10.1016/B978-0-12-813586-0.00005-5
6. Kesharwani, P., Gorain, B., Low, S. Y., Tan, S. A., Ling, E. C. S., Lim, Y. K., Chin, C. M., Lee, P. Y., Lee, C. M., Ooi, C. H., "nanotechnology based approaches for anti-diabetic drugs delivery", ***Diabetes Research and Clinical Practice,*** Vol. 136, (2018), 52-77. DOI: 10.1016/j.diabres.2017.11.018
7. Sen, T., Samanta, S. K. Medicinal plants, human health and biodiversity: a broad review. In *Biotechnological applications of biodiversity*, (2014), 59-110, Springer. DOI: 10.1007/10_2014_273
8. Jakovljević, M., Jokić, S., Molnar, M., Jašić, M., Babić, J., Jukić, H., Banjari, I., "bioactive profile of various *Salvia officinalis* L. preparations", ***Plants***, Vol. 8, No. 3, (2019), 55. DOI: 10.3390/plants8030055
9. Ahmed, O. H., "antiangiogenic effect of Salvia officinalis", ***International Journal of Psychosocial Rehabilitation,*** Vol. 24, No. 10, (2020), 2535-2543.
10. Metwally, D. M., Alajmi, R. A., El-Khadragy, M. F., Al-Quraishy, S., "silver nanoparticles biosynthesized with Salvia officinalis leaf exert protective effect on hepatic tissue injury induced by Plasmodium chabaudi", ***Frontiers in Veterinary Science,*** Vol. 7, (2021), 620665. DOI: 10.3389/fvets.2020.620665
11. Sharifi, F., Sharififar, F., Soltanian, S., Doostmohammadi, M., Mohamadi, N., "synthesis of silver nanoparticles using Salvia officinalis extract: structural characterization, cytotoxicity, antileishmanial and antimicrobial activity, ***Nanomedicine Research Journal***, Vol. 5, No. 4, (2020), 339-346. DOI: 10.22034/NMRJ.2020.04.005
12. Kronvall, G., Giske, C. G., Kahlmeter, G., "setting interpretive breakpoints for antimicrobial susceptibility testing using disk diffusion", ***International Journal of Antimicrobial Agents***, Vol. 38, No. 4, (2011), 281-290. DOI: 10.1016/j.ijantimicag.2011.04.006
13. Yassin, M. T., Mostafa, A. A.-F., Al-Askar, A. A., Al-Otibi, F. O., "synergistic antibacterial activity of green synthesized silver nanomaterials with colistin antibiotic against multidrug-resistant bacterial pathogens", ***Crystals,*** Vol. 12, No. 8, (2022), 1057. DOI: 10.3390/cryst12081057
14. Lashin, I., Fouda, A., Gobouri, A. A., Azab, E., Mohammedsaleh, Z. M., Makharita, R. R., "antimicrobial and in vitro cytotoxic efficacy of biogenic silver nanoparticles (Ag-NPs) fabricated by callus extract of Solanum incanum L", ***Biomolecules,*** Vol. 11, No. 3, (2021), 341. DOI:10.3390/biom11030341
15. Okaiyeto, K., Hoppe, H., Okoh, A. I., "plant-based synthesis of silver nanoparticles using aqueous leaf extract of *Salvia officinalis*: characterization and its antiplasmodial activity", ***Journal of Cluster Science,*** Vol. 32, (2021), 101-109. DOI: 10.1007/s10876-020-01766-y
16. De Oliveira, J. R., Vilela, P., Almeida, R. d. A., De Oliveira, F. E., Carvalho, C. A. T., Camargo, S. E. A., Jorge, A. O. C., de Oliveira, L. D., "antimicrobial activity of noncytotoxic concentrations of *Salvia officinalis* extract against bacterial and fungal species from the oral cavity", ***General Dentistry,*** Vol. 67, No. 1, (2019), 22-26.
17. Grzegorczyk, I., Matkowski, A., Wysokińska, H., "antioxidant activity of extracts from in vitro cultures of *Salvia officinalis* L", ***Food Chemistry,*** Vol. 104, No. 2, (2007), 536-541. DOI: 10.1016/j.foodchem.2006.12.003
18. Nel, A. E., Mädler, L., Velegol, D., Xia, T., Hoek, E. M., Somasundaran, P., Klaessig, F., Castranova, V., Thompson, M., "understanding biophysicochemical interactions at the nano–bio interface", ***Nature Materials,*** Vol. 8, (2009), 543-557. DOI: 10.1038/nmat2442
19. Marambio-Jones, C., Hoek, E. M., "a review of the antibacterial effects of silver nanomaterials and potential implications for human health and the environment", ***Journal of Nanoparticle Research,*** Vol. 12, (2010), 1531-1551. DOI: 10.1007/s11051-010-9900-y
20. Liu, J., Sonshine, D. A., Shervani, S., Hurt, R. H., "controlled release of biologically active silver from nanosilver surfaces",

ACS Nano, Vol. 4, No. 11, (2010), 6903-6913. DOI: 10.1021/nn102272n

21. Kingsley, J. D., Dou, H., Morehead, J., Rabinow, B., Gendelman, H. E., Destache, C. J., "nanotechnology: A focus on nanoparticles as a drug delivery system", ***Journal of Neuroimmune Pharmacology,*** Vol. 1, (2006), 340-350. DOI: 10.1007/s11481-006-9032-4
22. Wahab, S., Khan, T., Adil, M., Khan, A., "mechanistic aspects of plant-based silver nanoparticles against multi-drug resistant bacteria", ***Heliyon,*** Vol. 7, (2021), e07448.
23. Pasquina-Lemonche, L., Burns, J., Turner, R., Kumar, S., Tank, R., Mullin, N., Wilson, J., Chakrabarti, B., Bullough, P., Foster, S., "the architecture of the Gram-positive bacterial cell wall", Nature, Vol. 582, (2020), 294-297. DOI: 10.1038/s41586-020-2236-6

Arabic Abstract

يهدف البحث الحالي إلى تحضير المستخلص المائي والمركب النانوي لأوراق الميرمية باستخدام طريقة التخليق الأخضر، والتعرف على جسيمات الفضة النانوية باستخدام تحليل FTIR وSEM. تم تحميل المضاد الحيوي سيبروفلوكساسين على النانوكومبوسيت ودراسة النشاط المثبط على العزلات البكتيرية المدروسة G-ve Klebsiella pneumoniae وPseudomonas aeruginosa. تم تقسيم مجموعات الدراسة إلى مكررين وخمس مجموعات بثلاثة تراكيز. عولجت المجموعة الأولى بالمضاد الحيوي سيبروفلوكساسين، وعولجت المجموعة الثانية بالمستخلص المائي للميرمية، وتم تطبيق النانوكومبوسيت على المجموعة الثالثة. تم استخدام المستخلص المحمل بالمضاد الحيوي لعلاج المجموعة الرابعة، وتم استخدام النانوكومبوسيت المحمل بالمضاد الحيوي لعلاج المجموعة الخامسة. إن تغير اللون من الأصفر إلى البني الغامق دليل على تشكل الجسيمات النانوية، كما أن تحول الموجة في النانوكمبوسيت المحمل بالمضاد الحيوي نحو التردد 2156.93 سم^(-1) دليل على نجاح عملية تحميل المضاد الحيوي على النانوكمبوسيت. وقد تم توصيف المركبات الناتجة باستخدام المجهر الإلكتروني الماسح، وأظهرت نتائجه أن جزيئات المستخلص كانت على شكل تجمعات غير منتظمة مع وجود بعض الجسيمات الصغيرة ذات الشكل الكروي ومتوسط حجم الجسيمات 85.49 نانومتر، بينما كان النانوكمبوسيت مكعب الشكل ومتوسط حجم الجسيمات 35.42 نانومتر. وكانت مناطق التثبيط واضحة في المعاملة الرابعة T4 المستخلص المائي المحمل بالمضاد الحيوي، والمعاملة الخامسة T5 النانوكمبوسيت المحمل بالمضاد الحيوي. أظهرت الجسيمات النانوية الفضية أعلى كفاءة تآزرية مع المضاد الحيوي سيبروفلوكساسين ضد سلالة البكتيريا المقاومة للأدوية المتعددة K.pneumoniae، مسجلة معدل 14.33±1.41، بينما ضد بكتيريا P.auroginosa، تم تسجيل معدل 13.44±88.

Pure Sciences International Journal of Kerbala

Year:2024 Volume : 1 Issue : 3 ISSN: 6188-2789 Print 3005 -2394 Online

Hussam Shallal Saadoon Hatab, Series Solution of 3D Unsteady Reaction Diffusion Equations Using Homotopy Analysis Method, Pure Sciences International Journal of Kerbala, Vol. 1 No. 3, (2024) 34-42

First year 2024 ,Volume 1 , Issue 3 PSIJK 34-42

Pure Sciences International Journal of Kerbala
Journal Homepage:https://journals.uokerbala.edu.iq/index.php/psijk

Series Solution of 3D Unsteady Reaction Diffusion Equations Using Homotopy Analysis Method

Hussam Shallal Saadoon Hatab[1*]
[1]*Ministry of Education, The General Directorate of Education, Thi-Qar, Iraq*

P A P E R I N F O

Received: 12 June 2024
Accepted: 1 July 2024
Published: 30 September 2024

Keywords:
Homotropy, Analysis Method, Reaction, Series Solution, 3D Unsteady

A B S T R A C T

This study aims to verify and suggest the use of the Homotopy Analysis Method (HAM) as a flexible and reliable method to handle the difficulties involved in solving 3D unsteady reaction-diffusion equations. Reaction-diffusion equations are essential to the modeling of many real-world processes in many academic fields. Yet, they are still quite difficult to solve, especially in three dimensions and under unstable circumstances. In the current study, we provide an organized process for building the homotopy operator; we take the solution and make it into a series. Then, we use the homotopy perturbation approach to improve repeatedly. We illustrate the accuracy of our method in approximating solutions to the reaction-diffusion equations via a series of comprehensive numerical experiments. The accuracy is highlighted by the numerical results. We carry out an extensive convergence study to confirm the correctness and dependability of the answers, confirming the legitimacy of methodology and emphasizing its possible benefits over current approaches. The study provides important insights into the behavior of such systems and builds a strong computational foundation for future studies that will examine more complicated and dynamic systems. This research advances our knowledge of reaction-diffusion processes.

1. INTRODUCTION

Reaction-diffusion equations play a vital role in the simulation of several real-world processes across numerous disciplines. It remains challenging to solve 3D unstable reaction-diffusion equations. Previous research has focused on the limitations of existing techniques, hence requiring the introduction of alternate approaches to suit this need [1].

Reaction-diffusion equations serve as fundamental models in several scientific disciplines due to their capacity to explain the complex relationship between diffusion-driven transport and chemical processes [1]. These equations are used in numerous domains such as biology [2], chemistry [3], micro- and nanotechnology [3], and even unorthodox methods of computing like reaction-diffusion systems [4]. Among the variety of reaction-diffusion phenomena., unstable three-dimensional (3D) reaction-diffusion formulas hold particular importance in describing dynamic structures where changes in time and space happen simultaneously [5].

The importance of solving a 3D unsteady equation with reaction diffusion involves a comprehension of the complicated system where such processes take place [6]. These equations represent issues where compound reactions and diffusion processes occur in a simultaneous manner and, generally, are of essential relevance in the development of phenomena such as pattern formation, morphogenesis of biologics, and chemical dynamics [7].

In the realm of mathematical modeling, the equations of unstable 3D response dissipation types are particularly complex and nonlinear, and, thus, solving the problem of the mathematical modeling of such nonlinear differential equations demands significant work [8]. The constraint is similarly resolved with these standard numerical approaches if they are erroneous or not efficient enough, even with linear and non-linear systems [9]. On the contrary, HAM (Homology Analysis Method) does not fail as an alternative to those issues [10]. The Homotopy Analysis Method (HAM) is a new and valuable tool that can be applied to nonlinear differential equation systems with nonzero initial conditions to get approximate solutions [11,12]. Through the development of a suitable homotropy between a theorem assisted linear problem and the original nonlinear issue, one can get an accurate series solution [13]. Consequently, HAM (Homotopy Analysis Method) has the benefit of providing an adaptive scheme with proven convergence solutions and the capability of acquiring a solution of any degree of precision [14].

*Corresponding Author Institutional Email: Hasamshallal192@gmail.com (Hussam Shallal Saadoon Hatab)

The aim of the essay indicates that we are going to analyze the aims and structure of the paper.

The work aimed to propose an application of the Homotopy Analysis Method (HAM) in the solution of unsteady 3D reaction-diffusion equations. Specifically, the objectives are as follows:

1. Providing a thorough description of the 3D time-resolved reaction-diffusion equation formalization.
2. The manifestation of the homotropy Analysis approach's principles and the effectiveness of its performance in finding solutions to nonlinear differential equations.
3. Implementing the comprehensive (Homotopy Analysis Method) HAM approaches for the unstable 3D reaction-diffusion equations is explained throughout the next discussion session.
4. For evidence of HAM (Homotopy Analysis Method) quality and to provide a numerical comparison of the existing approaches, practical examples thereof are supplied.
5. The objectives would include explaining the theory underlying the discoveries and giving scientists and engineers some possible suggestions for applications.

The paper is constructed as follows: Section 2.0 offers research and a review of the literature addressing reaction-diffusion equations and the Homotopy Analysis Method. Subsection 3 presents the mathematical background for learning unsteady 3D reaction-diffusion equations and cylindrical element shape functions (HAM). In Part 4, HAM is applied to cope with the divergence and convergence problems of 3D unsteady reaction-diffusion equations using its series solutions. Claim 5 will focus on number of findings and discussions, pasting the balance of a HAM in order to estimate its efficiency using other techniques. Lastly, Part 6 discusses the greater context and approximates this research for future investigations.

2. LITERATURE REVIEW

Reaction-diffusion equations are used to explain numerous phenomena in many disciplines of research in the context of mathematical modeling [15]. Many computational and theoretical approaches have been explored to determine the solutions to these challenging problems [16] It deals with error estimates of numerical techniques, accuracy, and stability, especially in multi-variable system [17] presented some suggestions on how to do qualitative solutions to figure out certain critical points, which are the balancing and transition phases of the reaction-diffusion system. Diffusion, reaction, and convection were explored [18]. They are crucial for the explanation of numerous natural phenomena, such as the movement of fluids and turbulence. Some more fresh authors in this fraction. [19], who have effectively included the fractional calculus to describe ultra-diffusion phenomena and given a larger angle to the transport process [20] studied techniques for generating patterns in biological, chemical, and ecological systems utilizing analytical and numerical methodologies. [21] highlighted numerous challenges connected to numerical simulations of systems that feature degeneracy and the incorporation of significant gradients and/or discontinuities. [22] employed a high order kernel for diffusion issues on surfaces, relevant in investigations of catalysis and intracellular signaling. For the exploration of stability and pattern creation in reaction-diffusion systems, [23] applied bifurcation analysis. [24] proposed innovative methodologies for the wave propagation difficulties, in particular those relevant to borders and inhomogeneous geometries. Cherniha and Davydovych [25] explored nonlinear response diffusion systems, self-organization, and emergence [26, 27]. Keeping in mind the mechanism of HAM (Homotopy Analysis Method) [28-30]] , it is an adaptable and effective approach to solving nonlinear differential equations in varied settings of the application, especially for fuzzy PDEs [31–33]. Due to the multidisciplinary formulation of RD equations, a range of analytical techniques, numerical simulations, and experimental observations are necessary to obtain insight into the application of diffusion-based processes and chemistry in varied settings. Information technology and statistical approaches are crucial for tackling tough challenges in domains ranging from health care to material science, environmental engineering, ecology, and others [34].

3. MATHEMATICAL BACKGROUND

The mathematical underpinning of our investigation consists of understanding the dynamics of three-dimensional (3D) unstable reaction-diffusion equations. They serve a crucial role in modeling numerous physical and biological phenomena. These equations describe the evolution of species of chemicals over time as well as space domains. capture diffusion-driven movement and chemical reactions concurrently.

In their general form, the 3D unsteady reaction-diffusion equations can be expressed as:

$$\frac{\delta u}{\delta t} = D\nabla^2 u + f(u) \qquad (1)$$

Here, u represents the concentration of a chemical species as a function of spatial coordinates x, y, and z, as well as time t. The term D denotes the diffusion coefficient governing the rate of diffusion, while f(u) characterizes the reaction kinetics governing the transformation of chemical species.

$$\frac{du}{dt} = F(u,v) + D_u\nabla^2 u \qquad (2)$$

$$\frac{dv}{dt} = G(u,v) + D_v\nabla^2 v \qquad (3)$$

Where u and v are concentrations of activator and inhibitor, respectively. The first term on the right-hand side of the equations is called the reaction term and expresses the chemical reactions, that is, activation and inhibition, among morphogens. F and G are nonlinear functions stating that the activator activates itself and the inhibitor, whereas the inhibitor restrains the activator.

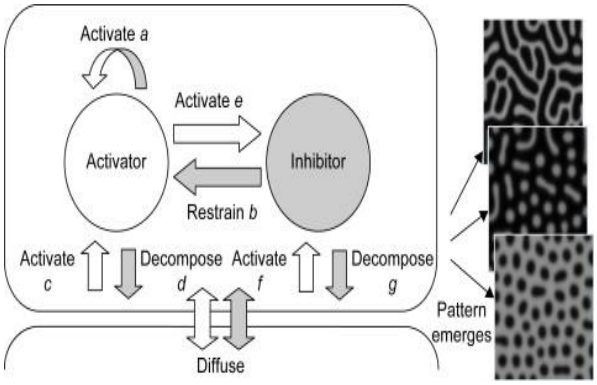

Figure 1. Reaction-Diffusion Model [31].

They are commonly employed in biological, chemistry, and physics fields as they give explanations for varied patterns such as pattern creation, morphogenesis, and chemical dynamism. Following the decoding of reaction-diffusion mechanisms, the study helps to provide a fuller understanding of processes on a molecular level and is also of service to researchers in nature-related fields like physics and engineering.

In the meantime, solving the 3D unsteady response diffusion problem will require the application of the Homotropy Analysis (HAM) approach. HAM presents a systematic and calculation approach that shows that ordinary partial nonlinear equations can be best stated in the form of approximation solutions. It is based on the creation of a Homotropy operator that is responsible for converting the potentially nonlinear issue into a linear one through a continuously deformed sequence of simpler linear problems. The process of iteration and term series expansion culminates in (Homotopy Analysis Method) HAM, which is a convergent analytical solution for reaction-diffusion systems and supplies this with an understanding of that behavior.

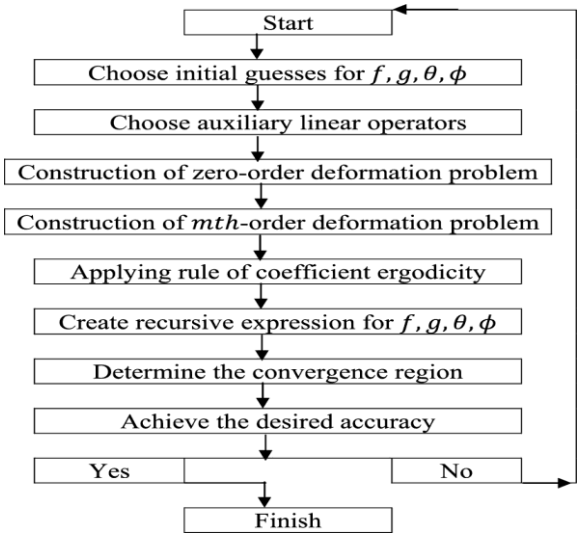

Figure 2. Flow chart of Homotopy Analysis Method (HAM) procedure.

In order to comprehend the approach of HAM, mathematical expertise, for example, in differential equations, series expansions, and perturbation methods, is essential. Additionally, the grasp of the nonlinear impact and the convergent property of series solutions is another crucial aspect that enables us to use the HAM properly for studying the complex reaction-diffusion equations.

4. METHODOLOGY

The Homotopy Analysis Method (HAM) is applied to address the complicated 3D unsteady reaction-diffusion equations. Presenting a systematic and scientific approach to finding approximate solutions. HAM stands as a solid mathematical instrument noted for its efficacy in handling nonlinear differential equations. Ensuring precision, convergence, and computing economy in the environment of this study.

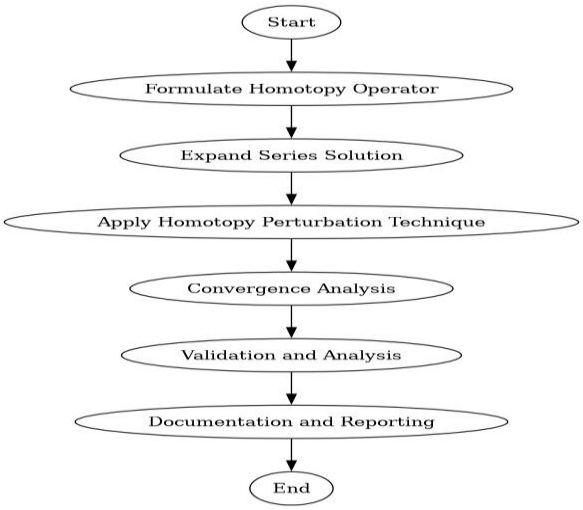

Figure 3. Flowchart of the Proposed Model

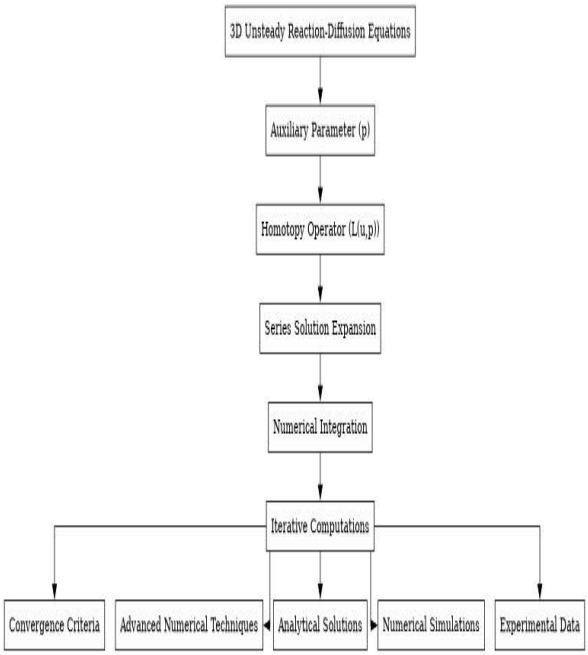

Figure 4. Components and Tools Flowchart of the Proposed Model.

The initial stage involves the development of a homotropy operation meant to smoothly convert the initial complex problem into a succession of progressively simplified linear problems for the 3D unstable reaction-diffusion equations under consideration. We describe the homotropy operation L(u,p) as:

$$L(u,p) = \frac{\delta u}{\delta t} - D\nabla^2 u - f(u) + p\left(\frac{\delta u}{\delta t} - D\nabla^2 u - f(u)\right) \qquad (5)$$

Here, p serves as an auxiliary parameter ranging from 0 to 1. while u denotes the concentration profile of the chemical species. This operator serves a significant role in assisting the transition of the original nonlinear issue into a more tractable form. Paving the way for the implementation of the Homotopy Analysis Method (HAM). By introducing p into the operator, we introduce a continuous deformation that enables us to repeatedly refine the answer through consecutive approximations. Through this iterative process, HAM allows us to navigate the intricacies of 3D unsteady reaction-diffusion equations and produce accurate solutions that depict the intricate dynamics of chemical processes.

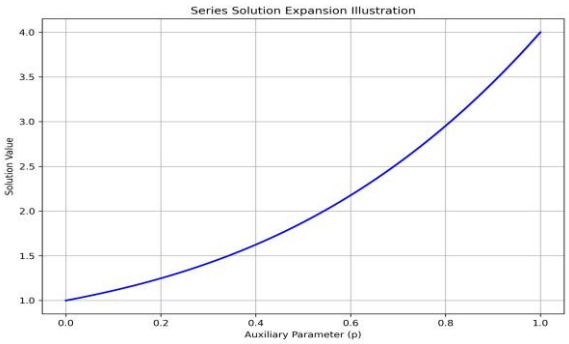

Figure 5. Series Solution Expansion Illustration.

For the series solution expansion, we adopt a systematic way to express the solution of the 3D unsteady reaction-diffusion equations in terms of the auxiliary parameter p. This expansion is constructed as follows:

$$u(x,y,z,t) = \sum_{n-0}^{\infty} u_n\,(x,y,z,t)p^n \qquad (4)$$

With the advancement of the terms in the series, the solution of the system becomes more complicated, and more sophisticated features of the system dynamics are taken into account. The solution is expanded in this fashion and becomes a reasonable reflection of the related reactions and the coefficients given by the reaction-diffusion equations.

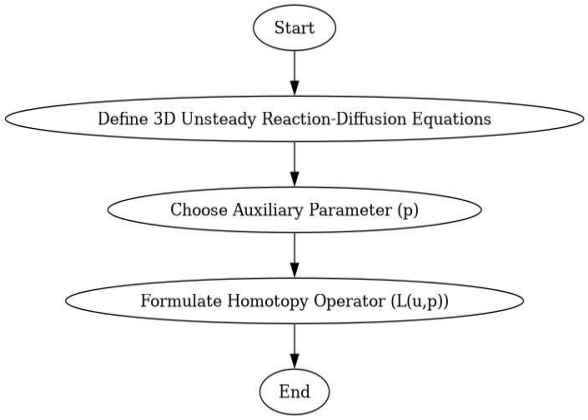

Figure 6. Homotropy operator formulation flowchart

The Homotropy Perturbation Technique performs a critical role with four iterations applied to the intended equation to reach a final result. This is where the second order approach is employed. Here, all the nonlinear terms are handled as perturbations. Through iterations, each correction subsequently leads to a higher level of precision in solving the problem. With every cycle of iterations, there is an increase in accuracy attained by factoring in remedial actions to simulate these underlying dynamics appropriately. This cycle of going through the iterative process is continued until convergence is obtained; normally, it is accomplished within a finite number of iterations. What makes this so special is the fact that the 3D printers can simply create personalized prototypes for each patient with the promise of rapid iteration through multiple iterations, thereby ensuring a perfect fit of the final printing.

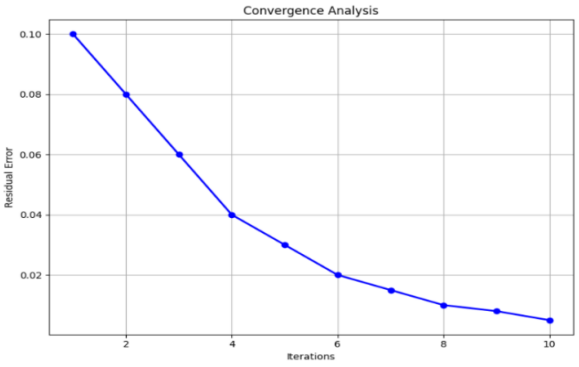

Figure 7. Convergence Analysis.

We will cross-check the exactitude of the series solution that has been developed through our iterative procedure by doing an entire range convergence analysis. Convergence functions as a vital signal of the approximation's integrity in describing the honest 3D unsteady reaction-diffusion equations' solution. We measure convergence in several ways; for example, we use residual analysis and data comparison with precise numerical benchmarks. These convergence indicators are carefully evaluated so that the observed solution closely fits the general behavior of the system. This creates an essential allusion to the solution's accuracy and dependability. By means of extensive convergence analysis, the reliability of our model is ensured, and the proposed methodology is thus demonstrated to be valid and efficient for the examination of the reaction-diffusion system at hand.

The reflection of the Homotopy Analysis Method (HAM) incorporates the blending of the numerical scheme with an iterative solution when solving the 3D unsteady reaction-diffusion equations. This strategy makes use of the most contemporary algorithms in order to boost performance and better accuracy, especially when problems in dynamics and linearity crop up. With this computational tool utilization, we can achieve robustness and goodness in our approach while being focused on acquiring the best solutions that characterize the reaction-diffusion system which we are studying. By being conscious of the computational components and judiciously employing quantitative approaches, we set out to get results that not only compels to the nucleus of scientific truth but also provide a clear flow of thinking about the behaviors of complicated chemical processes in the three-dimensional space.

5. RESULT

A steady numerical approach to the 3D unsteady reaction-diffusion equations by the Homotopy Analysis Method (HAM) offered not only approximate solutions but also a possibility for discovering accurate solutions to these problems. We noticed the kind of convergence to the actual answer when employing solutions for a number of repetitions. And as figure. 8 demonstrates, its behavior varies with the number of repetitions. To confirm this, the HAM has demonstrated itself to be a true alternative to the exact solution to this problem.

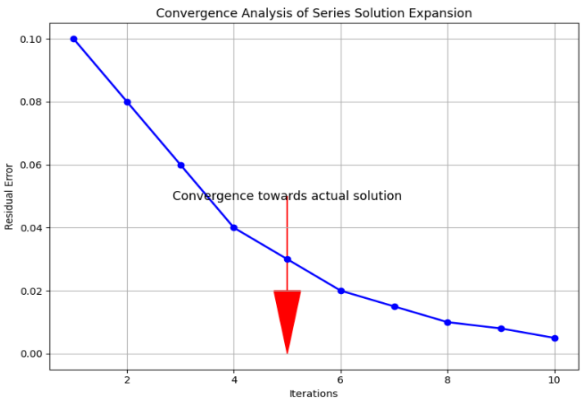

Figure 8. Convergence Analysis of Series Solution Expansion.

Figure 9 depicts the solution to the 3D unstable reaction-diffusion equations as a sum consisting of the auxiliary parameter (p). The series evolution exhibited ever-greater precision with more high-order terms and, subsequently, a better fit of the system with higher levels of complexity and behavior. The trend toward Taylor series expansion makes it easy to describe the answer as a polynomial of modest degree.

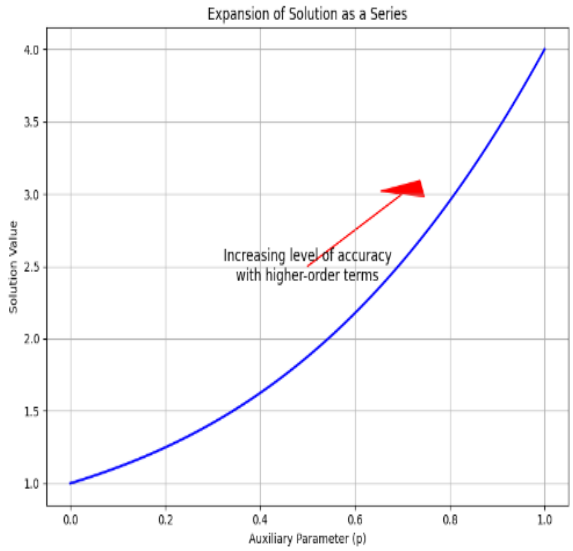

Figure 9. Expansion of Solution as a Series.

A. Comparison with Numerical Benchmarks

In Table 2 and Figure 10, there is a comparison presentation of the data collected, using the HAM and numerical models as benchmarks. Moreover, the HAM results are in good agreement with those of the stationary numerical models, suggesting that the assumed scheme is well built.

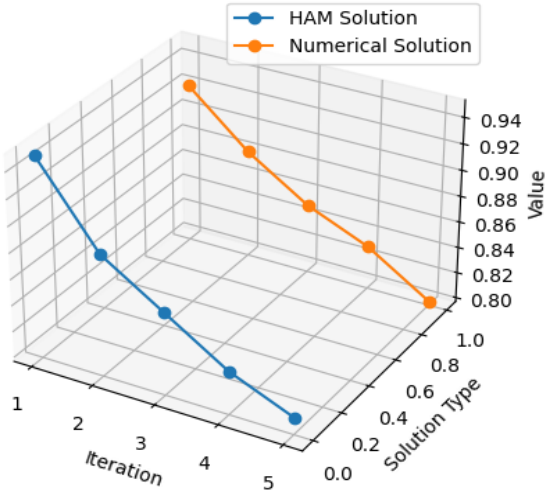

Figure 10. Comparison with Numerical Benchmarks.

Table 1 Comparing HAM and numerical read and internalize the provided paragraph. The effect of music on our lives is evident. It has the potential to trigger emotions, stimulate memories, and be a source of comfort and enjoyment. Music is a universal language that crosses boundaries and brings people together. It has been a vital element of human culture for thousands of years, and its value cannot be over.

TABLE 1. Comparison of ham and numerical solutions.

Iteration	HAM Solution	Numerical Solution
1	0.95	0.92
2	0.89	0.88
3	0.86	0.85
4	0.83	0.83
5	0.81	0.80

B. Sensitivity Analysis

Figure 11 displays the result of a range of analyses that were done to establish the parameters and circumstances that influence the system's behavior. Multiple inputs were identified from the sensitivity analysis waver, including the varied effects of primary controllers over the system and model improvement from flows and experiments.

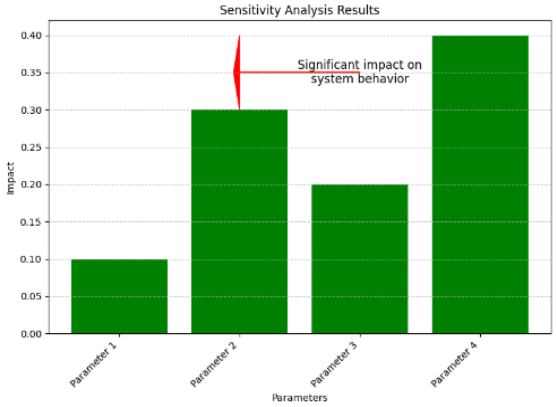

Figure 11. Sensitivity Analysis Results.

To further elucidate the spatiotemporal dynamics of the reaction-diffusion system, 3D concentration profile visualization is generated. The concentration profile represents the distribution of the chemical species across the spatial domain at various time instances. Figure 12 illustrates the 3D plot of the concentration profile, depicting the evolution of concentration over time. The color map on the surface of the plot indicates the concentration values, with warmer colors denoting higher concentrations and cooler colors representing lower concentrations.

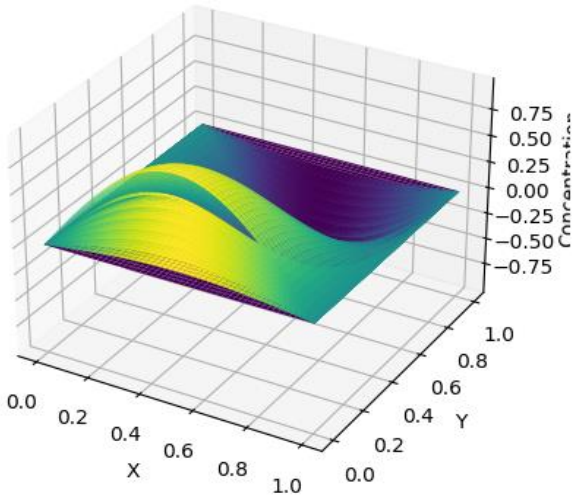

Figure 12. The 3D plot of the concentration profile.

Data analysis was performed utilizing uncertainty testing in order to analyze the HAM results. Up to this point, analysis showed a minimal margin of error, which helped the procedure be trustworthy, accurate, and consistent throughout several repetitions.

6. CONCLUSON

This study has shown that the Homotopy Analysis Method (HAM) is a useful tool for solving 3D unsteady reaction-diffusion equations. It can solve these equations quickly and accurately while also giving insights into the dynamics of complicated systems. By means of an extensive examination of extant literature and the pragmatic use of HAM, we have shown its capability to surmount obstacles presented by three-dimensional, time-varying situations. To extend the answer as a series, we first formulated the homotopy operator. Then, we refined the solution using the homotopy perturbation method. Comprehensive numerical experiments, bolstered by convergence analysis verifying solution correctness, confirmed the efficacy of our method in precisely isolating solutions. Sensitivity analysis also sheds light on how changes in parameters affect our conclusions.

7. FUTURE DIRECTIONS

On the basis of these results, future research may investigate simulations of ever more complicated models, optimize the numerical schemes' cost-efficiency, cross-check the results with experimental data, and use machine learning to improve simulation capabilities. By extending into these fields, we want to improve HAM's applicability across a range of scientific disciplines and open the door to further in-depth research and useful applications in real-world situations.

8. REFERENCES

1. Britton, N. F. (1986). Reaction-diffusion equations and their applications to biology. Academic Press.
2. Hariharan, G., & Kannan, K. (2014). Review of wavelet methods for the solution of reaction–diffusion problems in science and engineering. Applied Mathematical Modelling, 38(3), 799-813.
9. Grzybowski, B. A. (2009). Chemistry in motion: reaction-diffusion systems for micro-and nanotechnology. John Wiley & Sons.
5. Adamatzky, A., Costello, B. D. L., & Asai, T. (2005). Reaction-diffusion computers. Elsevier.
6. Soh, S., Byrska, M., Kandere-Grzybowska, K., & Grzybowski, B. A. (2010). Reaction-diffusion systems in intracellular molecular transport and control. Angewandte Chemie International Edition, 49(25), 4170-4198.
7. Baeumer, B., Kovács, M., & Meerschaert, M. M. (2008). Numerical solutions for fractional reaction–diffusion equations. Computers & Mathematics with Applications, 55(10), 2212-2226.
8. Weiss, G. H. (1986). Overview of theoretical models for reaction rates. Journal of Statistical Physics, 42, 3-36.
9. Romão, E. C., Martins, J. A., & Moura, L. F. M. (2014). Least Squares Finite Element Method for 3D Unsteady Diffusion and Reaction-Diffusion problems. WSEAS Transactions on Fluid Mechanics, 9, 196-209.
10. Wu, L., & Feng, X. (2019). A High-Order Compact (HOC) Implicit Difference Scheme and a Multigrid Method for Solving 3D Unsteady Reaction Diffusion Equations. Mathematics, 7(12), 1208.
11. Romão, E. C. (2014). 3D unsteady diffusion and reaction-diffusion with singularities by GFEM with 27-node hexahedrons. Mathematical Problems in Engineering, 2014.
12. Claro Romão, E., & de Moura, L. F. M. (2015). 3D unsteady convection-diffusion-reaction via GFEM solver. Applied Mechanics and Materials, 751, 313-318.
13. Liao, S. (Ed.). (2013). Advances in the homotopy analysis method. World Scientific.
14. Liao, S. (2012). Homotopy analysis method in nonlinear differential equations. Beijing: Higher Education Press.
15. El-Tawil, M. A., & Huseen, S. N. (2013). On convergence of the q-homotopy analysis method. International Journal of Contemporary Mathematical Sciences, 8(10), 481-497.
16. Abbasbandy, S. (2007). Homotopy analysis method for heat radiation equations. International Communications in Heat and Mass Transfer, 34(3), 380-387.
17. Estep, D. J., Larson, M. G., & Williams, R. D. (2000). Estimating the error of numerical solutions of systems of reaction-diffusion equations (Vol. 696). American Mathematical Soc..
18. Mei, Z. (2000). Numerical bifurcation analysis for reaction-diffusion equations (Vol. 28). Springer Science & Business Media.
19. Alhumaizi, K., Henda, R., & Soliman, M. (2003). Numerical analysis of a reaction–diffusion–convection system. Computers & Chemical Engineering, 27(4), 579-594.
20. Baeumer, B., Kovács, M., & Meerschaert, M. M. (2008). Numerical solutions for fractional reaction–diffusion equations. Computers & Mathematics with Applications, 55(10), 2212-2226.
21. Owolabi, K. M. (2016). Mathematical analysis and numerical simulation of patterns in fractional and classical reaction-diffusion systems. Chaos, Solitons & Fractals, 93, 89-98.

22. Baier, R. R. (2008). Numerical methods and analysis for degenerate parabolic equations and reaction-diffusion systems (Doctoral dissertation, Universidad de Concepcion).
23. Fuselier, E. J., & Wright, G. B. (2013). A high-order kernel method for diffusion and reaction-diffusion equations on surfaces. Journal of Scientific Computing, 56(3), 535-565.
24. Herschkowitz-Kaufman, M. (1975). Bifurcation analysis of nonlinear reaction-diffusion equations—II. Steady state solutions and comparison with numerical simulations. Bulletin of Mathematical Biology, 37, 589-636.
25. Lin, J., Chen, W., & Chen, C. (2014). A new scheme for the solution of reaction diffusion and wave propagation problems. Applied Mathematical Modelling, 38(23), 5651-5664.
26. Cherniha, R., & Davydovych, V. (2017). Nonlinear reaction-diffusion systems. Springer Lecture Notes in Mathematics LNM, 2196.
27. Kopell, N., & Howard, L. N. (1973). Plane wave solutions to reaction-diffusion equations. Studies in Applied Mathematics, 52(4), 291-328.
28. Wei, J., Ge, Y., & Wang, Y. (2022). High-Order Compact Difference Method for Solving Two-and Three-Dimensional Unsteady Convection Diffusion Reaction Equations. Axioms, 11(3), 111.
29. Askar, A. H., Nagy, Á., Barna, I. F., & Kovács, E. (2023). Analytical and Numerical Results for the Diffusion-Reaction Equation When the Reaction Coefficient Depends on Simultaneously the Space and Time Coordinates. Computation, 11(7), 127.
30. Giraldo, J. F., & Calo, V. M. (2023). An adaptive in space, stabilized finite element method via residual minimization for linear and nonlinear unsteady advection–diffusion–reaction equations. Mathematical and Computational Applications, 28(1), 7.
31. Zhu, X., & Ge, Y. (2023). Adaptive ADI difference solution of quenching problems based on the 3D convection–reaction–diffusion equation. International Journal of Nonlinear Sciences and Numerical Simulation, 24(6), 2325-2345.
32. Zamani-Gharaghoshi, H., Dehghan, M., & Abbaszadeh, M. (2024). A meshless collocation method based on Pascal polynomial approximation and implicit closest point method for solving reaction–diffusion systems on surfaces. Engineering with Computers, 40(1), 313-322.
33. Altaie, S. A., Anakira, N., Jameel, A., Ababneh, O., Qazza, A., & Alomari, A. K. (2022). Homotopy analysis method analytical scheme for developing a solution to partial differential equations in a fuzzy environment. Fractal and Fractional, 6(8), 419.
34. Al-Qudah, A., Odibat, Z., & Shawagfeh, N. (2022). An optimal homotopy analysis transform method for handling nonlinear PDEs. International Journal of Applied and Computational Mathematics, 8(5), 260.
35. Ahmad, I., Faisal, M., Loganathan, K., Kiyani, M. Z., & Namgyel, N. (2022). Nonlinear mixed convective bidirectional dynamics of double stratified radiative Oldroyd-B nanofluid flow with heat source/sink and higher-order chemical reaction. Mathematical Problems in Engineering, 2022, 1-16.

Arabic Abstract

تلعب معادلات رد الفعل والانتشار دورًا حيويًا في محاكاة العديد من عمليات العالم الحقيقي عبر العديد من التخصصات. لا يزال من الصعب حل معادلات انتشار التفاعل غير المستقرة ثلاثية الأبعاد. وقد ركزت الأبحاث السابقة على القيود المفروضة على التقنيات الحالية، وبالتالي تتطلب إدخال أساليب بديلة لتناسب هذه الحاجة. الهدف من هذه الدراسة هو اقتراح وتأكيد استخدام طريقة التحليل الهوموتوبي (HAM) كتقنية مرنة لحل معادلات تفاعل وانتشار التفاعل غير المستقرة ثلاثية الأبعاد. نحن نقدم طريقة منهجية لإنشاء مشغل homotropy من خلال توسيع الحل كسلسلة وتحسينه باستمرار من خلال تقنية الاضطراب homotropy عن طريق إجراء اختبارات عددية متعددة. نعرض فعالية طريقتنا في تقريب الاستجابات بالضبط. تدعم دراسة التقارب أيضًا صحة حلولنا. إن نتائج بحثنا لا تساعد فقط في فهم أحداث انتشار التفاعل. كما أنه يوفر أساسًا حسابيًا مفيدًا للبحث في الأنظمة الديناميكية المتطورة.

Pure Sciences International Journal of kerbala

Year:2024 Volume : 1 Issue : 3 ISSN: 6188-2789 Print 3005 -2394 Online

Nadia Hashim Al-Noor, Akbal Jabbar Sultan, A New Extended Inverse Exponential Distribution with Medical and Engineering Applications, Pure Sciences International Journal of Kerbala, Vol. 1 No. 3, (2024) 43-50

First year 2024 ,Volume 1 , Issue 3 PSIJK 43-50

Pure Sciences International Journal of Kerbala
Journal Homepage:https://journals.uokerbala.edu.iq/index.php/psijk

A New Extended Inverse Exponential Distribution with Medical and Engineering Applications

Nadia Hashim Al-Noor[1*], Akbal Jabbar Sultan[2]

[1,2] *Department of Mathematics, College of Science, Al-Mustansiriyah University, Baghdad, Iraq*

P A P E R I N F O

Received: 21 July 2024
Accepted: 5 August 2024
Published: 30 September 2024

Keywords:
Generator family, extended distribution, inverse exponential distribution, maximum likelihood estimation, essential statistical features.

A B S T R A C T

A new probability distribution named Truncated Rayleigh Odd Weibull Inverse Exponential distribution that extends the traditional inverse exponential distribution is proposed. The essential statistical properties including moments, quantile function, linear representation, measures of reliability, entropies, and reliability stress strength model are derived. The unknown three parameters are estimated with the method of maximum likelihood and a simulation study is introduced to examine the accuracy of the estimates. Two applications based on real-life datasets - medical and engineering - are considered. Due to its flexible features, the new extended distribution is preferable to number of well-known comparable models.

1. INTRODUCTION

Statistical data modeling is a crucial part of statistics that has drawn the attention of many researchers. A suitable statistical model is necessary for the accurate actualization of the data when modeling real-life data in various fields such as economics, reliability analysis, engineering, environment, biological investigations, and medical sciences. However, there are still issues when real-life data does not fit any of the conventional probability models. Indeed, statistical and applied researchers have expressed a strong interest in developing new extended probability distributions that are more adaptable to data modeling. The literature describes numerous methods for extending well-known distributions. One of the most prevalent approaches is to think about distribution generators [1,2].

For the generator (G) approach adding parameter (s) to the well-known distributions may introduce new modified/or extended distributions with high flexibility in data-driven modeling of real-life phenomena. In the literature, many generator families of probability distributions with several desirable properties have been proposed. A summary of the varied and useful proposed families includes the Marshall–Olkin-G [3], beta-G [4], Kumaraswamy-G [5], gamma-G [6], exponentiated generalized-G [7], logistic-G [8], Weibull-G [9], truncated Fréchet-G [10], Gompertz-G [11], generalized inverse Weibull-G [12], truncated general-G [13], exponentiated truncated inverse Weibull-G [14], and recently truncated Rayleigh odd Weibull-G [15] to the bounded interval [0,1]. For more families and details, the interested reader may refer to [14] and [15]. For lifetime data analysis, the exponential distribution is one of the most often used distributions related to the scale family of distributions due to its simplicity and mathematical viability. However, in real life, rarely come across engineering systems that have a consistent danger rate throughout their lifetime. As a result, it appears reasonable to assume hazard rate as a function of time which led to the development of an alternative modified/extended model for lifetime data analysis [16].

The inverse exponential (IE) distribution is an alternative modified version of the traditional exponential distribution proposed by [17]. But this modified version also has a limitation which is its inability to effectively represent various skewed datasets. The goal of this paper is centered around introducing a new version of the IE distribution based on employing the truncated Rayleigh odd Weibull-G (TROW − G) family. The new extended version is called truncated Rayleigh odd Weibull inverse exponential (TROWIE) to the bounded interval [0,1].

For $x > 0$ and $\bar{G}(x;\omega) = 1 - G(x;\omega)$, suppose $G(x;\omega)$ and $g(x;\omega) = dG(x;\omega)/dx$ are the cumulative distribution function (CDF) and probability density function (PDF) of a baseline distribution with parameter vector ω, then the CDF of TROW − G family is [15]

*Corresponding Author Institutional Email:
nadialnoor@uomustansiriyah.edu.iq (Nadia Hashim Al-Noor)

$$F(x)=\frac{1}{1-e^{-\theta/2}}\left(1-e^{-\frac{\theta}{2}\left(1-e^{-\left(G(x)/\bar{G}(x)\right)^{\beta}}\right)^{2}}\right) \quad (1)$$

The corresponding PDF of (1) is defined by

$$f(x)=\frac{\theta\beta}{1-e^{-\theta/2}}g(x)\frac{G^{\beta-1}(x)}{\bar{G}^{\beta+1}(x)}e^{-\left(\frac{G(x)}{\bar{G}(x)}\right)^{\beta}} \left(1-e^{-\left(G(x)/\bar{G}(x)\right)^{\beta}}\right)e^{-\frac{\theta}{2}\left(1-e^{-\left(G(x)/\bar{G}(x)\right)^{\beta}}\right)^{2}} \quad (2)$$

where θ and β are positive scales and shape parameters.

The random variable with PDF (2) is denoted by $X\sim TROW-G(\theta,\beta,\omega)$. By inverting (1), the form of quantile function related to the TROW − G family is

$$Q(q)=\psi(q)\left(\frac{G(x)}{\bar{G}(x)}\right)^{-1} \; ; \; 0<q<1 \quad (3)$$

with

$$\psi(q)=\left[-\ln\left(1-\left(\frac{-2}{\theta}\ln\left(1-\left(1-e^{-\frac{\theta}{2}}\right)q\right)\right)^{\frac{1}{2}}\right)\right]^{\frac{1}{\beta}} \quad (4)$$

2. THE TROWIE DISTRIBUTION

The PDF and CDF of the one scale-parameter IE distribution are $g(x;\lambda)=\frac{\lambda}{x^2}e^{-\lambda/x}$ and $G(x;\lambda)=e^{-\lambda/x}$ with $x>0$ and $\lambda>0$ (see [16]-[18]). By inserting the CDF of IE in (1), the CDF of a new extended version TROWIE can be obtained as

$$F(x)=\frac{1}{1-e^{-\theta/2}}\left(1-e^{-\frac{\theta}{2}\left(1-e^{-\left(e^{\lambda/x}-1\right)^{-\beta}}\right)^{2}}\right) \quad (5)$$

By inserting the PDF and CDF of IE in (2), the corresponding PDF follows, is

$$f(x)=\frac{\theta\beta\lambda}{1-e^{-\theta/2}}\frac{e^{-\beta\lambda/x}}{x^2(1-e^{-\lambda/x})^{\beta+1}}e^{-\left(e^{\lambda/x}-1\right)^{-\beta}} \left(1-e^{-\left(e^{\lambda/x}-1\right)^{-\beta}}\right)e^{-\frac{\theta}{2}\left(1-e^{-\left(e^{\lambda/x}-1\right)^{-\beta}}\right)^{2}} \quad (6)$$

The random variable with PDF (6) is denoted by $X\sim TROWIE(\theta,\beta,\lambda)$, and the PDF's natural logarithm of (6) is

$$\ln(f(x))=\ln\left(\frac{\theta\beta\lambda}{1-e^{-\theta/2}}\right)-\frac{\beta\lambda}{x}-2\ln(x) -(\beta+1)\ln\left(1-e^{-\lambda/x}\right)-\left(e^{\lambda/x}-1\right)^{-\beta} +\ln\left(1-e^{-\left(e^{\lambda/x}-1\right)^{-\beta}}\right)-\frac{\theta}{2}\left(1-e^{-\left(e^{\lambda/x}-1\right)^{-\beta}}\right)^{2} \quad (7)$$

With the aid of the following extended special formulas,

$$(S1)\;\; e^{-z}=\sum_{m=0}^{\infty}\frac{(-1)^m}{m!}z^m$$

$$(S2)\;\; (1-z)^a=\sum_{m=0}^{\infty}(-1)^m\binom{a}{m}z^m;\; |z|<1, a>0$$

$$(S3)\;\; (1-z)^{-a}=\sum_{m=0}^{\infty}\binom{m+a-1}{m}z^m; |z|<1, a>0$$

The essential expanded form of the CDF (5) is

$$F(x)^e=\frac{1}{1-e^{-\theta/2}}\left(1-\sum_{i,j,k=0}^{\infty}\frac{(-1)^{i+j+k}j^k}{i!\,k!}\binom{2i}{j}\left(\frac{\theta}{2}\right)^i\left(e^{\lambda/x}-1\right)^{-\beta k}\right) \quad (8)$$

The corresponding essential expanded form of the PDF (6) is

$$f(x)^e=\sum_{k,\ell=0}^{\infty}\Upsilon^{(k,\ell)}\frac{\lambda}{x^2}e^{-\lambda[\beta(k+1)+\ell]/x} \quad (9)$$

where

$$\Upsilon^{(k,\ell)}=\frac{\theta\beta}{1-e^{-\theta/2}}\sum_{i,j=0}^{\infty}\frac{(-1)^{i+j+k}}{i!\,k!}(j+1)^k \binom{2i+1}{j}\left(\frac{\theta}{2}\right)^i\binom{\beta(k+1)+\ell}{\ell} \quad (10)$$

Plots of the CDF and PDF of the TROWIE distribution for few parameter values are shown in Figures 1 and 2. Figure 1 clearly demonstrates the common CDF's features. Figure 2 displays some PDF shapes including decreasing, right-skewed, left-skewed, reversed J, and symmetric, which denote the suitability of TROWIE to model different positive data.

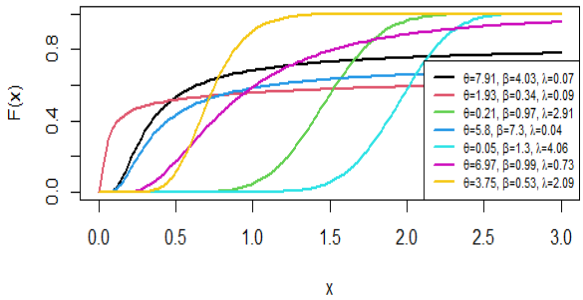

Figure 1. A plot of the CDF with some particular parameter values.

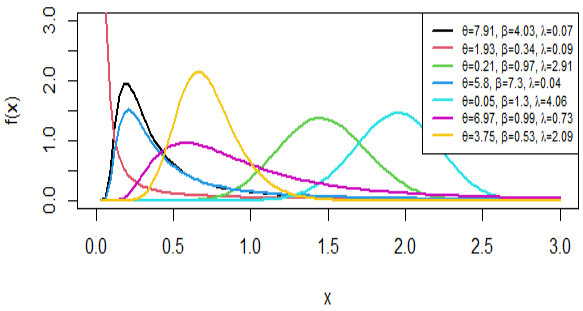

Figure 2. A plot of the PDF with some particular parameter values.

The other essential properties of TROWIE distribution are discussed in the following sub-sections.

2.1. Linear Representation and Related Measures Capital Each Word of Title

The $f(x)^e$ in (9) can rewrite as

$$f(x)^e = \sum_{k,\ell=0}^{\infty} \Upsilon^{(k,\ell)} \frac{\lambda[\beta(k+1)+\ell]}{x^2\,[\beta(k+1)+\ell]} e^{-\lambda[\beta(k+1)+\ell]/x}$$

$$= \sum_{k,\ell=0}^{\infty} \Upsilon^{(k,\ell)} \frac{1}{\beta(k+1)+\ell} \frac{\lambda[\beta(k+1)+\ell]}{x^2} e^{-\lambda[\beta(k+1)+\ell]/x}$$

Therefore

$$f(x)^e = \sum_{k,\ell=0}^{\infty} \Upsilon^{(k,\ell)} \frac{1}{\beta(k+1)+\ell} g(x;\lambda[\beta(k+1)+\ell])_{IE} \quad (11)$$

where $g(x;\lambda[\beta(k+1)+\ell])_{IE}$ represents the PDF of the traditional IE with parameter $\lambda[\beta(k+1)+\ell]$. That is the PDF of TROWIE is expressed as a linear combination of the IE distribution.

Regards to (11), rthnon-central moment can be found as

$$E(X^r) = \sum_{k,\ell=0}^{\infty} \Upsilon^{(k,\ell)} \frac{1}{\beta(k+1)+\ell} E(X^r)_{g(x;\lambda[\beta(k+1)+\ell])_{IE}}$$

where $E(X^r)_{g(x;\lambda[\beta(k+1)+\ell])_{IE}}$ represents the r^{th}non-central moment of IE with parameter $\lambda[\beta(k+1)+\ell]$. Thus, with $r<1$

$$E(X^r) = \sum_{k,\ell=0}^{\infty} \Upsilon^{(k,\ell)} \lambda^r(\beta(k+1)+\ell)^{r-1}\Gamma(1-r) \quad (12)$$

Further, based on the linear representation, the characteristic function of the TROWIE is given by

$$\varphi_X(t) = \sum_{k,\ell=0}^{\infty} \Upsilon^{(k,\ell)} \frac{1}{\beta(k+1)+\ell} \varphi_X(t)_{g(x;\lambda[\beta(k+1)+\ell])_{IE}}$$

where $\varphi_X(t)_{g(x;\lambda[\beta(k+1)+\ell])_{IE}}$ is the characteristic function of IE with parameter $\lambda[\beta(k+1)+\ell]$. Thus, the form of the characteristic function is

$$\varphi_X(t) = \sum_{k,\ell=0}^{\infty} \Upsilon^{(k,\ell)} \frac{2\sqrt{-it\lambda[\beta(k+1)+\ell]}}{\beta(k+1)+\ell} K_1\left(2\sqrt{-it\lambda[\beta(k+1)+\ell]}\right) \quad (13)$$

where $K_1\left(2\sqrt{-it\lambda[\beta(k+1)+\ell]}\right)$ is the Bessel's modified function, $K_\alpha(v) = \frac{1}{2}\int_0^\infty y^{\alpha-1}\, e^{-\frac{v}{2}(y+y^{-1})}dy$, with $\alpha = 1$ and $v = 2\sqrt{-it\lambda[\beta(k+1)+\ell]}$.

2.2. Quantile Function and Related Measures

Recall (3) with baseline distribution IE, $\psi(q)\left(\frac{G(x)}{\bar{G}(x)}\right)^{-1} = \psi(q)\left(e^{\lambda/x}-1\right) \Rightarrow \psi^{-1}(q) = e^{\lambda/x}-1 \Rightarrow e^{\lambda/x} = 1+\psi^{-1}(q)$. After taking the natural logarithm for both sides, the quantile function is

$$Q(q) = \lambda\left[\ln\left(1+\psi^{-1}(q)\right)\right]^{-1} \quad (14)$$

where

$$\psi^{-1}(q) = \left[-\ln\left(1-\left(\frac{-2}{\theta}\ln\left(1-\left(1-e^{-\theta/2}\right)q\right)\right)^{1/2}\right)\right]^{-1/\beta} \quad (15)$$

The median and simulated data of TROWIE random variable can be attained respectively via putting $q = 1/2$ and replacing q with U where U~Uniform (0,1).

2.3. Reliability Measures

The reliability measures of any lifetime equipment are the core tools for analyzing aging and associated aspects. The most commonly used measures in real-life data analysis and especially in reliability engineering are [19] reliability $R(x) = 1-F(x)$, hazard $h(x) = f(x)/R(x)$, cumulative hazard $ch(x) = -\ln(R(x))$, and reverse hazard $rh(x) = f(x)/F(x)$ functions that employed to assess how well an item (component or system) performs. Related to CDF and PDF of $TROWIE$ in (5) and (6), the four mentioned measures can easily attend. Figures 3 and 4 display the plots of the reliability and hazard of $TROWIE$ distribution for some parameter values. Figure 3 clearly demonstrates the common features of the reliability function. Figure 4 displays some hazard shapes including increasing, decreasing, right-skewed, J, and reversed J, which indicate the suitability of $TROWIE$ to analyze various sorts of lifetime data.

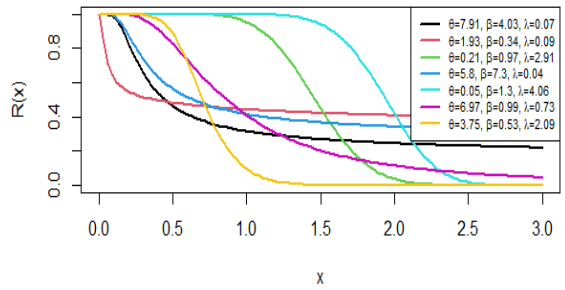

Figure 3. A plot of the reliabilty with some particular parameter values.

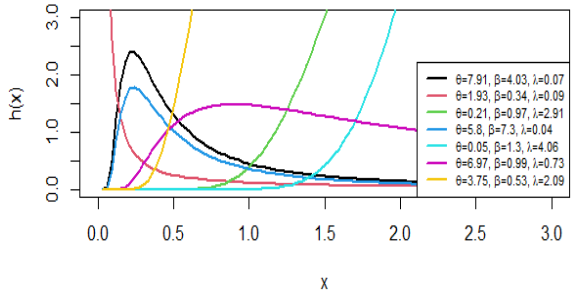

Figure 4. A plot of the hazard with some particular parameter values.

2.4. Entropies

Information theory uses entropy to describe the degree of uncertainty linked with random variable. The entropy of $TROWIE$ random variable can be measured in different ways, two of them are considered in this sub-section.

The first entropy (Shannon entropy) with formula $E_1 = -E\big(\ln(f(x))\big)$ [15] and [19] can be achieved from (7) as

$$\begin{aligned} E_1 &= \ln\left(\frac{1-e^{-\theta/2}}{\theta\beta\lambda}\right) + \beta\lambda E\left(\frac{1}{X}\right) + 2E(\ln(X)) \\ &+(\beta+1)E\big(\ln\big(1-e^{-\lambda/X}\big)\big) \\ &-E\left(\ln\left(1-e^{-\left(e^{\lambda/X}-1\right)^{-\beta}}\right)\right) + E\left(\left(e^{\lambda/X}-1\right)^{-\beta}\right) \\ &+\frac{\theta}{2}E\left(\left(1-e^{-\left(e^{\lambda/X}-1\right)^{-\beta}}\right)^2\right) \end{aligned} \tag{16}$$

where $E\left(\frac{1}{X}\right)$ as in (12) with $r=-1$, and $E(\ln(X))$ can be obtained related to PDF (9) as

$$\begin{aligned} E(\ln(X)) &= \int_0^\infty \ln(x)\, f(x)^e\, dx \\ &= \sum_{k,\ell=0}^{\infty} \Upsilon^{(k,\ell)} \int_0^\infty \ln(x)\, \frac{\lambda}{x^2} e^{-\lambda[\beta(k+1)+\ell]/x} dx \end{aligned}$$

After using the transformation $u = \lambda[\beta(k+1)+\ell]/x \longrightarrow x = \lambda[\beta(k+1)+\ell]/u$ and $dx = -\lambda[\beta(k+1)+\ell]\frac{1}{u^2}du$, and recalling the special formula $S4$,

$$(S4)\quad \int_0^\infty z^{s-1}\ln(z)\, e^{-mz} dz = m^{-s}\Gamma(s)(\psi(s)-\ln(m))$$

Thus

$$\begin{aligned} E(\ln(X)) = \sum_{k,\ell=0}^{\infty} \Upsilon^{(k,\ell)} \frac{1}{\beta(k+1)+\ell} \\ [\ln(\lambda[\beta(k+1)+\ell]) - \psi(1)] \end{aligned} \tag{17}$$

where digamma function $\psi(1) = \int_0^\infty \ln(u)\, e^{-u}\, du \cong -0.577$.More over, with the assistance of $S1-S3$ and extension formula $S5$,

$$(S5)\quad \ln(1-z) = -\sum_{m=1}^{\infty} \frac{1}{m} z^m \,;\, |z|<1$$

The other expectations in (16) can be obtained with some simple mathematical steps as

$$E\big(\ln\big(1-e^{-\lambda/X}\big)\big) = \sum_{m=1}^{\infty}\sum_{s=0}^{\infty} \frac{(-1)^{s+1}}{s!} m^{s-1}\lambda^s E(X^{-s}) \tag{18}$$

$$E\left(\left(e^{\lambda/X}-1\right)^{-\beta}\right) = \sum_{m,s=0}^{\infty} \frac{(-1)^s}{s!}\binom{m+\beta-1}{m} \tag{19}$$

$$\begin{aligned} E\left(\ln\left(1-e^{-\left(e^{\lambda/X}-1\right)^{-\beta}}\right)\right) = \sum_{v=1}^{\infty}\sum_{t,m,s=0}^{\infty} \frac{(-1)^{t+s+1}}{t!\,s!} \\ v^{t-1}\binom{m+\beta t-1}{m} (\lambda(m+\beta t))^s\, E(X^{-s}) \end{aligned} \tag{20}$$

$$\begin{aligned} E\left(\left(1-e^{-\left(e^{\lambda/X}-1\right)^{-\beta}}\right)^2\right) = \sum_{v,t,m,s=0}^{\infty} \frac{(-1)^{v+t+s}}{t!\,s!} \\ v^t\binom{2}{v}\binom{m+\beta t-1}{m} (\lambda(m+\beta t))^s\, E(X^{-s}) \end{aligned} \tag{21}$$

where $E(X^{-s})$ as in (12) with $r=-s$.

To obtain the second entropy (relative entropy), consider $f(x)$ and $f_1(x)$ to be the PDFs of two independent random variables following TROWIE respectively with parameters (θ,β,λ) and $(\theta_1,\beta_1,\lambda_1)$, then

$$\begin{aligned} E_2 &= E\left(\ln\left(\frac{f(x)}{f_1(x)}\right)\right) \\ &= E\big(\ln(f(x))\big) - E\big(\ln(f_1(x))\big) \end{aligned} \tag{22}$$

where $E\big(\ln(f(x))\big)$ and $E\big(\ln(f_1(x))\big)$ can easily be obtained as mentioned before.

2.5. Reliability Stress Strength (RSS) Model

The RSS is a term used in reliability theory to describe the life of an experimental unit under random stress (Z) and random strength (X). The system operates well if $X>Z$, or when the strength exceeds the stress (see [19] and [20]), which means that the experimental unit breaks instantly when Z applied to it exceeds X. As a result, the measure of experimental unit reliability is $P(X>Z)$. The RSS of two independent variables $X\sim TROWIE(\theta,\beta,\lambda)$ and $Z\sim TROWIE(\theta_1,\beta_1,\lambda_1)$ can be obtained with recalling "(8)" with $(\theta_1,\beta_1,\lambda_1)$ by $RSS = E(F_Z(x)^e)$ as

$$RSS = \frac{1}{1-e^{-\theta_1/2}} \left(1 - \sum_{i,j,k=0}^{\infty} \frac{(-1)^{i+j+k}}{i!\,k!} j^k \binom{2i}{j} \left(\frac{\theta_1}{2}\right)^i E\left(\left(e^{\lambda_1/X}-1\right)^{-\beta_1 k}\right)\right)$$

Based on (19) with λ_1 and $\beta_1 k$ respectively instead of λ and β, the RSS is

$$RSS = \frac{1}{1-e^{-\theta_1/2}} \left(1 - \sum_{i,j,k,m,s=0}^{\infty} \frac{(-1)^{i+j+k+s}}{i!\,k!\,s!} j^k \binom{2i}{j} \left(\frac{\theta_1}{2}\right)^i \binom{m+\beta_1 k-1}{m} (\lambda_1(m+\beta_1 k))^s E(X^{-s})\right) \quad (23)$$

2.6. Maximum Likelihood Estimators (MLE)

Regarding PDF (6), for a complete random sample $(x_1, x_2, \dots, x_n)$ of size n, the natural logarithm likelihood function related to $TROWIE$ with the vector of parameters $\Delta = (\theta, \beta, \lambda)^T$ is

$$\begin{aligned}\ell(\Delta|\underline{x}) &= n\ln\left(\frac{\theta\beta\lambda}{1-e^{-\theta/2}}\right) - \beta\lambda\sum_{i=1}^{n}\frac{1}{x_i} \\ &-2\sum_{i=1}^{n}\ln(x_i) - (\beta+1)\sum_{i=1}^{n}\ln\left(1-e^{-\frac{\lambda}{x_i}}\right) \\ &-\sum_{i=1}^{n}\left(e^{\lambda/x_i}-1\right)^{-\beta} + \sum_{i=1}^{n}\ln\left(1-e^{-\left(e^{\lambda/x_i}-1\right)^{-\beta}}\right) \\ &-\frac{\theta}{2}\sum_{i=1}^{n}\left(1-e^{-\left(e^{\lambda/x_i}-1\right)^{-\beta}}\right)^2\end{aligned} \quad (24)$$

The MLE of three parameters can be obtained numerically through solving the not closed forms of nonlinear differential equations $\frac{\partial\ell(\Delta|\underline{x})}{\partial\theta} = 0$, $\frac{\partial\ell(\Delta|\underline{x})}{\partial\beta} = 0$, $\frac{\partial\ell(\Delta|\underline{x})}{\partial\lambda} = 0$.

3. SIMULATION STUDY

A simulation study is conducted to assess the performance of MLE to study how these estimators of the unknown parameters behave for several sample sizes and different parameter combinations.

For each sample size, 3000 random samples of $TROWIE(\theta, \beta, \lambda)$ are generated via simulated formula involved in (14). The MLEs are obtained using the iterative technique available in program R (optim function). The performance of MLE is evaluated with Average Estimates (AE) and Mean Square Error (MSE),

$AE(\hat{\Delta}) = \frac{1}{3000}\sum_{i=1}^{3000}(\hat{\Delta}_i)$; $\Delta = \theta, \beta,$ or λ and

$MSE(\hat{\Delta}) = \frac{1}{3000}\sum_{i=1}^{3000}(\hat{\Delta}_i - \Delta)^2$.

The simulation outcomes related to six different combinations of parameters (for the PDF shapes, see Figure 2 with four sample sizes are shown in Table 1. It is noted that as sample size increases, the values AE tend to be close to the true values, and MSE values seem to be decreasing as expected, demonstrating the consistency of the estimators.

TABLE 1. Values of AE and MSE related to the parameters

			$n = 15$			
Δ	*Tr.*	*AE*	*MSE*	*Tr.*	*AE*	*MSE*
θ	7.91	8.327320	8.087636	1.93	2.012803	3.082864
β	4.03	4.441194	1.374382	0.34	0.374973	0.009585
λ	0.07	0.069945	0.000015	0.09	0.098021	0.001762
θ	0.21	0.472502	7.274642	5.8	5.734592	1.749384
β	0.97	1.054819	0.054117	7.3	8.025454	3.670264
λ	2.91	3.051733	0.589844	0.04	0.039873	8×10^{-7}
θ	6.97	6.515750	4.235454	3.75	3.517010	8.892786
β	0.99	1.131390	0.100377	0.53	0.594638	0.030576
λ	0.73	0.698358	0.020149	2.09	2.139330	0.934870
			$n = 30$			
Δ	*Tr.*	*AE*	*MSE*	*Tr.*	*AE*	*MSE*
θ	7.91	8.232776	6.113207	1.93	2.023179	1.867331
β	4.03	4.216355	0.529582	0.34	0.354612	0.003453
λ	0.07	0.070072	0.000009	0.09	0.094913	0.000804
θ	0.21	0.463850	5.850661	5.8	5.803626	1.325745
β	0.97	1.002085	0.020135	7.3	7.657964	1.505122
λ	2.91	3.023564	0.421412	0.04	0.039949	5×10^{-7}
θ	6.97	6.482723	3.456168	3.75	3.700618	5.965475
β	0.99	1.068240	0.039921	0.53	0.555355	0.012235
λ	0.73	0.702371	0.012082	2.09	2.156232	0.569826
			$n = 60$			
Δ	*Tr.*	*AE*	*MSE*	*Tr.*	*AE*	*MSE*
θ	7.91	8.122817	3.651627	1.93	1.990555	1.180167
β	4.03	4.114413	0.243656	0.34	0.345894	0.001532
λ	0.07	0.070105	0.000006	0.09	0.093067	0.000408
θ	0.21	0.372998	4.254743	5.8	5.846645	0.977229
β	0.97	0.980548	0.009239	7.3	7.479026	0.693581
λ	2.91	2.987964	0.295312	0.04	0.039993	3×10^{-7}
θ	6.97	6.592483	3.418955	3.75	3.739122	3.585034
β	0.99	1.033369	0.019687	0.53	0.540339	0.005700
λ	0.73	0.711428	0.009384	2.09	2.136193	0.301010
			$n = 120$			
Δ	*Tr.*	*AE*	*MSE*	*Tr.*	*AE*	*MSE*
θ	7.91	8.125081	3.007407	1.93	1.962725	0.677580
β	4.03	4.061155	0.114222	0.34	0.342609	0.000712
λ	0.07	0.070149	0.000004	0.09	0.091480	0.000215
θ	0.21	0.309839	2.678956	5.8	5.929748	0.759765
β	0.97	0.972393	0.004317	7.3	7.378719	0.320927
λ	2.91	2.955075	0.176735	0.04	0.040035	2×10^{-7}
θ	6.97	6.719152	3.111888	3.75	3.733695	2.118044
β	0.99	1.013170	0.011206	0.53	0.534231	0.002852
λ	0.73	0.719259	0.007652	2.09	2.116098	0.167366

4. APPLICATIONS TO REAL DATA

In this section, the flexibility of $TROWIE$ distribution is proved by analyzing medical and engineering datasets given as follows.

Medical dataset: The data consist of 120 daily death cases of COVID-19 in Iraq from 1st August to 28th November 2021 accessible at the Iraqi Ministry of Health, Public Health's Directorate [15].

Engineering dataset: The data consists of 38 values of the lifetime period operating the inverter split air conditioner devices before failure happens, taken from an Iraqi Home Electronics Company from 2018 to 2022, are: 1.28, 2.20, 1.26, 27.00, 7.25, 28.17, 12.29, 10.00, 3.05, 3.20, 7.15, 5.27, 6.22, 5.10, 4.12, 8.15, 4.19, 8.03, 6.25, 1.15, 11.00, 5.27, 7.24, 5.12, 8.15, 8.20, 3.13, 1.21, 5.20, 3.18, 6.12, 2.10, 7.24,1.29, 2.22, 3.17, 28.22, 19.10. The integer number denotes the months and the decimal number denotes the days.

Tables 2 and 3 include summary descriptive statistics that can be used to infer the nature of the datasets. The first set of data is right-skewed and platykurtic, and the second is right-skewed and leptokurtic. The $TROWIE$'s fitting behavior is compared with other extended IE related to five families, namely Beta-G, Kumaraswamy-G, Exponentiated Generalized-G, Weibull-G, and Gompertz-G, respectively denoted by $BeIE$, $KuIE$, $EGIE$, $WeIE$, and $GoIE$. It is important to point out that the p-values of the goodness of fit test Kolmogorov-Smirnov (K-S) associated with fitted $TROWIE$ and competitive distributions are all significant values (greater than 0.05). The traditional distribution IE is also included in the comparison. For the comparing process, the negative estimated log-likelihood ($-\hat{\ell}$), and common information criteria (IC) related to Akaike (AIC), Consistent Akaike ($CAIC$), Bayesian (BIC), Hanan and Quinn ($HQIC$) (see [15] and [19]) are employed. The distribution with the lowest values of these criteria is the best fit for the considered dataset. Tables 4 - 7 exhibit the outcomes of various MLE values and IC values. The $TROWIE$ distribution clearly has the lowest values of IC making it the best suited to represent COVID-19 medical data and lifetime period engineering data compared to other competitor distributions.

TABLE 2. Descriptive Statistics related to medical data

Stat.	Mean	Median	Min.	Max.	Sk.	Ku.
Val.	42.758	36.5	7.00	87.00	0.39219	-1.11064

TABLE 3. Descriptive Statistics related to engineering data

Stat.	Mean	Median	Min.	Max.	Sk.	Ku.
Val.	7.33	5.27	1.15	28.22	2.07	3.91

TABLE 4. MLE values related to medical data

Dist.	θ	β	λ
TROWIE	0.084405	1.201666	24.000442
BeIE	11.94404	4.397245	11.041476
KuIE	7.794827	6.321404	10.946719
EGIE	4.528481	1.640757	57.672792
WeIE	4.050667	1.640752	10.005726
GoIE	0.005616	2.425328	4.1478026
IE	---	---	34.001800

TABLE 5. MLE values related to engineering data

Dist.	θ	β	λ
TROWIE	0.08389882	0.67202273	2.84322329
BeIE	0.13633080	3.52900290	32.2836614
KuIE	1.08488600	1.74442600	4.71216500
EGIE	4.22806020	0.15457620	28.5583330
WeIE	2.38650400	1.84243600	1.16782200
GoIE	0.85214660	0.66453520	3.74076890
IE	---	---	3.64531100

TABLE 6. Information criteria for fitting medical data

Dist.	$-\hat{\ell}$	AIC	CAIC	BIC	HQIC
TROWIE	519.715	1045.43	1045.64	1053.79	1048.83
BeIE	523.711	1053.42	1053.63	1061.78	1056.82
KuIE	522.228	1050.46	1050.66	1058.82	1053.85
EGIE	523.410	1052.82	1053.03	1061.18	1056.22
WeIE	519.946	1045.89	1046.10	1054.25	1049.29
GoIE	522.576	1051.15	1051.36	1059.51	1054.55
IE	571.603	1145.21	1145.24	1147.99	1146.34

TABLE 7. Information criteria for fitting engineering data

Dist.	$-\hat{\ell}$	AIC	CAIC	BIC	HQIC
TROWIE	109.331	224.662	225.368	229.575	226.410
BeIE	109.619	225.238	225.944	230.150	226.986
KuIE	110.562	227.124	227.830	232.037	228.872
EGIE	109.583	225.166	225.872	230.079	226.914
WeIE	109.459	224.918	225.624	229.831	226.666
GoIE	109.356	224.711	225.417	229.624	226.459
IE	113.050	228.099	228.210	229.737	228.682

5. CONCLUSIONS

A new extended version of inverse exponential distribution named Truncated Rayleigh Odd Weibull Inverse Exponential is proposed. The essential statistical functions, properties, entropies, linear representation, measures of reliability, and stress strength are derived. The shapes of the density and hazard functions are investigated. The density function may be decreasing, right-skewed, left-skewed, reversed J, and symmetric. Further, hazard function may be increasing, decreasing, right-skewed, J, and reversed J, which indicate the suitability of the new extended to analyze various lifetime data. The three unknown parameters are estimated with the method of maximum likelihood and a simulation study examines the accuracy of the estimates. Two applications based on real medical and engineering datasets are considered. Based on the numerical results of different information criteria, new distribution is preferable to several well-known comparable models including the traditional inverse

exponential distribution due to its flexible features. This adaptability might make it possible to use the new distribution in more application areas. Other parameter estimation techniques, like least squares, weighted least squares, moments, and Bayesian might also be taken into consideration as a potential field for future research.

REFERENCES

1. Cordeiro, G. M., Hashimoto, E. M., Ortega, E. M. M., "The Mc-Donald Weibull model," ***Statistics***, Vol. 48, (2014), 256-278. DOI: 10.1080/02331888.2012.748769.
2. Cordeiro, G. M., Lemonte, A. J., "The exponentiated generalized Birnbaum-Saunders distribution," ***Applied Mathematics and Computation***, Vol. 247, (2014), 762-779. DOI: 10.1016/j.amc.2014.09.054.
3. Marshall, A. N. , Olkin, I., "A new method for adding a parameter to a family of distributions with applications to the exponential and Weibull families," ***Biometrika***, Vol. 84, (1997), 641-652. DOI: 10.1093/biomet/84.3.641.
4. Eugene, N., Lee, C., Famoye, F., "Beta-normal distribution and its applications," ***Communications in Statistics - Theory and Methods***, Vol. 31, (2002), 497-512. DOI: 10.1081/STA-120003130.
5. Cordeiro, G. M., Castro, M. de, "A new family of generalized distributions," ***Journal of Statistical Computation and Simulation***, Vol. 81, (2011), 883-893. DOI: 10.1080/00949650903530745.
6. Torabi, H., Hedesh, N. M., "The gamma-uniform distribution and its applications," ***Kybernetika***, Vol. 48, (2012), 16-30. http://eudml.org/doc/246973.
7. Cordeiro, G. M., Ortega, E. M. M., da Cunha, D. C. C., "The exponentiated generalized class of distributions," ***Journal of Data Science***, Vol. 11, (2013), 1-27. DOI: 10.6339/JDS.2013.11(1).1086.
8. Torabi, H., Montazeri, N. H., "The logistic-uniform distribution and its applications," ***Communications in Statistics - Simulation and Computation***, Vol. 43, (2014), 2551-569. DOI: 10.1080/03610918.2012.737491.
9. Bourguignon, M., Silva, R. B., Cordeiro, G. M., "The Weibull-G family of probability distributions," ***Journal of Data Science***, Vol. 12, (2014), 53-68. DOI: 10.6339/JDS.2014.12(1).1210.
10. Abid, S. H., Abdulrazak, R. K., "[0,1] truncated Fréchet-G generator of distributions," ***Applied Mathematics***, Vol. 7, (2017), 51-66. DOI: 10.5923/j.am.20170703.03.
11. Alizadeh, M., Cordeiro, G. M., Pinho, L. G. B., Ghosh, I., "The Gompertz-G family of distributions," ***Journal of Statistical Theory and Practice***, Vol. 11, (2017), 179-207. DOI: 10.1080/15598608.2016.1267668.
12. Abid, S. H., Al-Noor, N. H., Boshi, M.A.A., "On the generalized inverse Weibull distribution," ***AIP Conference Proceedings***, Vol. 2086, 030002, (2019), 1-4. DOI: 10.1063/1.5095087.
13. Jamal, F., Bakouch, H. S., Nasir, M. A., "A Truncated general-G class of distributions with application to truncated Burr-G family," ***REVSTAT – Statistical Journal***, Vol. 19, (2021), 513-530. https://www.ine.pt/revstat/inicio.html.
14. Almarashi, A. M., Elgarhy, M., Jamal, F., Chesneau, C., "The exponentiated truncated inverse Weibull-generated family of distributions with applications," *Symmetry*, Vol. 12, (2020), 1-21. DOI: 10.3390/sym12040650.
15. Al-Noor, N. H., Sultan, A. J., "Truncated Rayleigh odd Weibull exponential distribution with application to COVID-19 data," ***IEEE Xplore***, 8th International Conference on Contemporary Information Technology and Mathematics (ICCITM), Mosul, Iraq, (2022), 410-416, DOI: 10.1109/ICCITM56309.2022.10031987.
16. Singh, S. K., Singh, U., Kumar, M., "Estimation of parameters of generalized inverted exponential distribution for progressive type-II censored sample with binomial removals," ***Journal of Probability and Statistics***, Vol. 2013, (2013), 1-12. DOI: 10.1155/2013/183652.
17. Keller, A. Z., Kamath, A. R., "Reliability analysis of CNC machine tools," ***Reliability Engineering***, Vol. 3, (1982), 449-473. DOI: 10.1016/0143-8174(82)90036-1.
18. Al-Noor, N. H., Bawi, S. F., "Bayes estimators for the parameter of the inverted exponential distribution under symmetric and asymmetric loss functions," ***Journal of Natural Sciences Research***, Vol. 5, (2015), 45-52. https://www.iiste.org/Journals/index.php/JNSR/article/view/20169.
19. Hilal, O. A., Al-Noor, N. H., "Theory and applications of truncated exponential Topp Leone Rayleigh distribution," ***AIP Conference Proceedings***, Vol. 2414, 040055, (2023), 1-12. DOI: 10.1063/5.0115492.
20. Qazi, J. A., Mohd, A., Nancy, K., "Statistical inference of reliability in multicomponent stress strength model for Pareto distribution based on upper record values," ***International Journal of Modelling and Simulation***, Vol. 42, (2022), 319-334. DOI: 10.1080/02286203.2021.1891496.

Arabic Abstract

تم اقتراح توزيع احتمالي جديد يسمى Truncated Rayleigh Odd Weibull Inverse Exponential كتوسيع للتوزيع الأسي المعكوس التقليدي. تم اشتقاق الخصائص الإحصائية الأساسية بما في ذلك العزوم، الدالة الكمية، التمثيل الخطي، مقاييس المعولية، الانتروبيا، وأنموذج معولية إلاجهاد المتانة. تم تقدير المعلمات الثلاث المجهولة بطريقة الامكان الاعظم وتقديم دراسة محاكاة لفحص دقة التقديرات. تم النظر في تطبيقين يعتمدان على مجموعتين من البيانات الحقيقية - الطبية والهندسية. نظرًا لميزاته المرنة، يُفضل التوزيع الموسع الجديد على عدد من النماذج المماثلة المعروفة.

Pure Sciences International Journal of kerbala

Year:2024 Volume : 1 Issue : 3 ISSN: 6188-2789 Print 3005 -2394 Online

Mustafa Hatem, Ali Al-Fayadh, Efficient Iterative Transform Approach for Solving Time-Fractional Fokker-Planck Equations, Pure Sciences International Journal of Kerbala, Vol. 1 No. 3, (2024) 51-57

First year 2024 ,Volume 1 , Issue 3 PSIJK 51-57

Pure Sciences International Journal of Kerbala
Journal Homepage:https://journals.uokerbala.edu.iq/index.php/psijk

Efficient Iterative Transform Approach for Solving Time-Fractional Fokker-Planck Equations

Mustafa Hatem[1]*, Ali Al-Fayadh[2]
[1]Department of Cyber Engineering Technologies, Privet al Esraa University, Baghdad, Iraq.
[2]Department of Mathematics and Computer Applications, College of Science Al-Nahrain University.

P A P E R I N F O

Received: 6 August 2024
Accepted: 27 August 2024
Published: 30 September 2024

Keywords:
Kashuri and Fundo transform, Variation Iteration Method, Fokker-Planck equation, Homotopy Perturbation Method.

A B S T R A C T

An iterative semi-analytical transform approach is suggested in this paper for solving a time-fractional Fokker-Planck (FrF-P) partial differential equations. The Kashuri-Fundo transform and the variational iteration method are the key components of the suggested method. The fractional derivative is taken in the Caputo sense. The solution is given as a rapidly converging fractional power series with simple coefficients. Some illustrative examples are solved to show how practical and effective the proposed approach is.

1. INTRODUCTION

Partial differential equations (PDEs) are frequently utilized to expressing engineering and natural activities in the various fields of physics, chemistry, biology and applied mathematics. A variety of nonlinear partial differential equations (NLPDEs) have been the focus of important studies by physicists, mathematicians, and scientists in the past decades.

Finding the solution to partial NLDEs is challenging because to their nonlinear components. Although obtaining approximate or exact solutions to nonlinear partial differential equations (NLPDEs) is essential in many study areas, it remains a difficult task that require the development of new methodologies. In order to get an analytical solution, dependable and effective approaches must be developed [1]. The exact solution of these DEs is significant since many practical sciences, including quantum mechanics, hydrodynamics, plasma physics, and nonlinear optics, depend on the ability of predicting the future behavior of a dynamic system.

In recent years, fractional calculus, which is seen as a generalization of standard integer-order integration and differentiation, has received a lot of attention due to the wide range of disciplines in which it is used in modern life. Fractional derivatives have been defined via many suggested definitions including Riesz, Riemann-Liouville, Grunwald-Letnikov, Caputo, and conformable fractional definitions [2]-[4]. Fractional partial differential equations (FrPDEs), are utilized for modeling wide range of real-life applications. The FrPDEs gained importance and popularity because of their wide applications across many fields, including quantum physics, electrical circuits, and theoretical biology [5,6].

A significant amount of research has been done to find solutions for the FrDEs [7-11] and references therein. However, it can be difficult to find exact analytical solutions to the majority of these equations because of the complexity of nonlinear components and fractional derivatives; as a result, approximation and numerical approaches are acceptable for handling the issue. Thus, many iterative and hybrid methods have been proposed, such as the homotopy perturbation method (HPM) [12], the generalized differential transform method [13], the fractional variational iteration method (FrVIM) [14], the Adomian decomposition method (ADM) [15], the homotopy perturbation Sumudu transform method [16], the Kashuri Fundo transform and homotopy perturbation method [17] and references therein.

One of the most well-known and significant equations in the fields of statistical physics, natural science is the Fokker-Planck (F-P) equation. It was first proposed by Fokker and Planck to explain the Brownian motion of particles and the change in probability of a random function in space and time [18].

The objective of this study is to propose an iterative semi-analytic transform approach to approximate the solution of a time-fractional Fokker-Planck (FrF-P) partial differential equations. The suggested approach is termed the fractional Kashuri Fundo variational homotopy method (Fr-KFVHM), it is a combination of

*Corresponding Author Institutional Email: *mustafa1234432111@gmail.com* (Mustafa Hatem)

the Kashuri-Fundo transform (KFT) [19], the VIM [20], and the HPM [21]. The Fr-KFVHM helps in avoiding the complications that often arise when trying to find the Lagrange multiplier (LagM) and the complex integrations that are employed in VIM.

2. OVERVIEW OF THE FOKKER-PLANCK (F-P) EQUATION

The following equation represents the general F-P equation [18]:

$$\frac{\partial z(x,t)}{\partial t} = \left[-\frac{\partial}{\partial x}Q(x) + \frac{\partial^2}{\partial x^2}R(x)\right] z(x,t) \quad (1)$$

subject to,

$$z(x,0) = f(x), \quad x \in \mathbb{R}, \quad (2)$$

The drift and the diffusion coefficients are $Q(x)$ and $R(x)$, respectively. The diffusion and drift coefficients might be time-dependent.That is, "(1)" can be written as:

$$\frac{\partial z(x,t)}{\partial t} = \left[-\frac{\partial}{\partial x}Q(x,t) + \frac{\partial^2}{\partial x^2}R(x,t)\right] z(x,t). \quad (3)$$

Equation (1) represents mathematically a linear second order PDE of parabolic type. The following equation is a generalized version of "(1)" for M variables $x_1, x_2, \dots x_M$:

$$\frac{\partial z(\boldsymbol{x},t)}{\partial t} = \left[-\sum_{r=1}^{M}\frac{\partial}{\partial x_r}Q_r(\boldsymbol{x}) + \sum_{r,s=1}^{M}\frac{\partial^2}{\partial x_r \partial x_s}R_{r,s}(\boldsymbol{x})\right] z(\boldsymbol{x},t) \quad (4)$$

subject to,

$$z(\boldsymbol{x},0) = f(\boldsymbol{x}), \boldsymbol{x} = (x_1, x_2, \dots x_M) \in \mathbb{R}^M \quad (5)$$

The nonlinear F-P (NLF-P) equation is the most common type of F-P equations and has significant applications in many fields, including engineering, pattern formation, psychology, neurosciences, population dynamics, nonlinear hydrodynamics, plasma physics, etc. The NLF-P equation is expressed as follows for the one variable case:

$$\frac{\partial z(x,t)}{\partial t} = \left[-\frac{\partial}{\partial x}Q(x,t,z) + \frac{\partial^2}{\partial x^2}R(x,t,z)\right] z(x,t) \quad (6)$$

3. VARIATIONAL ITERATION METHOD (VIM)

Illustration of the concept VIM based on NLPDE [20] is

$$U\mathrm{z} + T\mathrm{z} = P(x) \quad (7)$$

where T is nonlinear operator, U is linear operator, and $P(x)$ is an analytical function. Correction functional for "(7)" of VIM is

$$\mathrm{z}_{m+1}(x) = \mathrm{z}_m(x) + \int_0^x \lambda(\xi)\left[U\mathrm{z}_m(\xi) + T\mathrm{z}_m(\xi) - P(\xi)\right]d \quad (8)$$

The (LagM) $\lambda(\xi)$ may be determined by the variational theory. A restricted variation is z_m, i.e. $\delta\mathrm{z}_m = 0$ and the mth approximation is denoted by the index m.

The approximation z_{m+1}, $m \geq 0$ of z cab be computed by any selective function z_0 and using LagM. To determine $\lambda(\xi)$, integration by parts may be used; and the solution is given by,

$$z = \lim_{m\to\infty} \mathrm{z}_m \quad (9)$$

4. KASHURI AND FUNDO TRANSFORM

Let Ω be a set of functions of exponential order [19],

$$\Omega = \left(\hbar;\ |\hbar(t)| \leq Ne^{\frac{|t|}{(k_j)^2}}, t \in (-1)^j \times, [0,\infty)\right) \quad (10)$$

where $N, k_1, k_2 > 0$.

The KFT is defined as the following and denoted by the operator $(:)$,

$$\mathcal{K}[\hbar(t)](w) = \frac{1}{v}\int_0^\infty \hbar(t)e^{\frac{-t}{w^2}}dt = \mathcal{A}(w) \quad (11)$$

where $t \geq 0$; $-k_1 < w < k_2$.

Let $\mathcal{A}(w)$ be the KFT of $\hbar(t)$. The fundamental properties of KFT are [25]

$$1.\ \mathcal{K}[\hbar'(t)](w) = \frac{\mathcal{A}(w)}{w^2} - \frac{\hbar(0)}{w} \quad (12)$$

$$2.\ \mathcal{K}[\hbar''(t)](w) = \frac{\mathcal{A}(w)}{w^4} - \frac{\hbar(0)}{w^3} - \frac{\hbar'(0)}{w} \quad (13)$$

3. $\mathcal{K}\left[\hbar^{(n)}(t)\right](w) = \frac{\mathcal{A}(w)}{w^{2n}} - \sum_{k=0}^{n-1} \frac{\hbar^{(k)}(0)}{w^{2(n-k)-1}}$ (14)

TABLE 1. The typical kft for some functions [19]

$\hbar(t)$	$\mathcal{K}[\hbar(t)](w) = \mathcal{A}(w)$
1	w
$t^n,\ n \geq 0$	$n!\, w^{2n+1}$
$e^{-\mu t}$	$\frac{w}{1+\mu w^2}$
$sin(\mu t)$	$\frac{aw^2}{1+\mu^2\ w^4}$
$cos(\mu t)$	$\frac{w^2}{1+\mu^2 w^4}$

Theorem 1. [22]. The KFT of the Riemann-Liouville fractional integral $\mathfrak{Q}_t^\alpha z(x,t)$ and the Caputo fractional derivative $D_t^\alpha z(x,t)$ is given by

i. $\mathcal{K}\{\mathfrak{Q}_t^\alpha z(x,t)\} = w^{2m}\mathcal{A}(x,w)$,

ii. $\mathcal{K}\{D_t^\alpha z(x,t)\} = \frac{\mathcal{A}(x,w)}{w^{2m}} - \sum_{k=0}^{m-1} \frac{1}{w^{2(\alpha-k)-1}} \frac{\partial^k z(x,0^+)}{\partial t^k}$

where $m-1 < \alpha < m \in N$.

iii. $\mathcal{K}\left\{\frac{t^{n\alpha}}{\Gamma(1+m\alpha)}\right\} = w^{2m\alpha+1}$

5. HOMOTOPY PERTURBATION METHOD

The basic idea of the HPM is explained by considering the following nonlinear system[21] ,

$U(z) + T(z) - g(s) = 0$, $s \in \Phi$ (15)

$B\left(z, \frac{\partial z}{\partial m}\right) = 0$, $s \in \Pi$ (16)

where T is nonlinear operator, U is linear operator, and $g(s)$ is an analytical function.

The Homotopy technique for "(15)" is,

$w(r,p): \Phi \times [0,1] \to \mathbb{R}$ (18)

satisfying,

$\mathfrak{U}(w,p) = (1-p)[U(w) - U(z_0)] + P[U(w) + T(w) - g(s)] = 0,\quad s \in \Phi$ (19)

$\mathbb{R}$ is the real numbers, $p \in [0,1]$ increases from 0 to 1, and z_0 is initial approximate solution of "(19)" satisfying the boundary conditions "(15)". Obviously, from "(19)", we have

$\mathfrak{U}(w,0) = U(w) - L(z_0) = 0$ (20)

$\mathfrak{U}(w,1) = U(w) + T(w) - g(s) = 0$ (21)

Suppose that the solution of "(19)" can be written as a power series in p:

$w = w_0 + pw_1 + p^2 w_2 + \cdots$ (22)

The solution z of (19), by Setting $p = 1$ is,

$z = \lim_{p\to 1} w = w_0 + w_1 + w_2 + \cdots$ (23)

For most cases, "(23)" convergent, however the nonlinear operator affects a rate of convergence.

6. FRACTIONAL VARIATIONAL HOMOTOPY TRANSFORM METHOD (Fr-VHTM)

Fr-VHTM is combined from the KFT, VIM, and HPM. The method begins by applying the KFT for both sides of a given DE. The resulting equation will be multiplied by the LagM to generate the recurrence relation. Then, the recurrence relation is limited to determine the LagM. The technique is significant since it does not require the integral part or the convolution theorem neither the convolution theorem nor the integral part used in VIM.

Applying KFT of "(7)", yields,

$\mathcal{K}[Uz + Tz - P(x)] = 0$ (24)

Multiplying (24) by LagM $\lambda(w)$, we get

$\lambda(w)\mathcal{K}[Uz + Tz - P(x)] = 0.$ (25)

The recurrence relation to calculate the LagM is,

$z_{m+1}(x,w) = z_m(x,w) + \lambda(w)\mathcal{K}[Uz + Tz - P(x)]$ (26)

The optimality criterion is employed to calculate the LagM $\lambda(w)$ by using the KFT and

$\frac{\delta z_{m+1}(x,w)}{\delta z_m(x,w)} = 0.$ (27)

Then $\lambda(w) = -w^{2\alpha}$. By using the value of LagM and the inverse of KFT in "(26)", we obtain the approximate solution.

$z_{m+1}(x,w) = z_m(x,w) + \mathcal{K}^{-1}\left[-w^{2\alpha}\mathcal{K}[Uz + Tz - P(x)]\right],\quad m = 0,1,2,3,\ldots$ (28)

The HPM can be expressed as follows for nonlinear terms,

$T(z) = \sum_{j=0}^{\infty} p^j H_j = H_0 + pH_1 + p^2 H_2 + \cdots$ (29)

where $\mathrm{H}_m{}'$s denote the He's polynomials.

$$\mathrm{H}_m(\mathrm{z}_0+\mathrm{z}_1+\mathrm{z}_2+\cdots+\mathrm{z}_m)=\frac{1}{m!}\frac{\partial^m}{\partial p^m}\left[T\left(\sum_{j=0}^{\infty}p^j\mathrm{z}_j\right)\right]_{p=0},\quad m=0,1,2,3,\ldots \tag{30}$$

The following approximations can be found,

$$p^0=\mathrm{z}_0(x,t) \tag{31}$$

$$p^1=\mathrm{z}_1(x,t)=-\boldsymbol{\mathcal{K}}^{-1}(32)$$

$$p^2=\mathrm{z}_2(x,t)=-\boldsymbol{\mathcal{K}}^{-1}\left[w^{2\alpha}\boldsymbol{\mathcal{K}}\left[T\left(\mathrm{z}_1(x,t)\right)-\mathrm{H}\left(\mathrm{z}_1(x,t)\right)\right]\right] \tag{33}$$

$$p^3=\mathrm{z}_3(x,t)=-\boldsymbol{\mathcal{K}}^{-1}\left[w^{2\alpha}\boldsymbol{\mathcal{K}}\left[T\left(\mathrm{z}_2(x,t)\right)-\mathrm{H}\left(\mathrm{z}_2(x,t)\right)\right]\right] \tag{34}$$

and so on.

$$\mathrm{z}_m(x,t)=\mathrm{z}_0+\mathrm{z}_1+\mathrm{z}_2+\mathrm{z}_3+\cdots \tag{35}$$

7. APPLICATIONS

In number of practical scientific disciplines, including physics, engineering, the life sciences, and statistics, the Fokker-Planck equation has been considered as one of the most significant differential equations. The random motion of infinitesimally small particles in a changing medium is studied using the Fokker-Planck equation, and statistical processes and reactions in systems that rely on scattering and atomic activity are also examined. It is also a powerful tool for analyzing how materials are transported and how gases and liquids are distributed in engineering systems. To investigate heat transfer processes and the probability distribution of tiny particles, like electrons and photons, in electromagnetic systems, for instance, physicists utilize the Fokker-Planck equation. This equation is used in engineering to study the movement of matter and energy in physical and chemical systems. It is used to study biological reaction models and the activity of chemicals in living cells in the life sciences. The Fokker-Planck equation is additionally used in disciplines including statistics, economics, and finance. It is used to examine trends in stock price changes and market movements. In general, depending on the scientific field and the phenomenon being studied, the Fokker-Planck equation has a wide range of applications, whether in its form with integer derivatives or with fractional derivatives.

Example 1:

$$\frac{\partial^\alpha}{\partial t^\alpha}=\left[-\frac{\partial}{\partial x}x+\frac{\partial^2}{\partial x^2}\frac{x^2}{2}\right]z$$

$$z(x,0)=x\ ,\quad x\in[0,2]\,,t\geq 0\,,\ 0<\alpha\leq 1$$

$$\left[\frac{\partial^\alpha}{\partial t^\alpha}+\left[\frac{\partial}{\partial x}x-\frac{\partial^2}{\partial x^2}\frac{x^2}{2}\right]z\right]=0 \tag{36}$$

The recurrence relation after applying the KFT for both sides of "(36)" , then multiplying by $\lambda(w)$ is, we obtain

$$z_{m+1}(x,w)=z_m(x,w)+\lambda(w)\left[K\left[\frac{\partial^\alpha}{\partial t^\alpha}+\left[\frac{\partial}{\partial x}x-\frac{\partial^2}{\partial x^2}\frac{x^2}{2}\right]z\right]\right] \tag{37}$$

Using the KFT after considering the variation of "(37)" w.r.t the independent variable z_m.

$$\delta z_{m+1}(x,w)=\delta z_m(x,w)+\lambda(w)\left[\left(\frac{1}{w^{2\alpha}}\delta z_m(x,w)-z(x,0)+K\left[\left[\frac{\partial}{\partial x}x-\frac{\partial^2}{\partial x^2}\frac{x^2}{2}\right]z\right]\right)\right]$$

$$\delta z_{m+1}(x,w)=\delta z_m(x,w)\left(1+\frac{1}{w^{2\alpha}}\lambda(w)\right)$$

When $\frac{\delta z_{m+1}}{\delta z_m}=0$,

$(\frac{1}{w^2}\lambda(w)=-1)\times w^{2\alpha}$, then

$$\lambda(w)=-w^{2\alpha}$$

$$z_{m+1}(x,w)=z_m(x,w)-w^{2\alpha}\left[K\left[\frac{\partial^\alpha}{\partial t^\alpha}+\left[\frac{\partial}{\partial x}x-\frac{\partial^2}{\partial x^2}\frac{x^2}{2}\right]z\right]\right]$$

Taking the inverse of the KFT

$$z_{m+1}(x,w)=z_m(x,w)-K^{-1}\left[w^{2\alpha}\left[K[\frac{\partial^\alpha}{\partial t^\alpha}+\left[\frac{\partial}{\partial x}x-\frac{\partial^2}{\partial x^2}\frac{x^2}{2}\right]z]\right]\right]$$

The HMP can be applied to have

$$z_0+pz_1+p^2z_2+\cdots=z_m(x,t)+pK^{-1}\left[w^{2\alpha}\left[K\left[\left(\left[\left[-\frac{\partial}{\partial x}x+\frac{\partial^2}{\partial x^2}\frac{x^2}{2}\right]z_0\right)+p\left(\left[-\frac{\partial}{\partial x}x+\frac{\partial^2}{\partial x^2}\frac{x^2}{2}\right]z_1\right)+p^2\left(\left[-\frac{\partial}{\partial x}x+\frac{\partial^2}{\partial x^2}\frac{x^2}{2}\right]z_2\right)+\cdots\right]\right]\right] \tag{38}$$

$$p^0{:}\,z_0=z_0(x,t)=x\,,$$

$$p^1{:}\,z_1=K^{-1}\left[w^{2\alpha}\left[K\left[-\frac{\partial}{\partial x}x+\frac{\partial^2}{\partial x^2}\frac{x^2}{2}\right]z_0\right]\right]=K^{-1}[w^{2\alpha+1}x]=x\frac{t^\alpha}{\Gamma(\alpha+1)},$$

$$p^2{:}\,z_2=K^{-1}\left[w^{2\alpha}\left[K\left[-\frac{\partial}{\partial x}x+\frac{\partial^2}{\partial x^2}\frac{x^2}{2}\right]z_1\right]\right]$$

$$= K^{-1}[w^{4\alpha+1}x\,] = x\frac{t^{2\alpha}}{\Gamma(2\alpha+1)},$$

$$p^3: z_3 = K^{-1}\left[w^2\ \left[K\left[-\frac{\partial}{\partial x}x + \frac{\partial^2}{\partial x^2}\frac{x^2}{2}\right]z_2\right]\right]$$

$$= K^{-1}[w^{6\alpha+1}x\,] = x\frac{t^{3\alpha}}{\Gamma(3\alpha+1)},$$

$$p^m: z_m = x\frac{t^{m\alpha}}{\Gamma(m\alpha+1)} = x\left(1 + \frac{t^{\alpha}}{\Gamma(\alpha+1)} + \frac{t^{2\alpha}}{\Gamma(2\alpha+1)} + \frac{t^{3\alpha}}{\Gamma(3\alpha+1)} + \cdots\right) =$$

$$xE_{\alpha}(t^{\alpha}) \qquad (39)$$

TABLE 2. The 10th fr-vhtm approximate solutions of Example 1 at α=1

t	Exact solution	Approximation solution	Absolute error
0.1	1.1051709180756477	1.1051709180756475	0.222045×10^{-15}
0.2	1.2214027581601699	1.2214027581601692	0.666134×10^{-15}
0.3	1.3498588075760032	1.3498588075759577	0.455191×10^{-13}
0.4	1.4918246976412703	1.4918246976401834	0.108691×10^{-11}
0.5	1.6487212707001282	1.6487212706873657	0.176250×10^{-10}
0.6	1.8221188003905090	1.8221188002948574	0.956517×10^{-10}
0.7	2.0137527074704766	2.0137527069445813	0.525895×10^{-9}
0.8	2.2255409284924680	2.2255409261876826	0.230479×10^{-8}
0.9	2.4596031111569500	2.4596031026621 000	0.849485×10^{-8}

Example 2:

$$\frac{\partial^{\alpha}}{\partial t^{\alpha}} = \left[-\frac{\partial}{\partial x}\frac{x}{6} + \frac{\partial^2}{\partial x^2}\frac{x^2}{12}\right]z \qquad (40)$$

$x \in [0,2]\,, t \geq 0\,,\ 0 < \alpha \leq 1$

$z(x,0) = x^2$ The recurrence relation after applying the KFT for both sides of "(40)", then multiplying by $\lambda(w)$ is, we conclude that

$$z_{m+1}(x,w) = z_m(x,w) + \lambda(w)\left[K\left[\frac{\partial^{\alpha}}{\partial t^{\alpha}} + \left[\frac{\partial}{\partial x}\frac{x}{6} - \frac{\partial^{2}}{\partial x^{2}}\frac{x^2}{12}\right]z\right]\right] \qquad (41)$$

Applying the same steps as in Example1, we have

$\lambda(w) = -w^{2\alpha}$, and

$p^0: z_0 = z_0(x,t) = x^2,$

$$p^1: z_1 = K^{-1}\left[w^{2\alpha}\ \left[K\left[-\frac{\partial}{\partial x}\frac{x}{6} + \frac{\partial^2}{\partial x^2}\frac{x^2}{12}\right]z_0\right]\right]$$

$$= \frac{x^2}{2}\frac{t^{\alpha}}{\Gamma(\alpha+1)}$$

$$p^2: z_2 = K^{-1}\left[w^{2\alpha}\ \left[K\left[-\frac{\partial}{\partial x}\frac{x}{6} + \frac{\partial^2}{\partial x^2}\frac{x^2}{12}\right]z_1\right]\right]$$

$$p^3: z_3 = K^{-1}\left[w^2\ \left[K\left[-\frac{\partial}{\partial x}\frac{x}{6} + \frac{\partial^2}{\partial x^2}\frac{x^2}{12}\right]z_2\right]\right]$$

$$= K^{-1}\left[w^{6\alpha+1}\frac{x^2}{8}\right] = \frac{x^2}{8}\frac{t^{3\alpha}}{\Gamma(3\alpha+1)},$$

$$p^m: z_m = \frac{x^2}{2^m}\frac{t^{m\alpha}}{\Gamma(m\alpha+1)}$$

$$= x^2\left(1 + \frac{t^{\alpha}}{2\Gamma(\alpha+1)} + \frac{t^{2\alpha}}{2^2\Gamma(2\alpha+1)} + \frac{t^{3\alpha}}{2^3\Gamma(3\alpha+1)} + \cdots\right) = \frac{x^2}{4}\frac{t^{2\alpha}}{\Gamma(2\alpha+1)}$$

8. REFERENCES

1. M. A. AL-Jawary, "An efficient iterative method for solving the Fokker–Planck equation". Res. Phys.vol. 6,pp. 985-991,2016.
2. I. Podlubny, "Fractional differential equations". San Diego,CA: Academic Press, 1999.
3. M. Caputo, "Linear models of dissipation whose Q is almost frequency independent: part II". Geophys J Int vo.13,pp. 529–539, 1967.
4. M. Al-Smadi, A. Freihat, and H. Khalil, et al. "Numerical multistep approach for solving fractional partial differential equations". Int J Comput Method,vol.14,Doi:1750029, 2017.
5. K. Moaddy, A. Freihat, and M. Al-Smadi, et al. "Numerical investigation for handling fractional-order Rabinovich– Fabrikant model using the multistep approach". Soft Comput,vol. 22,pp.773–782, 2018.
6. M. Al-Smadi, "Solving fractional system of partial differential equations with parameters derivative by combining the GDTM and RDTM". Nonlin Stud,vol. 26,pp.587–601, 2019.
7. S. I .Mohammed, S. F.Fadhel, and A. H. Fayadh "Solution of multi-term fractional order delay differential equations using homotopy analysis method" ,The Second International Scientific Conference (Sisc2021), 2023.
8. Mohammed, R. Wurood, and M. F. Rand, "Numerical and analytical solutions of space-time fractional partial differential equations by using a new double integral transform method", Iraqi Journal of Science,vol. 64, no. 4, pp.1935-1947, 2023.
9. K. H. Auras, and M. M. Muna, "Numerical solution of linear fractional differential equation with delay through finite deference method", Iraqi Journal of Science,vol. 63, no. 3, pp.1232-1239, 2022.
10. M. Guechi, and A. Kadem, "On an analytical and numerical solutions within the conformable fractional derivative for Fitzhugh-Nagumo fractional equation", Italian Journal of Pure and Applied Mathematics, vol. 46 ,pp.530–539, 2021.
11. M. S. Ismael, F. S. Fadhel, and A. Al-Fayadh, "Approximate solution of multi-term fractional order delay differential equations using homotopy perturbation method", Al-Nahrain Journal of Science , vol.23, no. 2, pp.60–66, 2020,
12. K. A. Gepreel, "The homotopy perturbation method applied to the nonlinear fractional Kolmogorov-Petrovskii-Piskunov equations", Applied Mathematics Letters, vol.24,no. 8, pp.1428–1434, 2011.
13. Z. Odibat, S. Momani, and V. S. Erturk, "Generalized differential transform method: application to differential equations of fractional order", Applied Mathematics and Computation, vol.197, no.2, pp.467–477. 2008

14. G. C. Wu, “A fractional variational iteration method for solving fractional nonlinear differential equations”, Computers&Mathematics with Applications, vol.61, no.8, pp.2186 –2190, 2011.
15. D. Jun-Sheng, R. Rach, and A.M. Wazwaz, “A new modified Adomian decomposition method and its multistage form for solving nonlinear boundary value problems with Robin boundary conditions”, Applied Mathematical Modelling , vol.37, no.20-21, pp.8687-8708, 2013.
16. A. Karbalaie, M. M. Montazeri, and H. H. Muhammed, “Exact solution of time-fractional partial differential equations using Sumudu transform”. WSEAS Transactions on Mathematics, vol.13, pp.142-151, 2014.
17. H. A. Peker, and F. A. Cuha, “Application of Kashuri Fundo Transform and Homotopy Perturbation Methods to Fractional Heat Transfer and Porous Media Equations”. THERMAL SCIENCE, vol. 26, no. 4A, pp. 2877-2884, 2022 .
18. M. A. Firoozjaee, S. A. Yousefi, and H. A Jafari, “numerical approach to Fokker-Planck equation with space- and time-fractional and non-fractional derivatives”. MATCH Commun Math Comput Chem , vol. 74, pp. 449–464, 2015.
19. A. Kashuri, and A. Fundo, “A new integral transform”. Advances in Theoretical and Applied Mathematics, vol.8 , no.1, pp.27-43, 2013.
20. He J. Huan. “Variational iteration method - a kind of nonlinear analytical technique: Some examples”. Int. J. Nonlin. Mech., vol.34, pp.699-708, 1999.
21. H. J. Huan, “Homotopy perturbation technique”, Comput. Meth. Appl. Mech. Eng., vol.178, no.3–4, pp.257-262, 1999.
22. A. Kashuri, A. Fundo, and R. Liko, “New integral transform for solving some fractional differential equations”, International Journal of Pure and Applied Mathematics, vol.103, no.4, pp.675-682, 2015

Arabic Abstract

تم اقتراح طريقة تحويل شبه تحليلية تكرارية في هذه الورقة لحل معادلات فوكر-بلانك التفاضلية الجزئية للزمن الكسرية .(FrF-P) يعد تحويل Kashuri-Fundo وطريقة التكرار المتغير المكونات الرئيسية للطريقة المقترحة. يتم أخذ المشتق الكسري بمعنى كابوتو. يتم تقديم الحل على شكل سلسلة قوى كسرية متقاربة بسرعة مع معاملات بسيطة. تم حل بعض الأمثلة التوضيحية لتوضيح مدى عملية وفعالية النهج المقترح.

Pure Sciences International Journal of Kerbala

Year:2024 Volume : 1 Issue : 3 ISSN: 6188-2789 Print 3005 -2394 Online

Mahmood N. Hammood, Liqaa H. Saqban, Nazar J. Metib, The Role of Withania Somnifera against Levofloxacin Effect in Oxidative Stress, Sperm Parameters and DNA Integrity of Male Rats, Pure Sciences International Journal of Kerbala, Vol. 1 No. 3 (2024) 58-66

First year 2024 ,Volume 1 , Issue 3 PSIJK 58-66

Pure Sciences International Journal of Kerbala
Journal Homepage:https://journals.uokerbala.edu.iq/index.php/psijk

The Role of Withania Somnifera Against Levofloxacin Effect in Oxidative Stress, Sperm Parameters and DNA Integrity of Male Rats

Mahmood N. Hammood[1]* , Liqaa H. Saqba[2] , Nazar J. Metib[3]

[1] *Ministry of Education, General Directorate of Education in Karbala*
[2] *Department of Biology, Collage of Education for Pure Science, University of Kerbala, Kerbala, Iraq.*
[3] *Consulting Pathologist, Al-Hussein Medical City, Kerbala, Iraq.*

P A P E R I N F O

Received: 14 July 2024
Accepted: 30 July 2024
Published: 30 September 2024

Keywords:
Withania sominifera, Levofloxacin, Antioxidant, Sperm quality, Sperm DNA.

A B S T R A C T

Folk medicine across various cultures has relied on medicinal plants for their distinctive therapeutic properties. Among these plants is Withania somnifera, which is reputed for its potential to enhance sexual health and improve semen quality and inhibit lipid peroxidation as well as its anti-ageing, and anti-inflammatory properties. The primary objective of this study is to evaluate the inherent protective role of W. somnifera against the effects of Levofloxacin, specifically focusing on DNA damage and sperm quality in a rat model. In order to achieve this objective, a total of thirty adult male rats were carefully assigned to five separate experimental groups, including the Control group (C) saline-treated for 60 days. Group (W) W. somnifera root extract was orally treated for 60 days. Group (L) Levofloxacin orally treated for 60 days. Group (W+L) Levofloxacin was orally co-administered and pre-treated with W. somnifera root extract for 60 days. Group (L+W) Levofloxacin was orally co-administered and post-treated with W. somnifera root extract for 60 days. The degree of protection was estimated using the oxidative stress biomarkers, sperm concentration, motility, viability, morphology, and comet assay. The administration of Levofloxacin resulted in a significant increase ($P < 0.05$) in various parameters, including Total Oxidative Status (TOS), sperm abnormality (Head and Tail abnormality), and the presence of immotile sperm. Additionally, significant damage to sperm DNA was observed, as confirmed by the comet assay. Furthermore, Levofloxacin treatment led to a significant decrease ($P < 0.05$) in Super Oxide Dismutase (SOD) levels and reductions in sperm concentration, motility, and viability. W. somnifera root extract treatment post and pre-Levofloxacin improved recovery of these biochemical changes and boosted sperm quality. In conclusion, W. somnifera root extract may protect against levofloxacin-induced sperm damage in rats.

1. INTRODUCTION

Levofloxacin is classified as a fluoroquinolone antibiotic that effectively treats various bacterial infections such as respiratory tract infections, skin infections, urinary tract infections, and others. It belongs to the third generation of antibiotics called fluoroquinolones (FQs). It can penetrate bacterial cell walls and inhibit the activity of bacterial enzymes responsible for DNA replication [1]. It achieves this by binding to and blocking the action of the bacterial DNA gyrase enzymes, which are necessary for bacterial DNA synthesis and replication [2]. Like all medications, levofloxacin can cause side effects, some of which can be serious. Common adverse effects of levofloxacin include headaches, dizziness, nausea, and diarrhea. However, there are also rare but severe side effects, including aneurysms, prolongation of the Q-T interval, and tendon rupture, especially in the Achilles tendon. Additionally, levofloxacin may lead to muscle weakness, neuropsychiatric toxicity, and hepatotoxicity [3]. The reproductive side effects of FQs like levofloxacin can be concerning. These effects can include changes in libido, decrease sperm parameters and serum testosterone level, and also testicular damage [4,5]. It is not entirely clear why FQs can cause reproductive side effects. Still, it is thought that the drugs may interfere with the production of certain hormones or enzymes that are involved in reproductive function [6]. Furthermore, it is worth noting that besides the potential effect on reproductive functions, there exists compelling evidence indicating that the administration of levofloxacin has the capability to provoke a state of Oxidative Stress (OS) within the body. This oxidative stress is believed to be initiated by the discernible reduction in the functional capacities of vital antioxidant enzymes, namely Superoxide Dismutase (SOD), catalase (CAT), and Glutathione S-transferase (GST) activities [7,8]. Several studies have demonstrated a reasonable connection between

*Corresponding Author Institutional Email:
mahmood_neamah@karbala.edu.iq (Mahmood N. Hammood)

oxidative stress and certain reproductive side effects commonly associated with FQs, including but not limited to infertility and testicular damage [9,10]. Levofloxacin and other FQs have been shown to generate ROS in various cell types, including germ cells [11]. This can lead to damage to cellular components, including lipids, proteins, and DNA. Sperm DNA damage and low sperm quality can negatively impact male fertility and contribute to infertility [12]. Therefore, protecting sperm against oxidative stress and damage is a crucial field of research. Deeply rooted in the ancient traditions of Ayurvedic medicine, *Withania somnifera (WS)*, commonly referred to as Ashwagandha, emerges as a remarkable botanical entity that has garnered profound reverence for its profound healing properties. Over the course of countless generations, this medicinal plant has consistently proven its efficacy in alleviating a diverse spectrum of health challenges, earning it a well-deserved position of eminence within holistic healing practices [13]. Today, it is widely used as a dietary supplement and is gaining popularity for its potential health benefits [14]. Ashwagandha plants root is believed to have immunomodulatory, anti-inflammatory, and antioxidant properties, and is commonly used to manage stress, anxiety, depression, insomnia, and pain [15]. According to a comprehensive qualitative analysis of phytochemicals, it has been clearly emphasized that the extracts derived from the roots of *W. somnifera* contain a rich array of compounds, including terpenoids, tannins, flavonoids, alkaloids, carbohydrates, and saponins. These diverse components synergistically contribute to providing the plant with its remarkable antioxidant properties, protecting against oxidative processes. Furthermore, it is crucial to note that the presence of a specific class of compounds called withanolides further boosts the plant's potential to exhibit such exceptional antioxidant capabilities [16]. These compounds are believed to protect cells from oxidative stress by scavenging free radicals, which are highly reactive molecules that can damage cells and contribute to the development of various diseases [15]. *W. somnifera* can increase the activity of enzymes that help to protect cells against oxidative damage, such as SOD, CAT, and glutathione peroxidase [17]. In addition, *W. somnifera* has been found to increase the levels of antioxidants, such as Glutathione and vitamin C, in cells and tissues [18]. Several researches have been conducted to evaluate the possible protective benefits of *W. somnifera* on sperm cells against oxidative stress caused by a variety of stressors such as environmental pollutants and chemotherapy medicines [19,20]. Several studies have suggested that the root extract of *W. somnifera* can enhance sexual health and improve semen parameters by reducing levels of lipid peroxidation, stress, serum cortisol, and reactive oxygen species. Additionally, the extract increases antioxidant levels, improves overall sperm quality, and elevates testosterone and luteinizing hormone levels [13-21].

2. MATERIALS AND METHODS

2. 1. The Plants Extract Preparation

The *W. somnifera* (*WS*)plants were gathered from the garden at Baghdad University's Science College. The roots were carefully cleaned and left to naturally dry in the comforting shade. Once dried, the roots were grinned into a fine powder using a grinder. This finely powdered root was then immersed in a solution of 70% ethanol and left to soak for duration of 48 hours. The solution is then filtered with filter paper. The alcoholic extract method, employing the renowned Soxhlet apparatus, was employed to harness the desired constituents from the root powder. Following the extraction process, any excess alcoholic solvent was skillfully evaporated at a temperature of 60◦C, ensuring the excess alcoholic solvent was evaporated to gain the final extract [17]. And the dose was prepared according to previous report [18].

2.2. The Drug

Levofloxacin (COX pharmaceutical, LTD. Arcade House. Finchley Road. London NW11 7TL, UK) Tablets 500 mg obtained from local pharmacy. It was finely grinding and then dissolved in normal saline to prepare a dose of 10 mg / kg [11].

2.3. Animals

This experiment involved the utilization of a total of thirty adult albino rats, which were housed in breeding cages under carefully controlled conditions. The temperature within the facility was maintained at a range of 25 to 30 degrees Celsius, accompanied by a humidity level of 50 to 55 percent. The rats were provided with standard pellets as their regular diet and had unrestricted access to water (*Ad libitum*). To ensure fairness and statistical significance, the rats were evenly divided into five groups, with each group consisting of six rats (n=6/group).

Group C: These rats received normal saline orally via gavage for a period of 60 days.

Group W: Rats in this group were administered *W. somnifera* extracts orally via gavage at a dose of 500 mg/kg/body weight, also for a duration of 60 days [18].

Group L: The rats in this group were subjected to oral gavage of Levofloxacin at a dose of 10 mg/kg/body weight for 60 days [11].

Group W+L: Prior to receiving Levofloxacin, the rats in this group were pre-treated with *W. somnifera* extract at a dose of 500 mg/kg orally via gavage, and subsequently received Levofloxacin at a dose of 10 mg/kg via gavage for 60 days. Group L+W: In contrast to the previous group, the rats in this group were first administered Levofloxacin at a dose of 10 mg/kg orally via gavage, and were later post-treated with *W. somnifera* extract at a dose of 500 mg/kg/body weight orally via gavage for 60 days.

2.4. Estimation of TOS and SOD

The serum's total oxidant status (TOS) was measured using an automated analyzer (Thermo Scientific Multiskan FC, Waltham, MA) and Erel's method [22]. The method involved oxidizing the ferrous ion-o-dianisidine complex to the ferric ion in an acidic medium, forming a colored complex with xylenol orange. The color intensity was measured spectrophotometrically at 530 nm wavelengths and correlated with the total amount of oxidant molecules in the serum. Results were expressed in micromolar hydrogen peroxide equivalent per liter (μm H_2O_2 Equiv./L) after calibration with hydrogen peroxide.

2.5. Sperm Parameters Study

2.5.1. The Sperm Concentration

The animals were sacrificed by anaesthetized with chloroform, the epididymis was removed rapidly after the animals had been dissected. The epididymal sperm concentration was calculated according to [24] by cutting the left epididymis into thin slices in a petri-dish which contains 1ml of a normal saline (0.9% NaCl) to release swim sperm. after 10 minutes a drop of a homogenate was loaded on the improved Neubauer hemocytometer and counted under the light microscope (NOVEX, Euromex Co., Holland) a sperm count following WHO [25] criteria.

2.5.2. Sperm Motility

The sperm motility analysis was carried out in accordance with WHO guidelines [25]. Immediately the sperm solution was put on a microscopic slide and covered with a coverslip. Each animal had at least ten microscopic fields examined to evaluate sperm motility. The percentage of sperm motility was calculated for the following: motile parameters: progressive motility, non-progressive motility, and Immotile sperm [24].

2.5.3. Sperm Viability and Morphology

According to WHO [25] guidelines, eosin (1%) and nigrosine (10%) (Merck, Germany) staining were employed to assess sperm viability. One drop of sperm suspension and two drops of 1% eosin were combined. The mixture was then treated with two drops of nigrosine. Thin smears were then produced and examined under an oil immersion magnification. Live sperm remained colorless, but dead sperm colored. A total of 200 spermatozoa were characterized as normal, double head, headless, amorphous head, coiled mid-piece, coiled tail, bent tail, and cytoplasmic droplet in each sample. Sperm viability and abnormality were estimated as a percentage [24].

2.5.4. Quantitative Assessment of DNA Damage

The alkaline comet assay was used to determine the level of DNA damage in sperm. The method followed the protocol [26] with slight modifications. The right Epididymis was removed, and put in a test-tube which contains 1 ml a normal solution (0.9% NaCl) and a 1μl of a homogenate was placed on the improved Neubauer hemocytometer and counted. The cell suspension about (5000-10000) cells were combined and mixed with 1.2 ml low melting agarose (0.5%) before spread out on a slide covered with normal melting agarose (1%). The slides were then incubated in cold lysis prepared immediately at 4°C (18−20 h) in the dark, followed by alkaline buffer and electrophoresis for 25 min at a voltage of 0.6 V/ cm. The slides were then neutralized with 0.4 M Tris base. Then fixed in 100% cold ethanol, and stained with a solution containing SYBR green (1X diluted in PBS) for 20 min in the refrigerator. After that, slides were rinsed with 500ml distilled water to remove excess stain. The slides were examined by the ZEISS Primo Star fluorescence microscope in green light (Carl Zeiss, GmbH, Deutschland) equipped with a digital camera connected to the computer. The length of the comet tail was measured by 100 DNA of cells in each sample that were randomly analysed and scored for the tail intensity (% DNA in tail) using comet score 2.0 software (Rex Hoover, USA) [27].

2.6. Statistical Analysis

The values were represented as Mean ± Standard Error SE and analyzed by one-way ANOVA followed by Revised Least Significant Differences (LSD). Using GraphPad Prism 9.5GraphPad ® Software, CA, USA. The statistical significance was set at $P<0.05$.

3. RESULTS AND DISCUSSION

3.1. The Oxidative Stress

The findings of the study demonstrate that the use of Levofloxacin resulted in a significant elevate in TOS (Total Oxidant Status) levels and a significant lower in SOD (Superoxide Dismutase) levels when compared with the control group. However, the administration of *WS* extract in the L+W and W+L groups exhibited a significant reduction ($P<0.05$) in TOS levels compared with the L treatment alone. Interestingly, the SOD levels in the W+L group did not exhibit a significant change ($P>0.05$), whereas the L+W group displayed a significant increase ($P<0.05$) when compared with the L group, although it did not reach the level observed in the Control group as it appeared in Figures 1 and 2.

The Oxidative Stress (OS) play a significant role in the pathophysiology of reproductive dysfunction and sperm quality. In the present study, it was observed that rats treated with Levofloxacin exhibited significantly higher TOS levels compared with the control group, indicating elevated oxidative stress. Conversely, the SOD levels in the Levofloxacin-treated group were found to be lower than those in the control group, suggesting a reduction in the body's antioxidant defense mechanism. Similar findings showed that levofloxacin treatment caused a significant elevation ($P<0.05$) in MDA and it significantly reduced in SOD, CAT and GSH in the animals that received oral levofloxacin (40mg/kg/day)

for fourteen days [11]. Moreover, Olayinka *et al*. [8] found that administering different doses of levofloxacin (5mg/kg, 10mg/kg, 20mg/kg) caused oxidative stress in the hepatic and renal tissues of rats. This led to increased levels of MDA and reduced levels of GSH and Vitamin C. In addition, the activities of antioxidant enzymes such as SOD, CAT, and GST were decreased. As a result of being treated with FQs, an unbalance between oxidants and antioxidants increased the formation of ROS, which in turn caused oxidative stress. This is associated with pathogenic elements and contributes to cellular deterioration. [28],[29],[30]. Moreover, it may result in mitochondrial dysfunction and overproduction of ROS, leading to oxidative damage to proteins, DNA, and phospholipids of membranes [31]. Levofloxacin and *WS* extract co-treatment result in decreased lipid peroxidation by decreased TOS levels and increased SOD levels. *WS* extract contains various Antioxidants compounds such as fatty acid ester, essential amino acids, flavonoid, phenolic compounds, and antioxidant activities [19],[32].

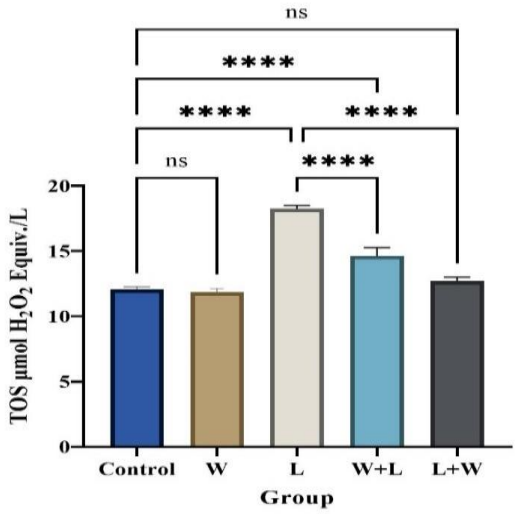

Figure 1. The effect of W. Somnifera and before/after treated Levofloxacin on TOS. Data are presented as mean ± SE (n = 6). The Asterisks represent significance differences from control: *(P<0.05), **(P<0.01), ***(P<0.001), ****(P<0.0001).

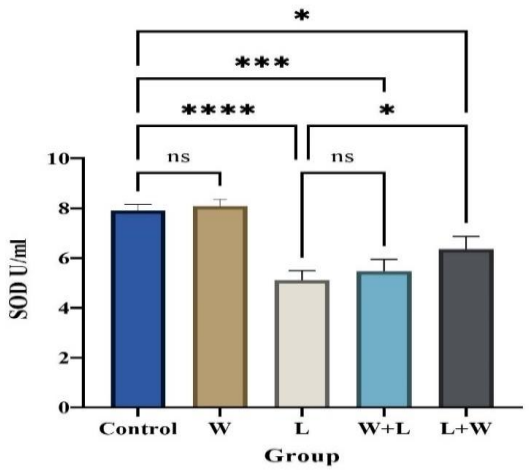

Figure 2. The effect of *W. Somnifera* and before/after treated Levofloxacin on SOD. Data are presented as mean ± SE (n = 6). The Asterisks represent significance differences from control: *(P<0.05), **(P<0.01), ***(P<0.001), ****(P<0.0001).

3.2. Sperm Parameters

The statistical analysis and means of various sperm parameters across the five groups are presented in Table 1. The table clearly indicates significant differences (P<0.05) between the groups regarding sperm concentration, motility (progressive, non-progressive, immotile), viability, as well as morphology (Normal, Head abnormal, and Tail abnormal). This study observed significant decreases in various sperm parameters, including motility, concentration, viability, and morphology. In addition, it showed significant increases in head and tail abnormality in the Levofloxacin treated groups. This finding agrees with previous studies that pointed out that FQs drugs especially levofloxacin cause a significant reduction in sperm count, vitality and motility [5,6]. The sperm membrane is particularly vulnerable to free radical attacks due to the substantial amount of polyunsaturated fatty acids. Sperm viability and concentration can be diminished because sperm membrane damage caused by lipid peroxidation makes it lose its integrity [28]. Oxidative stress influences sperm motility by modifying axoneme structure, resulting in sperm tail abnormalities and decreased motility [33]. This study revealed a significant increase in TOS in levofloxacin-treated rats, which would increase mitochondrial membrane permeability, disrupting the respiratory chain and ATP generation, as well as reduce phosphorylation of axonemal proteins, decreasing sperm quality [34]. Our results found a significant enhancement in baseline sperm viability; morphology and motility after 60 days of *WS* extract administration. This finding is in line with other research that investigated the *WS* extract potential benefits for male reproductive health. It has been

demonstrated that *WS* extract possesses antioxidant characteristics that can help protect sperm from damage caused by oxidative stress [19],[20].

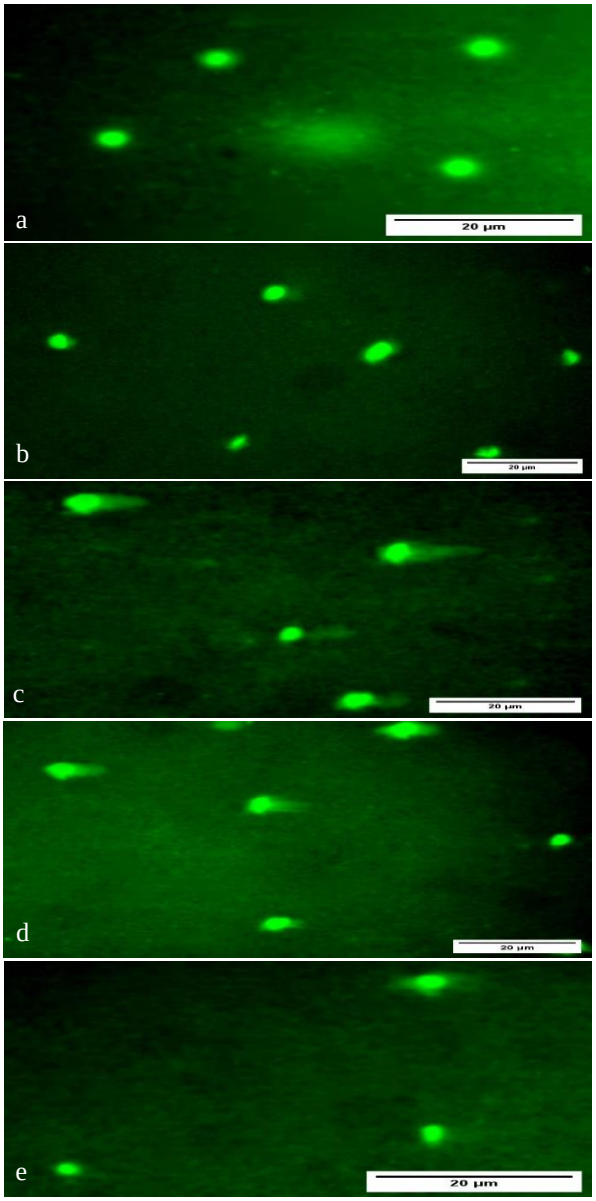

Figure 3. Microscopic photographs showing the DNA damage in rat sperm nuclei Fi shown by Comet assay. (a) Nucleus of sperm from the control group. (b) Nucleus of sperm from the W. sominifera treated group. (c) Nucleus of sperm from the Levofloxacin-treated group. (d) Nucleus of sperm from Levofloxacin + W. sominfera group. (e) Sperm nuclei from W. sominfera + Levofloxacin group. (Scale bar 20 µm. Dye: SYBR Green).

This study aimed at examining the impact of *WS* extract on DNA damage in rat sperm induced by Levofloxacin, the researchers employed a comet assay to evaluate genotoxicity. The results of this assay were visually represented in Figure 3. It was observed that the control group and the group treated with *WS* extract exhibited intact nuclei of undamaged cells, as depicted in Figure 3a and 3b, respectively. On the contrary, the group treated with Levofloxacin displayed evident DNA damage in the form of comet-like structures, as shown in Figure 3c. In contrast, the group receiving a combination of *WS* extract and Levofloxacin (W+L) exhibited a low level of DNA damage within the cell nuclei (Figure 3d). Similarly, the group receiving Levofloxacin followed by *WS* extract (L+W) displayed normal nuclei of undamaged cells (Figure 3e). It is important to note that the administration of *WS* extract alone did not cause any genotoxic effects on sperm. Furthermore, the statistical analysis revealed that the percentage of DNA in the comet tail was significantly increased in the Levofloxacin-treated group compared to the control group, indicating significant DNA damage. Conversely, the *WS* extract -treated group showed non-significant increases ($P>0.05$) in the percentage of DNA in the tail. When *WS* extract was co-administered with Levofloxacin, the group (W+L) exhibited a non-significant reduction ($P>0.05$) in the percentage of DNA in the comet tail, while the group (L+W) displayed a significant reduction compared to the Levofloxacin-treated group (Table 1). The results of this study indicate that exposure to Levofloxacin led to significant damage to rat sperm DNA, as demonstrated by the comet assay. This damage was evidenced by the appearance of comets in the nuclei of sperm cells. Several studies have reported that levofloxacin, a fluoroquinolone antibiotic, can induce Oxidative Stress and damage in DNA of sperm cells [9],[35],[36]. For instance, in a study by Al-Dujaily *et al*. [37], rats treated with levofloxacin showed significant increases in sperm DNA fragmentation, as measured by the sperm chromatin structure assay, compared to control. Because levofloxacin is a topoisomerase inhibitor, the current study assumed that it limits the formation and ligation of nicks in DNA, preventing protamination and, as a result, causing internal DNA damage by restricting repair and increasing sensitivity to damage [29],[36]. In a study by Al-Soufi & Al-Rekabi [38], rats were given different doses of levofloxacin (7.5mg/kg/bw and 15mg/kg/bw) orally for 2 or 4 weeks. There were no significant differences in micronuclei assay and chromosomal aberration among the groups. However, after a period of thirty days, a significant decrease was observed in both nuclear division index and mitotic index values, and the comet assay showed a significant reduction in both treated groups in comparison to the control. The study concluded that levofloxacin is cytotoxic but not genotoxic in male rats. However, co-administration of *WS* extract with Levofloxacin resulted in a reduction in DNA damage compared to Levofloxacin alone. Based on the comprehensive literature review, this study was the first to investigate the effects of *WS* extract on improving the comet assay, a test used to evaluate DNA damage in sperm. In recent research, it has been discovered that taking *WS* extract

can have positive effects on men's reproductive health. Specifically, it has been found that ashwagandha extract supplementation can boost important semen parameters such as sperm viability, motility, and protection against DNA damage [19]. These findings highlight the potential of *WS* extract as a natural and beneficial addition to support male fertility and overall reproductive well-being. In addition, *WS* extract has been suggested to enhance testosterone levels and reduce stress and anxiety, which can have positive effects on male fertility [39]. The beneficial impacts of specific medicinal herbs on specific sperm characteristics can be attributed to their potent antioxidant properties. This is particularly relevant in the case of *WS* extract, as it contains essential phytochemical components and antioxidant minerals that contribute to its significance in addressing infertility concerns [18]. These results highlight the potential of *WS* extract as a promising therapeutic option for mitigating the adverse effects of Levofloxacin on sperm health.

TABLE 1. Result of Sperm Parameters in The Different Groups.

Variables	Group (C)	Group W	Group L	Group W+L	Group L+W
Concentration ($\times 10^6$)	152.17 ±16.21 AB	158.0 ±8.30 B	75.17± 8.14 C	117.67 ±12.9 D	120.83 ±11.35 D
Progressive (%)	56.9 ±0.63 A	74.9 ±1.18 B	26.0 ±0.78 C	40.6 ±0.98 D	42.2 ±0.55 D
Non-progressive (%)	28.9 ±1.14 A	17.2 ±0.07 B	32.6 ±0.52 C	38.2 ±0.58 D	37.9 ±1.10 D
Immotile (%)	14.2 ±1.23 A	7.9 ±1.27 B	41.4 ±0.70 C	21.2 ±1.65 D	19.7 ±1.11 D
Viability (%)	77.8 ±1.12 A	83.9 ±0.58 B	51.3 ±0.87 C	64.6 ±1.58 D	72.2 ±0.90 E
Normal morphology (%)	82.0 ±0.65 A	85.8 ±1.21 B	60.8 ±0.56 C	76.1 ±0.76 D	79.3 ±0.61 AD
Abnormal Head (%)	6.4 ±0.66 AD	5.2 ±0.88 A	20.6 ±1.15 B	11.3 ±0.61 C	7.5 ±0.24 D
Abnormal Tail (%)	11.4 ±0.51 A	8.9 ±0.85 B	18.6 ±0.72 C	12.4 ±0.64 A	13.0 ±0.69 A
DNA Damage (Tail % DNA)	2.22 ±0.33 A	3.41 ±0.98 AC	7.54 ±1.11 B	5.48 ±0.96 BC	4.65 ±0.58 AC

-Data are presented as mean ± SE (n=6). Deferent latter refer to significant differences.

4. CONCLUTOIN & FUTURE STUDIES

In conclusion, the findings of this study suggest that *WS* extract may possess a protective effect against Levofloxacin-induced DNA damage in rat sperm. However, it is important to conduct further studies in this area to explore its full potential and provide more insights. More research is needed to understand how exactly this protection works and to determine the optimal dosage and duration of both levofloxacin and *WS* to use.

5. REFERENCES

1. Chen H, Yuan L, Ma X, Gong Z-P, Li Y-T, Chen S-Y, Pan J, Wang A-M, Zheng L, Huang Y. "Herb-drug interaction: The effect of Polygonum capitatum extract on pharmacokinetics of levofloxacin in rats.",***J. Pharm. Biomed. Anal.***, Vol. 195,(2021),113832. doi:10.1016/j.jpba.2020.113832.
2. Bennett AC, Bennett CL, Witherspoon BJ, Knopf KB. "An evaluation of reports of ciprofloxacin, levofloxacin, and moxifloxacin-association neuropsychiatric toxicities, long-term disability, and aortic aneurysms/dissections disseminated by the Food and Drug Administration and the European Medicines Agency",***Expert Opin. Drug Saf.***, Vol. 18,(2019),1055–63. doi:10.1080/14740338.2019.1665022.
3. Bennett CL, Champigneulle O, Bennett A, Witherspoon B, Bove C. Fluoroquinolone-Associated Disability and Other Fluoroquinolone-Associated Serious Adverse Events: Unexpected Toxicities Have Emerged in Recent Years. In: Bennett C, Lubaczewski C, Witherspoon B, editors., Cham: Springer International Publishing; ,(2022), p. 1–39. doi:10.1007/978-3-031-04402-1_1.
4. Ara C, Asmatullah A, Kanwal S, Chaudhary A, Siddiqua A. "Haematological and Histopathological Analyses of Levofloxacin Induced Toxicity in Mammals",***Punjab Univ. J. Zool.***,Vol.35,(2020),1–6.doi:10.17582/journal.pujz/2020.35.1.01.06.
5. Mokhimar HM, Kandiel MM, Amin AA, Elsawah HK, El Mahmoudy AM. "Ciprofloxacin and levofloxacin adversely affect male infertility indicated by pharmacological, andrological and pathological evidence",***Int. J. Basic Clin. Pharmacol.***, Vol. 9,(2020),353. doi:10.18203/2319-2003.ijbcp20200190.
6. Ahmadi R, Ahmadifar M, Safarpour E, Vahidi-Eyrisofla N, Darab M, Eini AM, Alizadeh A. "The effects of levofloxacin on testis tissue and spermatogenesis in rat",***Cell J.***, Vol. 18,(2016),112–6. doi:10.22074/cellj.2016.3994.
7. Afolabi O, Oyewo EB. "Effects of Ciprofloxacin and Levofloxacin Administration on Some Oxidative Stress Markers in the Rat",***World Acad. Sci. Eng. Technol. Int. J. Biol. Vet. Agric. Food Eng.***, Vol. 8,(2014),38–42. doi:10.5281/ZENODO.1090856.
8. Olayinka ET, Ore A, Ola OS. "Influence of Different Doses of Levofloxacin on Antioxidant Defense Systems and Markers of Renal and Hepatic Dysfunctions in Rats",***Adv. Toxicol.***, Vol. 2015,(2015),1–7. doi:10.1155/2015/385023.
9. Abd A, Al-Dujaily S, Al-Saray D. "EFFECTS OF CIPROFLOXACIN ON MALE FERTILITY PARAMETERS AND SPERM DNA INTEGRITY IN RATS",***Iraqi J. Med. Sci.***, Vol. 16,(2018),378–84. doi:10.22578/IJMS.16.4.4.
10. Ukwenya V, Oladiran O. "Garcinia cambogia modulates ciprofloxacin-induced testicular histopathology through regulatory effects on the pituitary hormones",***Endocr. Abstr.***, Vol. ,(2016),. doi:10.1530/endoabs.41.ep723.
11. Farid AS, Hegazy AM. "Ameliorative effects of Moringa oleifera leaf extract on levofloxacin-induced hepatic toxicity in rats",***Drug Chem. Toxicol.***, Vol. 43,(2020),616–22. doi:10.1080/01480545.2019.1574811.
12. Al-Dujaily, A.H., Al-Saray, D.A., " Effects of levofloxacin on male reproductive system parameters and sperm DNA normality in rats", ***J. Pharm. Sci. Res.***, Vol. 10, (2018), No. 3, pp. 462–466.
13. Sengupta P, Agarwal A, Pogrebetskaya M, Roychoudhury

S, Durairajanayagam D, Henkel R. "Role of Withania somnifera (Ashwagandha) in the management of male infertility",***Reprod. Biomed. Online***, Vol. 36,(2018),311–26. doi:10.1016/j.rbmo.2017.11.007.

14. Natarajan K, Purushotham PM, Rajendran A, Suresh S, Senthil K. "Comparative adaptogenic properties of Withania somnifera and Panax ginseng",***Curr. Bot.***, Vol. ,(2022),12–8. doi:10.25081/cb.2022.v13.7599.
15. Paul S, Chakraborty S, Anand U, Dey S, Nandy S, Ghorai M, Saha SC, Patil MT, Kandimalla R, Proćków J. "Withania somnifera (L.) Dunal (Ashwagandha): A comprehensive review on ethnopharmacology, pharmacotherapeutics, biomedicinal and toxicological aspects",***Biomed. Pharmacother.***, Vol. 143,(2021),112–75.
16. Trivedi M, Branton A, Trivedi D, Nayak G, Nykvist C, Lavelle C, Przybylski D, Vincent D, Felger D, Konersman D, Feeney E, Prague J, Starodub J, Rasdan K, Strassman K, Soboleff L, Mayne M, Keesee M, Pillai P, et al. "Liquid Chromatography – Mass Spectrometry (LC-MS) Analysis of Withania Somnifera (Ashwagandha) Root Extract Treated with the Energy of Consciousness",***Am. J. Quantum Chem. Mol. Spectrosc.***, Vol. 2,(2017),1–10. doi:10.11648/j.ajqcms.20170101.13.
17. Govindappa PK, Gautam V, Tripathi SM, Sahni YP, Raghavendra HLS. "Effect of Withania somnifera on gentamicin induced renal lesions in rats",***Rev. Bras. Farmacogn.***, Vol. 29,(2019),234–40. doi:10.1016/j.bjp.2018.12.005.
18. Kyathanahalli CN, Manjunath MJ, Muralidhara. "Oral supplementation of standardized extract of Withania somnifera protects against diabetes-induced testicular oxidative impairments in prepubertal rats",***Protoplasma***, Vol. 251,(2014),1021–9. doi:10.1007/s00709-014-0612-5.
19. Rautela NS, Sharma MD, Sharma N, Kishor K, Singh K, "Comparative Gc-Ms Analysis of Leaf and Root Extract of Medicinal Plant Withania somnifera," ***World J. Pharm. Res***., Vol. 7, (2018), No. 2, pp. 956–972.
20. Nasimi Doost Azgomi R, Nazemiyeh H, Sadeghi Bazargani H, Fazljou SMB, Nejatbakhsh F, Moini Jazani A, Ahmadi AsrBadr Y, Zomorrodi A. "Comparative evaluation of the effects of Withania somnifera with pentoxifylline on the sperm parameters in idiopathic male infertility: A triple-blind randomised clinical trial",***Andrologia***, Vol. 50,(2018),1–9. doi:10.1111/and.13041.
21. Nasimi Doost Azgomi R, Zomorrodi A, Nazemyieh H, Fazljou SMB, Sadeghi Bazargani H, Nejatbakhsh F, Moini Jazani A, Ahmadi Asrbadr Y. "Effects of Withania somnifera on Reproductive System: A Systematic Review of the Available Evidence",***Biomed Res. Int.***, Vol. 2018,(2018),. doi:10.1155/2018/4076430.
22. Erel O. "A new automated colorimetric method for measuring total oxidant status",***Clin. Biochem.***, Vol. 38,(2005),1103–11. doi:10.1016/j.clinbiochem.2005.08.008.
23. Marklund S, Marklund G. "Involvement of the Superoxide Anion Radical in the Autoxidation of Pyrogallol and a Convenient Assay for Superoxide Dismutase", 474,(1974),469–74.
24. Pourentezari M, Talebi AR, Mangoli E, Anvari M, Rahimipour M. "Additional deleterious effects of alcohol consumption on sperm parameters and DNA integrity in diabetic mice",***Andrologia***, Vol. 48,(2016),564–9. doi:10.1111/and.12481.
25. Organization WH. WHO laboratory manual for the examination and processing of human semen. World Health Organization; ,(2021),.
26. Olive PL, Banáth JP. "The comet assay: a method to measure DNA damage in individual cells",***Nat. Protoc.***, Vol. 1,(2006),23–9. doi:10.1038/nprot.2006.5.
27. Nowsheen S, Xia F, Yang ES. "Assaying DNA Damage in Hippocampal Neurons Using the Comet Assay", ,(2012),. doi:10.3791/50049.
28. Khan AM, Rampal S, Sood NK. "Effect of repeated oral administration of levofloxacin, enrofloxacin, and meloxicam on antioxidant parameters and lipid peroxidation in rabbits",***Hum. Exp. Toxicol.***, Vol. 36,(2017),42–50. doi:10.1177/0960327116637111.
29. Mani S, Tyagi S, Pal KV, Jaiswal H, Jain A, Gulati A, Singh M. Drug-Induced Oxidative Stress and Cellular Toxicity. ***Free Radic. Biol. Environ. Toxic.***, Springer; ,(2022), p. 73–113.
30. Srinivasu M., "Effect of enrofloxacin and ciprofloxacin on oxidative stress in rats," ***Journal of Veterinary Pharmacology and Toxicology***, 2022, Vol., 21, (2022), No., 1, p. 80-82.
31. Kalghatgi S, Spina CS, Costello JC, Liesa M, Morones-Ramirez JR, Slomovic S, Molina A, Shirihai OS, Collins JJ. "Bactericidal antibiotics induce mitochondrial dysfunction and oxidative damage in mammalian cells",***Sci. Transl. Med.***, Vol. 5,(2013),. doi:10.1126/scitranslmed.3006055.
32. Munir N, Mahmood Z, Shahid M, Afzal MN, Jahangir M, Ali Shah SM, Tahir IM, Riaz M, Hussain S, Akram M, Yousaf F. "Withania somnifera Chemical Constituents' In Vitro Antioxidant Potential and Their Response on Spermatozoa Parameters",***Dose-Response***, Vol. 20,(2022),1–13. doi:10.1177/15593258221074936.
33. Khaleel A., Shaari R., Nawi M., and Al-Yassiri A., "Toxicological Aspects of Fluoroquinolones Administration: A Literature Review," ***Egypt. J. Chem.,*** Vol. 65, (2022), No. 5, pp. 561–569.
34. Dutta S, Majzoub A, Agarwal A. "Oxidative stress and sperm function: A systematic review on evaluation and management",***Arab J. Urol.***, Vol. 17,(2019),87–97.
35. Mojoyinola AO, Ishaya HB, Makena W, Jacob CB, Jonga UM, Anochie VC, Denis EW, Gadzama MN. "Protective effect of ciprofloxacin-induced oxidative stress, testicular and hepatorenal injury by Citrullus lanatus L.(Watermelon) seeds in adult Wistar rats",***South African J. Bot.***, Vol. 156,(2023),365–75.
36. Ebadimanas G. "Protective effect of royal jelly on the DNA integrity of sperms and early in vitro embryonic development in ofloxacin treated rats",***Comp. Clin. Path.***, Vol. 28,(2019),541–7. doi:10.1007/s00580-018-2832-0.
37. Al-Dujaily S, Abd, AbdulKareem, Al-Saray D. "Effects of Levofloxacin on Male Reproductive System Parameters and Sperm DNA Normality in Rats",***Res. J. Pharm. Technol.***, Vol. 14,(2021),4897–902. doi:10.52711/0974-360X.2021.00851.
38. Al-Soufi WF, Al-Rekabi FMK. "The Cytogenetic Effects of Levofloxacin in Male Rats",***Adv. Anim. Vet. Sci.***, Vol. 7,(2019),138–50. doi:10.17582/journal.aavs/2019/7.3.138.150.
39. Namdev N, Chourasiya S, Rai G. "Five-Year Meta-analysis of Ashwagandha Used as an Antioxidant : A Systematic Review",***High Technol. Lett.***, Vol. 29,(2023),484–92.

Arabic Abstract

الطب الشعبي في مختلف الثقافات يعتمد على النباتات الطبية لما لها من خصائص علاجية مميزة ومن بين هذه النباتات نبات الأشواغندا *Withania somnifera*، الذي يشتهر بقدرته على تحسين الصحة الجنسية وتحسين جودة السائل المنوي وتثبيط من عملية الاكسدة الفوقية للدهون فضلا عن خصائصه المضادة للشيخوخة، والمضادة للالتهابات. الهدف الرئيسي من هذه الدراسة هو تقييم الدور الوقائي المحتمل لنبات الاشواغندا *W. somnifera* ضد تأثيرات الجانبية لدواء الليفوفلوكساسين Levofloxacin على مستوى جودة النطف والتلف الحاصل للحامض النووي DNA للحيوانات المنوية في الجرذان. ومن أجل تحقيق هذا الهدف، تم أستخدام ثلاثين جرذا بالغًا من الذكور وتم تقسيمها بصورة عشوائية على خمس مجموعات تجريبية منفصلة، بما في ذلك المجموعة الاولى السيطرة (C) والمعاملة بمحلول ملحي لمدة 60 يومًا. المجموعة الثانية (W) وتم تجريعها بمستخلص جذر نبات الاشواغندا *W. somnifera* عن طريق الفم لمدة 60 يومًا. المجموعة الثالثة (L) تم تجريعها دواء الليفوفلوكساسين عن طريق الفم لمدة 60 يوما. تم إعطاء المجموعة الرابعة (W+L) دواء الليفوفلوكساسين عن طريق الفم ومعالجتها مسبقًا بمستخلص جذر نبات الاشواغندا *W. somnifera* لمدة 60 يومًا. المجموعة الخامسة (L+W) تم إعطاء دواء الليفوفلوكساسين وبعد ذلك تم معالجته بمستخلص جذر نبات الاشواغندا *W. somnifera* عن طريق الفم ولمدة 60 يومًا. وقد تم قياس درجة التأثير باستخدام بعض المعايير الحيوية كالإجهاد التأكسدي، وتركيز الحيوانات المنوية والنسبة المئوية للحركة والحيوية وأيضا النسبة المئوية للنطف السوية، وأختبار نسبة تحطم جزيئة DNA (فحص المذنب). أدى تجريع دواء الليفوفلوكساسين إلى زيادة معنوية ($P < 0.05$) في العديد من المعايير، بما في ذلك حالة الأكسدة الكلية (TOS)، النسبة المئوية للنطف غير السوية (تشوه الرأس والذيل)، الحيوانات المنوية غير المتحركة. فضلا عن ذلك، لوحظ وجود تلف كبير في الحامض النووي DNA للحيوانات المنوية، كما أكد ذلك فحص المذنب. علاوة على ذلك، أدى تجريع بالليفوفلوكساسين إلى انخفاض معنوي ($P < 0.05$) في مستويات أنزيم سوبر أوكسيد ديسموتاز (SOD) وانخفاض معنوي ($P < 0.05$) في تركيز الحيوانات المنوية وحركتها وحيويتها. كما أدت المعالجة بمستخلص جذور نبات الاشواغندا *W. somnifera* قبل وبعد تجريع دواء الليفوفلوكساسين إلى تحسين بعض هذه التغيرات في المعايير الكيموحيوية وكذلك تحسين من جودة الحيوانات المنوية. في الختام، نستنتج من هذه الدراسة قد كان لمستخلص جذور نبات الاشواغندا *W. somnifera* دورا أيجابيا للحماية من ضرر الحيوانات المنوية الناجم عن دواء الليفوفلوكساسين في الجرذان.

Pure Sciences International Journal of kerbala

Year:2024 Volume : 1 Issue : 3 ISSN: 6188-2789 Print 3005 -2394 Online

Hadeel Amoori Abd Ali , Neepal Imtair AlGaraawi , Suaad W. Kadium, Evaluation of the Biological Activity of Saccharomyces Boulardii in the Synthesis of Silver Nanoparticles, Pure Sciences International Journal of Kerbala, Vol. 1 No. 3 (2024) 67-71

First year 2024 ,Volume 1 , Issue 3 PSIJK 67-71

Pure Sciences International Journal of Kerbala
Journal Homepage:https://journals.uokerbala.edu.iq/index.php/psijk

Evaluation of the Biological Activity of Saccharomyces Boulardii in the Synthesis of Silver Nanoparticles

Hadeel Amoori Abd Ali[1*] , Neepal Imtair AlGaraawi[2] , Suaad W. Kadium[3]

[1,2] *University of Kerbala, College of Education for Pure Sciences, Department of Biology, Kerbala, Iraq*
[3] *University of Kufa, College of Science, Department of Biology, Kufa, Iraq*

P A P E R I N F O

Received: 14 July 2024
Accepted: 29 July 2024
Published: 30 September 2024

Keywords:
silver nanoparticles, XRD, AFM, Saccharomyces boulardii

A B S T R A C T

The intention of this study was to determine the efficacy of Saccharomyces boulardii as a biological catalyst.to generate silver nanoparticles using silver nitrate. Diffraction of X-rays (XRD) .The atomic force microscope (AFM) was employed to investigate the surface traits of the produced silver nanoparticles. According to the conclusions, silver nanoparticles with a standard crystalline size of 14.25 nm, as determined by x-ray spectroscopy (xrd), may potentially be manufactured. The Standard X-ray diffraction (XRD) chart for silver nanoparticles (JCPDS silver: 04-0783) revealed four diffraction values at the two values: 38.6, 44.2, 64.2, and 77.3, which equate to 111, 200, 220, and 311 respectively. Additionally, the silver nitrate solution's color changed to brown with constant shaking after being added to a solution of suspended S. boulardii, which proved that nanoparticles were formed. The appearance of these peaks between the specific wavelength of silver nanoparticles, which ranges between 200 and 800 nm, indicates the presence of nanoparticles. The results of the UV/Vis Spectrophotometer revealed the emergence of three peak levels of absorption at 234, 355, and 488 nm in wavelength. The outcomes also showed that silver nanoparticles' surface topography by atomic force microscopy has a mean diameter of 49.61 nm.

1. INTRODUCTION

Medicinal plants and fungy are the major sources of numerous valuable chemicals and drugs[1-6]. Medicinal plants have been discovered since prehistoric times and they were used in traditional medicine. Hundreds of chemical components have been synthesized from plants for using in combating insects, fungi, diseases, and herbivorous mammals. Many phytochemicals with proven or potential biological activity have been known, but the fact that a single plant possesses a large number of diverse chemical substances makes the effect of using the whole plant ineffective, and prevents the evaluation of the activities related to these substances found in many plants in precise scientific research aimed at determining their effectiveness and safety it has been the basis of treatment of various diseases [7-11].

According to [12], the term "nano" is Greek in derivation and refers to an item that is one billionth (9–10) of a meter in size. It also implies "dwarf" in this context.

Groups of atoms between 1 and 100 nanometers in size are referred to as nanoparticles, and the physical and chemical characteristics of nanomaterials can differ significantly from those of the same substance in a greater mass form That is, it deals with atomic clusters ranging from five atoms to a thousand atoms. These dimensions are much smaller than the dimensions of bacteria and a living cell. So far, this technology is not specific to biology, but rather is concerned with the properties of materials, and its fields vary widely from semiconductors to completely modern methods based on molecular self-assembly. This limitation in scale is matched by a broadening of the nature of the materials used, as nanotechnology deals with any phenomena or structures at the nano-level. Such nanoscale phenomena could involve quantum confinement that leads to new electromagnetic and optical phenomena for matter whose size is between the size of a molecule and the visible size of a solid [13].

According to [14], nanoparticles are the essential building blocks of nanotechnology. They are defined as pieces with multiple dimensions , a size of 100 nanometers or fewer, and a number of characteristics that differ from conventional size. Due to their excellent conductivity to heat and electricity, chemically stable nature, strong enzyme activity, and antibacterial characteristics, silver nanoparticles have received particular attention from researchers [15]. Due to its use in industries as varied as medical treatment, coverings, packaging, electronics, and biological technology, silver

*Corresponding Author Institutional Email:
hadeelamoori1989@gmail.com (Hadeel Amoori Abd Ali)

nanoparticles (AgNPs) have attracted a lot of attention [16].

For the aforementioned purposes, silver nanoparticles can be used in several kinds of industries, including clothing, wound care, and other sectors [17].

In general, there are various approaches to manufacture silver nanoparticles: 1: Physical methods 2: Chemical methods Biological modalities

The disadvantages of physicochemical synthesis techniques include higher costs, energy consumption, environmental toxicity, and unsuitability for biological applications because they employ dangerous and toxic substances that can lead to a variety of biohazards [18]. The use of hazardous chemicals during the manufacture of silver nanoparticles (AgNPs) may restrict their use. As a result, finding alternative agents that can reduce silver salts to form nanoparticles without endangering human health or the environment is crucial for science Animal studies indicate that carbon nanotubes and carbon nanofibers can cause pulmonary effects including inflammation, granulomas, and pulmonary fibrosis, and are of similar or greater potential when compared with other known fibrogenic materials such as silica, asbestos, and ultrafine black carbon. Some studies in cells or animals have shown genotoxic or carcinogenic effects, or systemic cardiovascular effects from pulmonary exposure. Although the extent to which data from animal studies may predict clinically significant pulmonary effects in workers is unknown, the toxicity demonstrated in short-term animal studies suggests a need for preventative action for workers exposed to these nanomaterials.

As an alternate to physical and chemical synthesis, natural materials derived from terrestrial and marine living organisms (microorganisms, animals, and plants) were used to create nanoparticles. For the sake of the aforementioned and in order to find alternative, safe, non-harmful and inexpensive methods were used, The objective of the research was to assess Saccharomyces boulardii's efficiency in producing silver nanoparticles [19].

2. MATERIALS AND METHODS

S. boulardii is used in the biological manufacture of silver nanoparticles. This investigation looked at the viability of employing S. boulardii as a biological catalyst to convert silver nitrate into silver nanoparticles in the manner described below.

2.1. The S. Boulardii

The S. boulardii, were obtained from Al-Ameen Center for Research and Advanced Biotechnology in Al-Ataba Al-Alawiya - Najaf.

2.2. Development and Activation of S. Boulardii

Based to the manufacturer's instructions, solid PDA medium was made by dissolving 39 g of powder in 1 liter of distilled water, adjusting the pH to 7, sterilizing in an autoclave at 121 ℃ and under 1 atmosphere for 15 minutes, then pouring into Petri dishes. Bacterial culture was then performed on the solid PDA medium, and the results were reported by [20].

2.3. Preparation of S. Boulardii Solution

The yeast solution was created by putting 10 ml of deionized water into every Petri dish, harvesting the yeast by scraping off the top layer with a sterile razor, and then collecting the solution made up of the yeast and deionized water in opaque cans until it was used to create nanoparticles. This method was modified slightly from [21].

2.4. Prepare a Silver Nitrate Solution [22]

Followed the method of preparing a silver nitrate fluid with a concentration of 1 mM (0.169 mg) and 2 mM (0.340 mg) of silver nitrate in 1 liter of deionized water under dark conditions, covering the glass beaker with commercial aluminum (silophone) and keeping the solution. In a dark way until use.

E-Synthesis of silver nanoparticles mediated by the S. boulardii for the purpose of producing silver nanoparticles using yeast, [23] method was adopted with a few modifications. To do this, 10 ml of the yeast solution prepared as described in paragraph 3 was added in drops to 90 ml of the silver nitrate solution prepared as described in paragraph 4, and 30 minutes were spent stirring the substance on a Magnatic. at a temperature of 35 °C. Once the color change was visible, which was red, the procedure was complete.

3. RESULTS AND DISCUSSION

Evaluation of the effectiveness of S. boulardii synthesis of silver nanoparticles .This investigation examined the potential for employing S. boulardii as a biological catalyst to create silver nanoparticles from silver nitrate. After 120 hours, the hue gradually changed to brown, indicating the production of silver nanoparticles and the reduction of silver nitrate. The reason for the color change can be explained by the role of yeast, as well as the plant, in manufacturing nanoparticles, as the yeast and plant absorb metal ions from the environment or the solutions surrounding them and convert these metal ions into the form of a nano-sized element through enzymatic reduction, as indicated by the change in color is due to the excitation of surface plasmon vibrations in metal nanoparticles. Silver nanoparticles show interesting optical properties that are directly related to the surface plasmon resonance, which depends greatly on the appearance of the nanoparticles.

The rate of reduction and nanoparticle formation can be further increased by increasing the incubation time under experimentally controlled conditions. The reason for the color change can be explained by the role of yeast, as well as the plant, in manufacturing nanoparticles, as the yeast and plant absorb
metal ions from the environment or the solutions surrounding them and convert these metal ions into the form of a nano-sized element through enzymatic reduction . The change in color also indicates the excitation of surface plasmon vibrations in metal nanoparticles. Silver nanoparticles, the rate of reduction and formation of nanoparticles can also be increased further by increasing the incubation time under experimentally controlled conditions, and thus the color intensity increases with increasing reaction time.This shows interesting optical properties that are directly related to the surface plasmon resonance, which depend greatly on the appearance of the nanoparticles. Thus, the color intensity increases with increasing reaction time, as illustrated in Figures. 1 and 2 .

Figure 1. The color change during the synthesis of silver nanoparticles by the S. boulardii .A- Silver nitrate solution + S. boulardii solution after 1 hour. B- Silver nitrate solution only. C- Silver nitrate solution + S. boulardii solution after 120 hours.

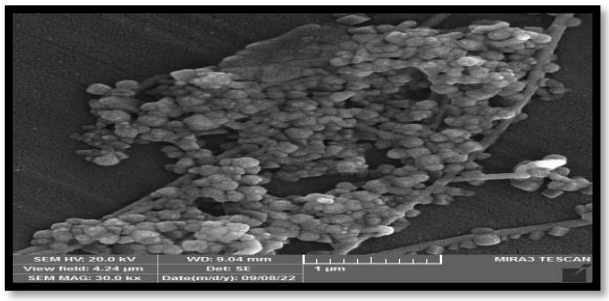

Figure 2. Different shapes and sizes of silver particles formed by S. boulardii under a scanning electron microscope (SEM) at a unit of measurement of 1 col.

4. CONCLUSIONS

The study proved that the possibility of manufacturing silver nanoparticles from S. boulardii .the outcomes also showed that silver nanoparticles' surface topography by atomic force microscopy has a mean diameter of 49.61 nm.

5. APPLICATIONS

In this study, male laboratory rats were used, weighing between (140-160) grams, which were placed in plastic cages and examined in the laboratory by the veterinarian to ensure their safety, then they were given food and water, and then the experiment was carried out.

6. REFERENCES

1. A.S., Abd and L.H. Saqban . “Study of the effect of cytotoxicity of extracts from Origanum Majorana leaves on human breast cancer cell line” (AMJ13) in vitro. AIP Conference Proceedings 2414, 020027 (2023).
2. Z.A., Mezher and L.H., Saqban. “The cytotoxicity effect for the crude extract of Cyperus esculentus tuber on human breast cancer cell line” (MCF-7)in vitro.Indian Journal of Forensic Medicine and Toxicology .vol.14.No.4.2020.
3. M.N., Al-Darraji1, L.H., Saqban,M., Rasheed, A.J., Hussein, T.F., Mutar . “Association of candidate genes polymorphisms in Iraqi patients with chronic kidney disease”. J Adv Biotechnol Exp Ther. 5(3): 687-701.2022.
4. H. H. Obaid, L. H. Saqban and L. Y. Mohammed. “Cytotoxic Effect of Vinca rosea Aqueous Extracts on (L20B) Cell Line In Vitro. Indian Journal of Public Health Research & Development”, Vol. 10, No. 11.2019.
5. L. H., Saqban , A.M., Mezher and H., Ali. “Cytotoxic Effect of the Crude Alcoholic Extract of the Fruits of Citrullus Colocynthis on Human Hepatocyte Carcinoma” (Hep-G2) Archives of Razi Institute, Vol. 77, No. 4 ,1389-1395.2022.
6. N A Abu-Serag, N I Al-Gara,awi, A M Ali, M A Alsirrag. “Analysis of bioactive phytochemical compound of (Cyperusaucheri Jaub.)” by using gas chromatography – mass spectrometry . IOP Conf. Series: Earth and Environmental Science 388 ,012063.2019.
7. N.I., Al-Garaawi, N.A. Abu-Serag, K.A. Shaheed, and Z.K.A., Bahadly. “Analysis of bioactive phytochemical compound of (Cyperus alternifolius L.) by using gas chromatography-mass spectrometry” , IOP Conference Series: Materials Science and Engineering 571(1):1-19.2019.
8. N., AlGaraawi, I., AlAmery, S, F., M. A.,Alwahed Alsirrag. “First record of phytochemical and the antifungal activity of methanol extracts from vegetative parts of Juncus rigidus plants in Iraq”. Caspian Journal of Environmental Sciences, 20: 1011-1021.2022.
9. S.F., AlAmery & N.I., AlGaraawi, “Phytochemical profile and antifungal activity of stems and leaves methanol extract from the Juncus maritimus linn. Juncaceae fam”.2020.
10. N.I., Al-Gara,awi , A.H., AL Edhari and F.K., ALAsadi, “Molecular taxonomic study for the genus juncus l”. (juncaceae) in iraq based on chloroplast gene rpl16. ann. for. res. 65(1): 6313-6319, 2022.
11. Y. K. Alghanimi, and A., Ghasemian , “Inhibitory trait of Dendrosome Curcumin(DNC)on breast cancer compared to curcumin single compound.Journal of Gastrointestinal cancer” 51:527-533.2022.

12. S., Bykkam, ,M., Ahmadipour, S.,Narisngam, V. R., Kalagadda, & S.C., Chidurala . “Extensive studies on X-ray diffraction of green synthesized silver nanoparticles”. Adv. Nanopart, 4(1), 1-10.2 .2015.
13. L., Castro, M.L., Blázquez, F.G.,González &A., Ballester . “Mechanism and applications of metal nanoparticles prepared by bio-mediated process”. Reviews in Advanced Sciences and Engineering, 3(3), 199-216.2014.
14. A., Fariq, T., Khan & A.,Yasmin . “Microbial synthesis of nanoparticles and their potential applications in biomedicine”. Journal of Applied Biomedicine, 15(4), 241-248.2017.
15. J., Harley and L., Prescott. “Laboratory exercises microbiology”. 5th ed. WCB. The Mcgraw-Hill, Companies. New York.2002.
16. B., Koul , A. K., Poonia , D.,Yadav & J.O., Jin. “Microbe-mediated biosynthesis of nanoparticles: Applications and future prospects”. Biomolecules, 11(6), 886.2021.
17. P.,Kouvaris ; A., Delimitis; V.,Zaspalis ;D., Papadopoulos ; S.A.,Tsipas and N., Michailidis. “Green synthesis and characterization of silver nanoparticles produced using Arbutus Unedo leaf extract”. Materials Lett, 76: 18-20.2012.
18. A., Labanni, Z., Zulhadjri,D., Handayani,Y., Ohya andS., Arief . “The effect of monoethanolamine as stabilizing agent in Uncaria gambir Roxb”. mediated synthesis of silver nanoparticles and its antibacterial activity. Journal of Dispersion Science and Technology, 41(10), 1480-1487.2020.
19. X., Li, H., Xu, Z.S., Chen &G., Chen, “Biosynthesis of nanoparticles by microorganisms and their applications. Journal of Nanomaterials”, 2011.
20. X., Li, H., Xu, ,Z.S., Chen &G., Chen “Biosynthesis of nanoparticles by microorganisms and their applications”. Journal of Nanomaterials, 2011.
21. Q.A., Naseer, X., Xue, X., Wang, S., Dang, S. U., Din & J., Jamil. “Synthesis of silver nanoparticles using Lactobacillus bulgaricus and assessment of their antibacterial potential”. Brazilian Journal of Biology, 82.2021.
22. N., Saifuddin,C.W., Wong &A., Yasumira, “ Rapid biosynthesis of silver nanoparticles using culture supernatant of bacteria with microwave irradiation. E-journal of Chemistry, 6(1), 61-70.2009.
23. S.S., Salem, &A., Fouda . “Green synthesis of metallic nanoparticles and their prospective biotechnological applications: an overview. Biological Trace Element Research”, 199(1), 344-370.2011.

Arabic Abstract

تهدف هذه الدراسة إلى تحديد مدى فعالية Saccharomyces boulardii كمحفز بيولوجي لتوليد جسيمات الفضة النانوية باستخدام نترات الفضة. حيود الأشعة السينية (XRD) تم استخدام مجهر القوة الذرية (AFM) لفحص الصفات السطحية. من جسيمات الفضة النانوية المنتجة. وفقا للاستنتاجات، من المحتمل أن يتم تصنيع جسيمات الفضة النانوية ذات الحجم البلوري القياسي البالغ 14.25 نانومتر، كما هو محدد بواسطة التحليل الطيفي للأشعة السينية (xrd). كشف مخطط حيود الأشعة السينية القياسي (XRD) لجسيمات الفضة النانوية (JCPDS Silver: 04-0783) عن أربع قيم حيود عند القيمتين: 38.6، 44.2، 64.2، و77.3، والتي تعادل 111، 200، 220، و311. على التوالي، بالإضافة إلى ذلك، تغير لون محلول نترات الفضة إلى اللون البني مع الاهتزاز المستمر بعد إضافته إلى محلول معلق S. boulardii، وهو دليل على تشكل الجسيمات النانوية. وظهور هذه القمم بين الطول الموجي المحدد لجسيمات الفضة النانوية والذي يتراوح بين 200 و800 نانومتر يدل على وجود الجسيمات النانوية. كشفت نتائج مقياس الطيف الضوئي للأشعة فوق البنفسجية/المرئية عن ظهور ثلاثة مستويات ذروة للامتصاص عند 234، 355، و488 نانومتر في الطول الموجي. كما أظهرت النتائج أن تضاريس سطح جسيمات الفضة النانوية بواسطة مجهر القوة الذرية يبلغ متوسط قطرها 49.61 نانومتر.

Pure Sciences International Journal of Kerbala

Year:2024 Volume : 1 Issue : 3 ISSN: 6188-2789 Print 3005 -2394 Online

Rehab Jasim Mohmmed, Abdulmutalb Badr Manhy Al khaleeli, Nada Habeeb Obaid, The Correlation Between Higher of Human Interleukin-6 and C-reactive Protein in Female Patients with Diabetes Type 2, Pure Sciences International Journal of Kerbala, Vol. 1, No. 3, (2024) 72-78

Pure Sciences International Journal of Kerbala

Journal Homepage:https://journals.uokerbala.edu.iq/index.php/psijk

The Correlation Between Higher of Human Interleukin-6 and C-reactive Protein in Female Patients with Diabetes Type 2

Rehab Jasim Mohmmed[1]*, Abdulmutalb Badr Manhy Al khaleeli[2] , Nada Habeeb Obaid[3]

[1,2,3] *Department of Chemistry, College of Education for Pure Sciences, University of Kerbala*

P A P E R I N F O

Received: 3 June 2024
Accepted: 15 July 2024
Published: 30 September 2024

Keywords:
diabetes mullites type , c-reactive protein, human-IL-6.

A B S T R A C T

Insulin resistance, glucose intolerance, fat deposition, dyslipidemia, and systemic inflammation are all symptoms of type (2) diabetes (T2D). Giving to the Universal Diabetes Confederation, millions of people worldwide will get diabetes. Genetic and environmental variables play a character in the development of T2D. In this investigation, samples were taken from 40 healthy women and 46 female patients with diabetes mellitus type 2. The serum levels of insulin, C-reactive protein, and Human interleukin-6 were measured in all patients and control groups. The results revealed that patient levels of these parameters were significantly more advanced than those in the control group, but the P value was less than 0.001.

1. INTRODUCTION

The umbrella term diabetes mellitus (DM) refers to a group of metabolic disorders brought on by either excessive or inadequate insulin synthesis. It typically presentes hyperglycemia and glucose intolerance, in addition to disrupting the processes that regulate the loading and enlistment of metabolic fuel and producing abnormalities in the metabolism of proteins, lipids, and carbohydrates [1].The International Diabetes Federation (IDF) estimates that 4.2 million individuals worldwide lost their lives to diabetes in 2019. Compared to the current 463 million, it is predicted that 700 million people between the ages of twenty and seventy will have diabetes by millions. The main reason for the at least several billion US dollars that were spent on healthcare in 2019 was diabetes [2].
Furthermore, gestational diabetes significantly increases the patient's offspring's genetic and environmental risk of developing diabetes and obesity due to the intrauterine diabetic environment. Financial statistics for Type 2 Diabetes (T2DM) date back to 1990, and 95% of all instances of diabetes reported in the US and worldwide are on the rise [3]. The aging population, urbanization, socioeconomic advancement, consumption of more highly processed food, and a decline in physical activity are some of the factors behind the exponential expansion. Nearly half of those with T2.DM are unaware that they have it because there are not many symptoms or markers in the early stages of the disorder.
Diabetes problems develop prior to a diagnosis being confirmed due to undiagnosed symptoms [4]. Despite the concerning prevalence of diabetes mellitus, around 193 million individuals lack a diagnosis. Many people are unaware that they have the condition due to factors such as a lack of symptoms or indicators and restricted access to medical care [5].
Based on where it originated, the American Diabetes Association (ADA) has divided diabetes mellitus into the following categories:
The first is
-Type 1 autoimmune idiopathic diabetes (T1DM).
-Type 2 Diabetes Mellitus (T2DM).
- Different forms of diabetes, including gestational diabetes mellitus (GDM) [6].

1.1. Diabetes Mellitus Type 2

Type 2 diabetes is the cause of 90–95 percent of cases of diabetes. In the context of hyperinsulinemia, which is characterized by both metabolic inefficiency and insufficient insulin production to meet the body's needs, insulin resistance leads to hyperglycemia [7]. Because of reduced insulin-mediated glucose uptake by muscle and fat in peripheral tissues, inadequate hepatic glucose output decrease, and ineffective fat-mediated triglyceride uptake, insulin resistance must be fought with increased insulin production [8]. The primary symptoms of this condition are polyuria, polydipsia, polyphagia, weight loss, fatigue, and eyes that seem far from objects. If their chronic hyperglycemia is not treated, diabetic patients may experience serious

*Corresponding Author Institutional Email: *rehab.j@uokerbala.edu.iq* (Rehab Jasim Mohmmed)

consequences [9].

the reasons for type 2 diabetes

For the past ten years, the sole significant element in identifying the congenital etiology of type 2 diabetes (T2DM) has been hypothesis-free genome-wide association studies (GWAS). More than 100 related genetic loci have been discovered using GWAS. Overindulgence and idleness are indicators of excess fat; genetic research has addressed this extensively. Comprehensive evaluations of BMI and related metrics indicate that among people of different descents, genes with high expression of the central nervous system are associated with general obesity [10].

1.2. Human Interleukin-6

Human interleukin-6 (IL-6) was once known by a number of names, including interferon, 26 K factor, B-cell stimulatory factor 2 [11], hybridoma growth factor, plasmacytoma growth factor, hepatocytestimulatory factor [12], hematopoietic factor, and cytotoxic T-cell differentiation factor. The biological activity linked to each name was tested using the same protein. Nowadays, most people are aware of the critical function IL-6 plays in several host defense mechanisms, including immunological response, acute-phase reactions, and hematopoiesis [13,14]. While IL-6 does not seem to have much impact on the body's "housekeeping" duties, when combined with other cytokines, it acts as the body's first line of defense against tissue damage or infection [15]. The functional pleiotropic effect of IL-6 has been shown, wherein. The pathophysiology of IL-6 has been linked to a number of diseases, including psoriasis, osteoporosis, rheumatoid arthritis, multiple myeloma, meningeal proliferative glomerulonephritis, AIDS, and Kaposi's sarcoma [16, 17]. Given the connection between clinical illnesses and abnormal IL-6 production, there has been a lot of interest in understanding the biochemical pathways regulated by IL-6 and in developing functional agonists and antagonists as potential therapeutic drugs for the treatment of IL-6-associated disorders [18]. Depending on the type of target cell, IL-6 influences a variety of proliferative, differentiated, and maturation events. The majority of cytokines and growth factors involved in the immunohemopoietic system share this functional pleiotropy [19].

There may be biological activities that overlap (functional redundancy) or that these cytokines are regulated at their receptors or along their intracellular signal transduction pathways, given that a single cell frequently reacts to several cytokines and growth factors that cooperate. Additionally, it has been demonstrated that several cytokines can function similarly or identically on the same cell. Numerous cells spread throughout the body create cytokines, which are distinct from traditional hormones.

It is a widely accepted belief that the body can more affordably produce pleiotropic biological effects by acting locally on the same cytokine. It is commonly known that the body can manufacture the same cytokine and use it locally to produce pleiotropic biological activity, more reasonably priced [20].

1.3. C.reactive Protein

An acute-phase protein called C-reactive protein (CRP) is a marker for inflammation or infection. When the level of blood protein falls below 10 mg/L, the liver begins to produce the protein. CRP levels rise quickly during the first six to eight hours of an infectious or inflammatory disease and peak 48 hours later at 350–400 mg/L [21]. CRP binds to Pepto saccharides and polysaccharides found on bacteria, parasites, and fungus in addition to the phosphocholine produced on the surface of injured cells. The immune system's classical complement cascade is triggered by this binding, which modifies the activity of phagocytic cells and strengthens the action of CRP in the opsonization of harmful microbes, boosting pathogen and living or dead cell opsonization by CRP, production is a good indicator of disease activity since it reduces when tissue damage or inflammation is treated [22]. Anemia, protein levels, red blood cell shape, patient age, or sex have no effect on CRP levels. However, by the conclusion of pregnancy, women usually have greater CRP levels [23].

The iron of the body and vitamin A status have been measured by serum ferritin, serum retinol, and other acute-phase proteins, which have all been used to compare the various levels of CRP in response to inflammation or infection. In any viral or inflammatory disease, serum ferritin levels increase along with a drop in serum retinol levels. As a result, an inflammatory or viral state could cause an overestimation whereas an underestimating could take place [24].

2. METHOD

In this study, the first group included 46 female patients with type 2 diabetes mellitus who were all between the ages of 35 and 60; the control group included 40 healthy female patients. The patients were seen at Al-Hussein Hospital in Kerbala. Name, age, weight, height, other diseases, and duration were among the details collected from patients and the control group in questionnaires. Each participant in the groups had their antecubital veins punctured with disposable sterile plastic syringes to collect three milliliters of venous blood. The blood samples were drawn into simple tubes without any anticoagulant, and they were left in a 37°C water bath for 15 minutes to clot. To extract serum samples, centrifugation was employed. Using a kit, the levels of human Interleukin-6, high Sensitivity C-reactive protein, and insulin were measured.

3. RESULTS

The results of the study showed that, in contrast to the control group, the patient group had considerably higher concentrations of serum insulin, C-reactive protein, and IL-6. Nevertheless, there was no significant difference in age or BMI, as Table 1 illustrates.

TABLE1. Serum biomarkers in women patients with diabetes type 2 and control subjects.

Parameter	Subject	Mean ± SD	P value
Age year	Patients	38.50 ± 9.12	NS
	Control	36.08 ± 8.55	
BMI kg/m2	Patients	55.22 ± 18.33	NS
	Control	53.10 ± 15.70	
Insulin ng/ml	Patients	18.66 ± 4.22	≤ 0.001
	Control	3.80 ± 1.71	
C-reactive protein(mg/l)	Patients	2.00 ± 2.61	≤ 0.001
	Control	0.52 ± 0.33	
Human IL-6 (pg/ml)	Patients	2.60 ± 1.82	≤ 0.001
	Control	1.32 ± 0.95	

Figure 1 shows the distribution of patients of diabetes mellitus according to age (years) including (35-60 years). Majority of patients (N=23, 58%) presented with age 46-60 years and 17 patients (42%) with age 35-45 years.

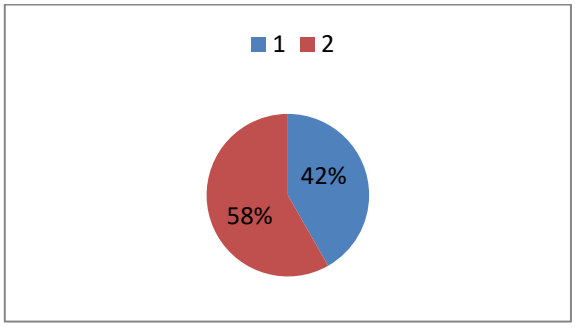

Figure 1. Distribution of patients with diabetes mellitus according to age (N=40).
1: patients of age 35-45 years 2: patients of age 46-60 years.

TABLE 2. Results of relation of age on parameters in women patients and healthy women.

Parameter	Subject	number	Mean ± SD	P value
Insulin ng/ml	35-45 years	17	17.88 ± 4.23	NS
	23			
	46-60 years		18.56 ± 3.31	
C-reactive protein (mg/l)	35-45 years	17	2.10 ± 0.74	≤ 0.001
	23			
	46-60 years		3.41 ± 0.52	
Human IL-6 (pg/ml)	35-45 years	17	2.06 ± 1.87	≤ 0.001
	23			
	46-60 years		3.85 ± 1.11	

4. DISCUSSION

The results in Table 1 of our investigation are explained by recent research showing a correlation between obesity and the development of type 2 diabetes (T2D) and greater amounts of IL-6, C-reactive proteins, and intestinal symbiosis [25]. Because adipocytes produce the essential CRP stimulators, tumor necrosis factor (TNF-) and interleukin 6 (IL-6), high CRP levels have been linked to excess body weight. Furthermore, it is known that under healthy conditions, hepatocytes create substantially less CRP than do T2DM patients, who have elevated levels of inflammatory markers like CRP.

Elevated CRP levels are closely associated with endothelial dysfunction, the synthesis of vasodilators, metabolic syndrome, and vascular system disease. Furthermore, insulin-based therapies may alter CRP levels in T2DM patients [26]. CRP production may be triggered by a number of metabolic and inflammatory factors, such as high blood glucose, adipokines, and free fatty acid levels, which are associated with the onset of type 2 diabetes. Moreover, a high CRP level in individuals with diabetes is a reliable indicator of vascular issues and the onset of cardiovascular disease [27].

Moreover, numerous studies on humans and animals have demonstrated connections between obesity and elevated serum CRP levels, as well as the progression of insulin resistance into type 2 diabetes. These findings provide credence to the hypothesis that the inflammatory state suggested by high CRP levels plays a major role in the pathogenesis of type 2 diabetes. Numerous studies have found a substantial positive correlation between elevated CRP levels and the probability of acquiring type 2 diabetes (28). However, when adjusting for a number of factors known to cause type 2 diabetes, including obesity and hyperinsulinemia, several studies fail to discover this connection. Owing to the fact that obesity and elevated body fat are significant risk factors for the development of type 2 diabetes and they are associated with a higher risk of inflammation and the advancement of insulin resistance (29).

Age, obesity, and inactivity are probably the main factors that affect the onset of type 2 diabetes. Long before the clinical signs of type 2 diabetes appear, IR, which is characterized by hyperinsulinemia and is commonly linked to obesity, hypertension, and dyslipidemia, starts [30]. During insulin resistance (IR), compensatory hyperinsulinemia keeps blood glucose levels normal. Yet, cells lose their capacity to do so due to hypersecretion, which causes hyperglycemia. Subclinical inflammation is a key component of inflammatory response (IR), and there is a positive link between IR and a number of inflammatory markers, including CRP. The innate immune system also produces serum amyloid A and fibrinogen in addition to CRP, the amounts of which change noticeably in response to inflammation, tissue injury, or infection. High concentrations of fibrinogen, sialic acid, CRP, and other

Low levels of albumin, transferrin, and serum amyloid A have all been linked to an increased risk of type 2 diabetes [31]. Inflammation of the adipose tissue and high levels of TNF-, IL-6, and IL-1 in obese people are factors that influence the onset and progression of type 2 diabetes. According to some writers, TNF-inhibits Akt substrate and increases IL-18 synthesis, which helps induce inflammation (IR) in human skeletal muscle. Moreover, TNF-reduces insulin-induced endothelial vasodilation and glucose absorption. TNF- receptors also have an impact on proteins that interfere with insulin signaling, trigger an inflammatory response, and make it easier for the NF-B pathway to activate [32].

However, in the liver and skeletal muscle tissues, IL-6 affects the production and activity of the insulin-degrading enzyme, and the manipulation of this enzyme may be connected to type 2 diabetes and obesity. In fact, a recent meta-analysis found that IL-6 contributes to chronic inflammation in people with T2DM. Because the general population appears to be exposed to insufficient amounts of IL-6, targeting the IL-6 pathway may not reduce the risk of developing type 2 diabetes. Although there is some evidence that CRP contributes to the microvascular effects of diabetes, such as neuropathy, retinopathy, and nephropathy, IL-6 is required for liver homeostasis [33].

Despite the fact that there is some evidence linking CRP to the microvascular effects of diabetes, such as nephropathy, retinopathy, and neuropathy. Elevated glucose levels may lead to increased production of inflammatory factors such TNF-, IL-6, and CRP, which may also cause microvascular alterations. Serum HS-CRP is linked to the development of diabetic neuropathy, one of the most prevalent effects of diabetes. Still, in both male and female patients, peripheral diabetic neuropathy symptoms and inflammation are connected with endothelial dysfunction and elevated CRP blood levels. It is assumed that in individuals with T2DM peripheral neuropathy, increased CRP levels are positively correlated with inflammatory grade [34]. Even though these results provide new insight into the pathophysiology of diabetes, further research is still needed to address unresolved issues.

Animal studies have shown that CRP plays a critical role in infections and inflammatory processes, and that it is produced in response to monocytic mediators such as IL-1 and IL-6 during the acute phase of infections [35]. CRP recognizes and attaches to specific polysaccharides in the bacterial wall to opsonize infections. The complement pathway is further triggered by this. Moreover, evidence suggests that CRP contributes to both proliferative and apoptotic processes by activating Fc receptors, which causes proapoptotic and proinflammatory mediators to produce cytokines. Male Sprague-Dawley rats given streptozotocin show greater serum CRP levels than untreated rats [36].

The antioxidant qualities of vitamin E, according to the same investigators, significantly decreased CRP levels and vascular issues in diabetic mice. A link between elevated CRP levels and the development of type 2 diabetes has been observed in certain human investigations, even after adjusting for other variables such as obesity, hyperinsulinemia, hypertriglyceridemia, and low HDL cholesterol [37]. Additionally, middle-aged diabetic women with elevated CRP levels have higher levels than the group of healthy controls, as reported by Pradhan et al. This finding raises the possibility that inflammation contributes to the etiology of type 2 diabetes. Han et al. also observed variations in the association between the prevalence of T2DM and elevated CRP levels by sex. This significant correlation may be explained by women's higher fat content and distinct hormone profiles [38, 39].

In 44% of the patients, Magrinelli et al. found a significant inverse relationship between serum IL-6 levels and compound muscle action potentials as well as sensory nerve action potentials. They argue that IL-6 plays a role in peripheral nerve axonal damage [40]. According to the study by Brazil, Lebro et al., there was a 19% occurrence of self-reported diabetes among women up to the age of 60 in the United States and Canada between 2005 and 2008. This study explains why the majority of women with type 2 diabetes between the ages of 46 and 60 were in the second group and had higher levels of inflammatory factors than the first group of female patients.

According to estimates, 26.9% of adults over 65 had diabetes. Previous studies using occupational cohorts have suggested that the self-rated health is mainly a reflection of physical and mental health problems and, to a lesser degree, of age, early life circumstances, family history, sociodemographic traits, psychosocial factors, and behavior related to health. It was found that living alone was linked to type 2 diabetes in men but not in women in a population cohort comprising both sexes [42].

The results of the study by Lidfeldt et al. [43] may be explained by the fact that women in Brazil who are most likely to have type 2 diabetes are older and live with others because they require care. It is also feasible that these women are in worse health and have lower incomes than other women. An rise in BMI between the ages of 20 and 30 was another factor that led to the onset of diabetes and its effects on inflammatory variables. Studies have shown that being obese or overweight when you are younger may increase your risk of developing diabetes [44].

Kim et al. found that among women in the Diabetes Prevention Program who were at high risk for the condition, going through a normal menopause did not increase their risk of developing diabetes. The lack of correlation between menopausal state and diabetes risk may be explained by the fact that the majority of women were postmenopausal at the time the condition developed [45]. The doctor's diagnosis report also established the age at which diabetes first became apparent. Other levels of aberrant glucose tolerance were not taken into account.

5. CONCLUSION

Human IL-6, C-reactive" protein, and type" 2 diabetes in women are strongly correlated.

5. REFERENCES

1. Padhi, S., Nayak, A. K., & Behera, A .)2020(.Type II diabetes mellitus: A review on recent drug based therapeutics. Biomedicine & Pharmacotherapy, 131, 110708 .
2. Galicia-Garcia, U., Benito-Vicente, A., Jebari, S., Larrea-Sebal, A., Siddiqi, H., Uribe, K. B., Ostolaza, H., & Martín, C. (2020). Pathophysiology of type 2 diabetes mellitus .International journal of molecular sciences, 21(17), 6275.
3. Kirtland, K. A., Cho, P., & Geiss, L. S. (2015). Diabetes among Asians and Native Hawaiians or other Pacific Islanders—United States, 2011–2014. Morbidity and Mortality Weekly Report, 64(45), 1261-1266 .
4. ATLAS, I. (2019). 2017: http://www. diabetesatlas. org. Accessed on Feb 10th .
5. Saeedi, P., Petersohn, I., Salpea, P., Malanda, B., Karuranga, S., Unwin, N., Colagiuri, S., Guariguata, L., Motala, A. A., & Ogurtsova, K. (2019). Global and regional diabetes prevalence estimates for 2019 and projections for 2030 and 2045: Results from the International Diabetes Federation Diabetes Atlas. Diabetes research and clinical practice, 157, 107843 .
6. Saini, V. (2010). Molecular mechanisms of insulin resistance in type 2 diabetes mellitus. World journal of diabetes, 1(3), 68.
7. Cancienne, J. M., Brockmeier, S. F., & Werner, B. C. (2018). Association of perioperative glycemic control with deep postoperative infection after shoulder arthroplasty in patients with diabetes. JAAOS-Journal of the American Academy of Orthopaedic Surgeons, 26(11), e238-e245 .
8. Zierath, J. R. (2019 .)Major advances and discoveries in diabetes-2019 in review. Current diabetes reports, 19(11), 1-9 .
9. Morris, A. P. (2018). Progress in defining the genetic contribution to type 2 diabetes susceptibility. Current opinion in genetics & development, 50, 41-51 .
10. Heitkamp, M., Siegrist, M., & Halle, M. (2021). Consideration of Sex Differences in Children With Obesity—Reply. JAMA pediatrics, 175(7), 748- 749.
11. Kishimoto, T., Akira, S., Narazaki, M., &Taga, T. (1995). Interleukin-6 family of cytokines and gp130.
12. Moore, J. B., & June, C. H. (2020). Cytokine release syndrome in severe COVID-19. Science, 368(6490), 473-474.
13. Ohsugi, Y. (2020). The immunobiology of humanized Anti-IL6 receptor antibody: From basic research to breakthrough medicine. Journal of Translational Autoimmunity, 3, 100030.
14. Scheller, J., Garbers, C., & Rose-John, S. (2014, February). Interleukin-6: from basic biology to selective blockade of pro-inflammatory activities. In Seminars in immunology (Vol. 26, No. 1, pp. 2-12). Academic Press.
15. Gabay, C. (2006). Interleukin-6 and chronic inflammation. Arthritis research & therapy, 8(2), 1-6.
16. Hunter, C. A., & Jones, S. A. (2015). IL-6 as a keystone cytokine in health and disease. Nature immunology, 16(5), 448-457.
17. Jones, S. A., & Jenkins, B. J. (2018). Recent insights into targeting the IL-6 cytokine family in inflammatory diseases and cancer. Nature reviews immunology, 18(12), 773-789.
18. Bastard, J. P., Jardel, C., Delattre, J., Hainque, B., Bruckert, E., & Oberlin, F. (1999). Evidence for a link between adipose tissue interleukin-6 content and serum C-reactive protein concentrations in obese subjects. Circulation.
19. Held, C., White, H. D., Stewart, R. A., Budaj, A., Cannon, C. P., Hochman, J. S., ... & STABILITY Investigators. (2017). inflammatory biomarkers interleukin-6 and C-reactive protein and outcomes in stable coronary heart disease: experiences from the STABILITY (stabilization of atherosclerotic plaque by initiation of darapladib therapy) trial. Journal of the American Heart Association, 6(10), 005077.
20. Nesbitt JE, Fuller GM. 1992. Dynamics of interleukin-6 internalization and degradation in rat hepatocytes. J Eiol Chem 2675739-5742.
21. Cals JW, Schot MJ, de Jong SA, Dinant GJ, Hopstaken RM. Point-of-care C-reactive protein testing and antibiotic prescribing for respiratory tract infections: a randomized controlled trial. Annals of family medicine. 2010;8(2):124-33.
22. Calvino O, Llor C, Gomez F, Gonzalez E, Sarvise C, Hernandez S. Association between C-reactive protein rapid test and group A streptococcus infection in acute pharyngitis. Journal of the American Board of Family Medicine : JABFM. 2014;27(3):424-6.
23. Bjerrum L, Gahrn-Hansen B, Munck AP. C-reactive protein measurement in general practice may lead to lower antibiotic prescribing for sinusitis. The British journal of general practice: the journal of the Royal College of General Practitioners. 2004; 54(506):659-62.
24. Llor C, Bjerrum L, Arranz J, Garcia G, Cots JM, Gonzalez Lopez-Valcarcel B, et al. C-reactive protein testing in patients with acute rhinosinusitis leads to a reduction in antibiotic use. Familypractice. 2012;29(6):653-8.
25. Thorand B., Löwel H., Schneider A., et al. C-reactive protein as a predictor for incident diabetes mellitus among middle-aged men: results from the MONICA Augsburg cohort study, 1984-1998. Archives of Internal Medicine . 2003;163(1):93–99. doi: 10.1001/archinte.163.1.93. [PubMed] [CrossRef] [Google Scholar]
26. Abernethy T. J., Avery O. T. The occurrence during acute infections of a protein not normally present in the blood : i. distribution of the reactive protein in patients' sera and the effect of calcium on the flocculation reaction with c polysaccharide of pneumococcus. The Journal of Experimental Medicine. 1941;73(2):173–182. doi: 10.1084/jem.73.2.173. [PMC free article] [PubMed] [CrossRef] [Google Scholar].
27. Esser N, Paquot N, Scheen A. J. Inflammatory markers and cardiometabolic diseases. Acta Clinica Belgica . 2015; 70(3):193–199. doi: 10.1179/2295333715Y.0000000004. [PubMed][CrossRef] [Google Scholar].
28. van Woudenbergh G. J., Kuijsten A., Sijbrands E. J. G., Hofman A., Witteman J. C. M., Feskens E. J. M. Glycemic index and glycemic load and their association with C-reactive protein and incident type 2 diabetes. Journal of Nutrition and Metabolism. 2011;2011:623077. doi: 10.1155/2011/623076. [PMC free article] [PubMed] [CrossRef] [Google Scholar]
29. Cani PD, Delzenne NM. The role of the gut microbiota in energy metabolism and metabolic disease. Curr Pharm Des (2009) 15:1546–58. doi:10.2174/138161209788168164. PubMed Abstract | CrossRef Full Text | Google Scholar.
30. Rao G. Insulin resistance syndrome. American Family Physician . 2001;63(6):1159–1163. [PubMed] [Google Scholar].
31. Crook M. Type 2 diabetes mellitus: a disease of the innate immune system? An update. Diabetic Medicine . 2004;21(3):203–207. doi: 10.1046/j.1464-5491.2003.01030.x. [PubMed] [CrossRef] [Google Scholar].
32. Mohallem R., Aryal U. K. Regulators of TNFα mediated insulin resistance elucidated by quantitative proteomics. Scientific Reports . 2020;10(1):p. 20878. doi: 10.1038/s41598-020-77914-1. [PMC free article] [PubMed] [CrossRef] [Google Scholar].

33. Bowker N., Shah R. L., Sharp S. J., et al. Meta-analysis investigating the role of interleukin-6 mediated inflammation in type 2 diabetes. eBioMedicine. 2020;61, article 103062 doi: 10.1016/j.ebiom.2020.103062. [PMC free article] [PubMed] [CrossRef] [Google Scholar].
34. Zhang H. H., Han X., Wang M., et al. The association between genomic DNA methylation and diabetic peripheral neuropathy in patients with type 2 diabetes mellitus. Journal of Diabetes Research . 2019;2019 doi: 10.1155/2019/2494057.2494057 [PMC free article] [PubMed] [CrossRef] [Google Scholar].
35. Ryu J., Lee C., Shin J., et al. FcγRIIa mediates C-reactive protein-induced inflammatory responses of human vascular smooth muscle cells by activating NADPH oxidase 4. Cardiovascular Research . 2007;75(3):555–565. doi: 10.1016/j.cardiores.2007.04.027. [PubMed] [CrossRef] [Google Scholar].
36. Zou X. L., Yang J., Yang J. M., et al. Brief communication (original). Immune injury in rat models of type 2 diabetes mellitus. Asian Biomedicine . 2017;6(6):903–908. [Google Scholar].
37. Cho W. C., Yip T. T., Chung W. S., Leung A. W., Cheng C. H., Yue K. K. Differential expression of proteins in kidney, eye, aorta, and serum of diabetic and non-diabetic rats. Journal of Cellular Biochemistry . 2006;99(1):256–268. doi: 10.1002/jcb.20923. [PubMed] [CrossRef] [Google Scholar].
38. Han T. S., Sattar N., Williams K., Gonzalez-Villalpando C., Lean M. E. J., Haffner S. M. Prospective study of C-reactive protein in relation to the development of diabetes and metabolic syndrome in the Mexico City Diabetes Study. Diabetes Care . 2002;25(11):2016–2021. doi: 10.2337/diacare.25.11.2016. [PubMed] [CrossRef] [Google Scholar]
39. Thorand B., Baumert J., Kolb H., et al. Sex differences in the prediction of type 2 diabetes by inflammatory Markers. Diabetes Care 2007;30(4):854–860. doi: 10.2337/dc06-1693. [PubMed] [CrossRef] [Google Scholar].
40. Mohallem R., Aryal U. K. Regulators of TNFα mediated insulin resistance elucidated by quantitative proteomics. Scientific Reports . 2020;10(1):p. 20878. doi: 10.1038/s41598-020-77914-1. [PMC free article] [PubMed] [CrossRef] [Google Scholar].
41. National Diabetes Statistics. 2011. http://diabetes.niddk.nih.gov/dm/ pubs/statistics/ (accessed 1 Aug 2012).
42. Agardh E, Allebeck P, Hallqvist J, et al. Type 2 diabetes incidence and socio-economic position: a systematic review and metaanalysis. Int J Epidemiol 2011;40:804–18.
43. Lidfeldt J, Nerbrand C, Samsioe G, et al. Women living alone have an increased risk to develop diabetes, which is explained mainly by lifestyle factors. Diabetes Care 2005;28:2531–6.
44. Talaei M, Sadeghi M, Marshall T, et al. Anthropometric indices predicting incident type 2 diabetes in an Iranian population: the Isfahan Cohort Study. Diabetes Metab 2013;39:424–31.
45. Kim C, Edelstein SL, Crandall JP, et al.; Diabetes Prevention Program Research Group. Menopause and risk of diabetes in the Diabetes Prevention Program. Menopause 2011;18:857–68.

Arabic Abstract

مقاومة الأنسولين، عدم تحمل الجلوكوز، ترسب الدهون، دسليبيدميا، والالتهابات الجهازية كلها أعراض لمرض السكري من النوع (2) T2D من خلال التبرع للاتحاد العالمي للسكري، سيصاب ملايين الأشخاص في جميع أنحاء العالم بمرض السكري. تلعب المتغيرات الجينية والبيئية دورًا في تطور مرض السكري من النوع الثاني. في هذا البحث، تم أخذ عينات من 40 امرأة سليمة و46 مريضة مصابة بداء السكري من النوع 2. تم قياس مستويات الأنسولين والبروتين التفاعلي C والإنترلوكين البشري 6 في جميع المرضى ومجموعات المراقبة. وكشفت النتائج أن مستويات هذه المعلمات لدى المرضى كانت متقدمة بشكل ملحوظ عن تلك الموجودة في المجموعة الضابطة، ولكن قيمة P كانت أقل من 0.001.

Pure Sciences International Journal of Kerbala

Year:2024 Volume : 1 Issue : 3 ISSN: 6188-2789 Print 3005 -2394 Online

Shaymaa Malik Yasir, Hanaa Mumtaz Hussein, Dalal Abdel-Hussein Kadhim AL–Essawi, Histological Influences and Liver Weight Measurements in Female Rats and Their Embryos After Spasmine Drug Administration, Pure Sciences International Journal of Kerbala, Vol. 1 No. 3, (2024) 79-87

2024 ,Volume 1 , Issue 3 PSIJK 79-87

Pure Sciences International Journal of Kerbala
Journal Homepage:https://journals.uokerbala.edu.iq/index.php/psijk

Histological Influences and Liver Weight Measurements in Female Rats and Their Embryos After Spasmine Drug Administration

Shaymaa Malik Yasir[1*], Hanaa Mumtaz Hussein[2], Dalal Abdel-Hussein Kadhim AL–Essawi[3]

[1]Biology Department, College of Education for Pure Sciences, Kerbala University, Karbala, Iraq
[2,3]Biology Department , Education for Girls Faculty , Kufa University , Iraq

P A P E R I N F O

Received: 5 September 2024
Accepted: 26 September 2024
Published: 30 September 2024

Keywords:
Spasmine, Weights, Livers, Embryo, Pregnant, Rats, Histological Influences.

A B S T R A C T

A study was conducted to determine the role of spasmin in some weight and histological parameters of the livers of pregnant female rats and their fetuses on the nineteenth day of pregnancy. The study was conducted at the College of Education for women at the University of Kufa for the period from January 1- 2022, until June 15- 2022. After obtaining 8 pregnant rats, 4 of them were dosed with a dose of the physiological solution. This group represented the control (G1), while 4 pregnant female rats were dosed with spasmin drug at a dose of (0.48 mg/kg/body weight) (G2) for 19 days. The pregnant rats in the control group were (12) weeks old and weighed (231) grams, while the pregnant animals in the group treated with spasmin were (11) weeks old and weighed (230) grams.

The results of the study recorded a significant decrease ($P < 0.05$) in the liver weights of both pregnant animals and their fetuses in groups of rats treated with spasmin. The results also showed that treating rats with spasmin until the nineteenth day of pregnancy led to histopathological and abnormal changes in liver tissue such as damage to the central vein wall, hepatocyte necrosis, sinusoidal expansion, hepatic tissue necrosis and inflammatory cell infiltration in pregnant rats and their fetuses compared to pregnant rats and their fetuses in control groups during pregnancy on the nineteenth day.

The study concludes that the treatment with spasming drug reduced the weight of pregnants and embryos' liver of embryos and also caused various histopathological changes in the structure of the livers of the pregnant rats and their embryos during the 19th day of gestation.

1. INTRODUCTION

Medical drugs are prescribed for the treatment of many diseases, as each drug has a therapeutic effect for different diseases but these drugs may cause many side effects that may be mild in some or severe in other types of them which affect many body systems. Since the wrong and unauthorized use of drugs induces dangerous and threatening effects on humans[1,2], some studies have pointed to that different drugs may pass through the placenta from the mother to the embryo during the differen stages of gestation causing harmful effects in the body systems of pregnant women and their embryos alike.This happens because these drugs when they enter the body the pharmacological action is not limited to the affected organs but they cause harmful effects on the healthy organs of the body as well when they are present in them.This is due to the fact that they stimulate disorders in their metabolic functions [3,4], as these drugs have the ability to stimulate congenital disorders in embryos during gestation and newborns after birth and even adults alike.This may cause death and for this reason many drugs are prepared during the different stages of gestation to ensure the safety of these medical drugs as the stage of gestation is critical for mothers as well as embryos [5]. The spasmine medication is classified as a p-methoxybenzoic acid derivative and it is commonly used to treat gastrointestinal disorders. Specifically, it functions as an antispasmodic to alleviate symptoms associated with chronic irritable colon , colitis of spastic and mucous and irritable bowel syndrome, and spastic constipation. Its mechanism of action involves direct sedation and muscle relaxation of the smooth muscles within the digestive system, thereby reducing painful cramps. Additionally, Spasmine is effective in treating accompanying symptoms of irritable bowel syndrome, including intestinal colic, flatulence, diarrhoea, constipation, and the passage of small, hard stools. The exact mechanism of action of this drug is still unknown but it is considered one of the santispasmodic effect through its direct activity on a smooth muscles of the digestive system .This causes these muscles to relax without impacting the normal bowel movement and several mechanisms are postulated to construe the action of spasmine on the digestive system .The most

*Corresponding Author Institutional Email:
shaimaa.malik@uokerbala.edu.iq (Shaymaa Malik Yasir)

important one is that the inhibition of receptors for acetylcholine, alters in the process for water absorption, reduced permeability of ion channels, local anesthetic effects in addition to the reuptake inhibitor of norepinephrine [8,9]. Spasmine drugs come in multiple forms such as oral capsules and pills in addition to oral liquid [10].The efficiency of this drug begins about an hour after taking it and the patient feels the disappearance of pathological symptoms after (1-3) hours of implementing the drug.However, this period may increase depending on the health status of patients [11]. Spasmine drug is like any other drug whose use is supported by some side effects like as loss of appetite, dry mouth, skin irritation headache, insomnia, depression, heartburn, indigestion, difficulty sleeping, diarrhoea, feeling unwell and tired, slow heartbeat, immune system disorders such as allergic responses causing hypersensitivity which appear in the form of skin rashes, urticaria and facial edema.Taking this drug with other drugs or certain meals may cause interactions that may reduce the effectiveness of the drugs used as the effectiveness of one drug might reduce the effectiveness of the other drug or may affect the patient's health [12,13]. The purpose of the study is due to the lack of research and studies on the impact of spasming on the tissue of the liver during pregnancy. That is, the present study investigates the potential impact of spasming drugs on weights as well as histological structures of the livers of pregnant rats and their embryos for gestation of nineteenth day.

2. MATERIALS AND METHODS

2.1. Study Animals

White female of rat animals from species Rattus rattus with ages (12 weeks)and weights (231g) were used, along with white male of rats from same species in a typical ages (11 weeks)and a weights (229 g). These animals were obtained to the College of Sciences / University of Kufa, and both sexes were housed in plastic cages with identical ventilation, temperature, and lighting conditions.

2.2. Drug Dose

Spasmin was administered in pill form at a dose of 100 mg. The concentration for the study was adjusted based on the weight of the animals and then administered to pregnant rats.

2.3. Pregnant Rats

To obtain pregnant female rats, a single adult female rat was placed with one fertile male rat in every pairing up a cage in the evening, and the animals were left overnight. The following morning, the female rats were tested for seeing the vaginal plug in the female's vagina or in cage and as depicted in Figure A .It was determined that gestation had occurred based on the presence of the vaginal plug, which was thought about the zero-day of gestation. [14]

Figure A. (VP)Vaginal Plugs

2.4. Experiment Design

This study's main experiment was designed to examine the probable side impacts of spasmine on weights and tissue modifications of livers in embryos and pregnant rat animals treated of this drug during gestation for 19th day. After mating male and female rats and obtaining pregnant rats, 8 pregnant rats:4 of them as control group (G1) and 4 of pregnant female rats were given in spasming drug at the dose of (0.48 mg/kg / b.w.) (G2) by peritoneal intramembranous injection at the rate of one injection per day for 19 days of gestation.

2.5. Pregnant Rats Dissection

Pregnant rats were annotated on the 20th day of gestation after being anesthetized with chloroformthe pregnant rodents were pinned to a dissection dish before the abdominal cavity was cut opened with pointed scissors. the livers of the pregnant rats were extracted and washed with a physiological solution and dried with filter paper. Their weight was measured by a normal weight balance, the uterine horns containing the embryos were also removed after removing the connective tissue and the fatty substances attached to it.

2.6. Embryos Dissection

After pregnant female rats dissection during gestation for 20th days, the two uterus horns and its contents of the embryos, then two horns of the uterus were opening by scissors to extract the embryos which were washed with physiological solution and dried with filter paper, then the embryos were anesthetized by placing a quantity of chlorform in the cotton, after that they were dissected by opening the cavity abdominal and the livers were extracted from the body and their weights were measured with a sensitive balance, then embryo livers were preserved with formalin solution at a concentration of 10% for 48 hours in order to prepare them for histological sections.

2.7. Histological Section of Livers of Pregnant Rats and Embryos

During gestation for 19th days, tissue sections of livers of pregnant animals and their embryos were made using this method. [15]

2.8. Examination of Histological Liver Sections Embryos

The sections of liver tissues of all pregnant rats and their embryos during gestation for 19th days were prepared.Then, these tissue sections were examined and photographed using a MEIJT light microtope equipped with a samsung imaging camera installed on the microscope and on the powers (10X and 40X) respectively.

2.9. Statistically Data Analysis

The studied data were calculated by using the statistical system (SPSS) for version 21. Values were mean ± standard error and ($P<0.05$) was a probability level used in this study to extract the least significant diffefences (LSD) for determining the significant differences among the groups. [16]

3. RESULTS AND DISCUSSION

Results of the study revealed a significant decrease at the probability level ($P<0.05$) in the liver weights of pregnant rats and embryos in the spasmine drug-treated pregnant rat group during the 19th day of gestation respectively when compared with the pregnant rat animals liver weights and embryos in group of control in a day 19 of gestation as shown in Table 1 and Table 2 respectively.Concerning the results of the histological study of the livers of the embryos whose mothers were handled with the spasmine drug,they suffered from different pathological effects on its histological structure. It was represented by the loss of the general structure of the hepatic tissue which may be a result of the lack of development and growth of a hepatic tissue.The developed tissue can be observed many pathological changes such as destruction of the central vein wall, necrosis and degeneration of hepatocyte, expanding of sinusoids, congestion and necrosis of hepatic tissue , bleed clotting and inflammatory cell infiltration as shown in the Figures (2,3,4,6,7,8,9,10,11,12,13 and 14) respectively when compared with the normal histological framework of the livers of embryos in the control group, Figures (1,5) and the examination results of histological sections of pregnant rats livers in control animals throughout 19th day of gestationwhich did not show any abnormal changes as shown in the Figures (15,19) respectively. The histological results of sections of pregnant female livers that were given with spasmin during the 19th day of gestation demonstrated different histopathological changes represented by expansion and destruction of the central vein wall, necrosis and degeneration of hepatocyte, widening of sinusoids, bleeding into hepatic tissue and blockages , necrosis and damage of hepatic tissue and inflammatory cell infiltration as in Figures (16,17,18, 20,21,22,23,24,25 and 26) respectively.

In view of lack of sufficient researches of spasmine drug effect on weights and structure of the various organ tissues of the body especially the liver in pregnant rats during gestationor or in embryos throughout the different stages of gestation,these results in this research can be attributed to the fact that spasmine drug caused the decrease in pregnant animal liver weights and the embryos due to its toxic effect which stimulated pathological effects on the histological structure of the liver during gestation as a result of its induction of programmed cell passing away (Apoptosis) and necrosis in addition to the occurrence of degenerative changes in it causing a destruction of the hepatic tissue and others organ tissues of the rats and the failure of the development and destruction of the liver tissue of embryos causing decrease in the weight of the livers in them .This is what the electricity study showed [17,18] , or it may be because that spasmine drug is the cause of the destruction of various pregnant rats' tissues, especially the horns of the uterus and placenta leading to a decrease of oxygen and various nutrients necessary for growth to embryos during gestation which triggered the destruction of different body tissues like livers and its absence of their growth and low weights [19] .As for the histopathological effects induced by the drug under study in the liver tissues of pregnant rats and embryos during nineteen days of gestation, it may be due to the ability of spasmine drug on the generation of free radicals in cells cells and organs of the body in general and liver tissue cells particularly causing programmed death of cells and necrosis thus destroying and wrecking liver tissue [20] as the production of free radicals, which are potent oxidising factors, stimulates the oxidation process of lipids in cell membranes as well as other essential macromolecules inside cells such as nuclear acidic substances (DNA), proteins, and others, causing oxidative stress to every part of the body including cells of the liver tissue, which ultimately results in necrosis of the cells for the various tissues and thus destroys them.This may be attributed to the fact that free radicals are effective oxidising factors [21] ,the free oxygen radicals arising from various medical drugs including spasmine plays a consequential role in the breakdown in body organs , as they are strong oxidizing agents for lipids in cell membranes causing their destruction especially when there levels exceed normal levels stimulating oxidative stress which leads to the depletion for various self-antioxidants in the body that it works to inhibit a activity of free radicals and stop their

destructive action to the cells of various organs but when the levels for free radicals exceed the levels of antioxidants and the destructive action of cells as well as tissues of these free radicals will increase stimulating distinct histological impacts on the tissue structure of the liver and other body systems in pregnant rats and eggs in which the systems of the defense against antioxidants is weak and that they are not developed to counter the action of free radicals generated by the drug when it passes from the mother to a embryo through the placenta blood leading to oxidative destruction in the fetal tissues and stimulating histopathological effects in them [22, 23, 24], since these free radicals cause the devastation of mother's tissues such as the uterus and placenta and what they contain of blood vessels which leads for a failure to reach the blood that provides oxygen as well as other nutrients to the cells as a result of necrosis and degeneration of the cells of these blood vessels and as an result the tissue cells are exposed to a lack of oxygen and nutrition necessary for cells to carry out their various functions and these promote harmful histological effects on body organs [24].

TABLE 1. Spasmine Effects on Embryos Liver Weights During the 19th Day of Gestation.

Treatments	weights (g) M±SE
Control Group (G1)	0.150 ± 0.002
Spasmin Drug Treated Group (G2)	0.071 ± 0.005
LeasSignificant Difference (LSD)	0.350

TABLE 2. Spasmine effects on pregnant Rats' liver weights during 19th day of gestation.

Treatments	weights (g) M±SE
Control Group (G1)	8.25±0.01
Spasmin Drug Treated Group (G2)	7.50±0.04
LeasSignificant Difference (LSD)	0.20

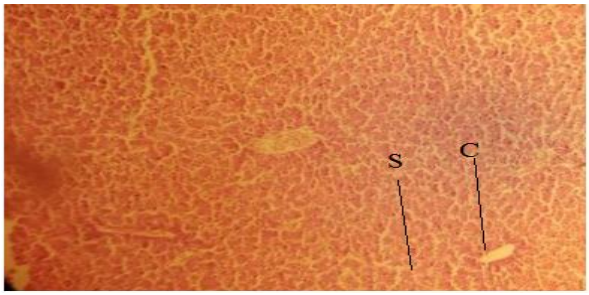

Figure 1. A Cross-section of liver tissue of a rat fetus from a control group: Hepatic tissue should have the following normal structure: Central vein (C), sinusoids (S) (H & E -stain, 10x).

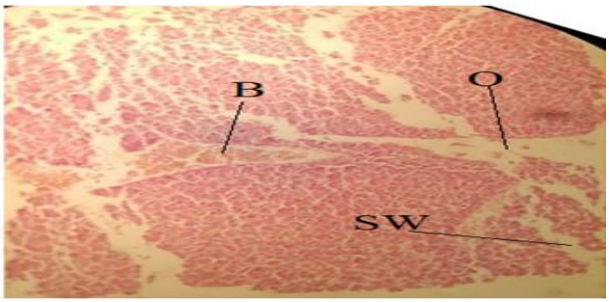

Figure 2. A Cross-section of liver tissue from a rat fetus from a dosed mother with spasmine. It shows: the following: Necrosis of hepatic tissue (O), expansion of sinusoids (Sw), and bleeding into hepatic tissue (B) (H & E -stain, 10x).

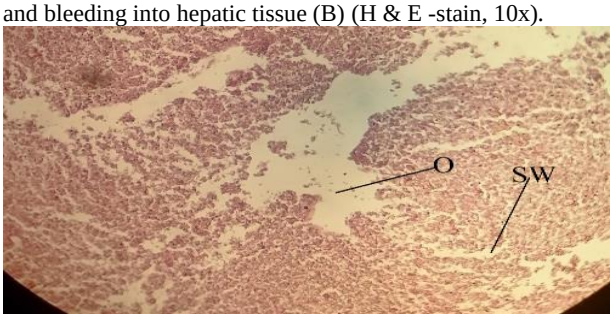

Figure 3. A Cross-section of liver tissue from a rat fetus from a dosed mother with spasmine: Expansion of the sinusoids (Sw), congestion into the hepatic tissue (B), and necrosis of the hepatic tissue (O) (H & E- stain, 10x).

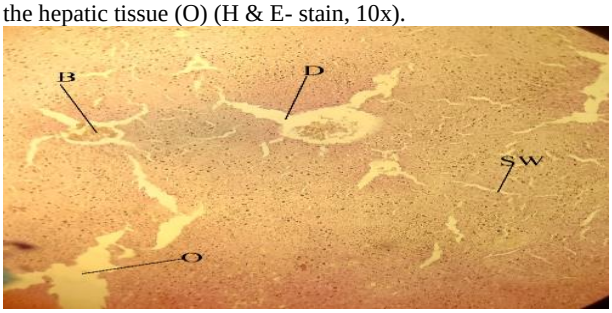

Figure 4. A Cross-section of liver tissue from a rat fetus from a dosed mother with spasmine: A breakdown in the fundamental architecture of the hepatic tissue, Widening of sinusoids (Sw) and necrosis of liver tissue (O) (H & E -stain, 10x).

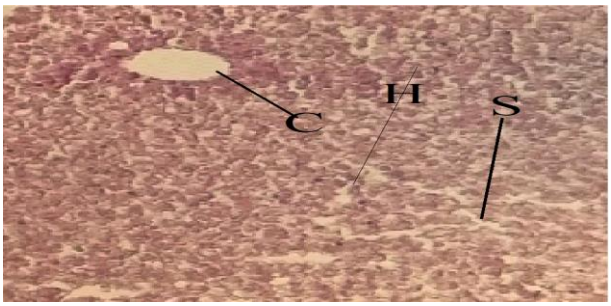

Figure 5. A Cross-section of liver tissue of a rat fetus from a control group :Normal structure of hepatic tissue, showing the central vein (C), sinusoids (S), and hepatic cells (H) (H & E-stain, 40X).

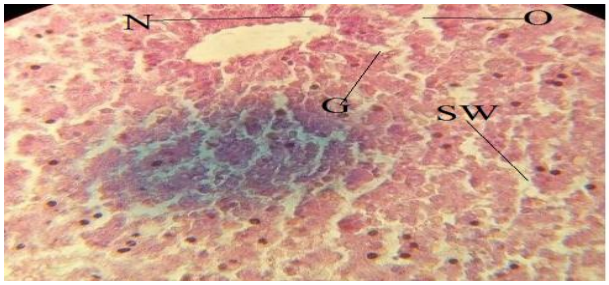

Figure 6. A Cross-section of liver tissue from a rat fetus from a dosed mother with spasmine::hepatocyte necrosis (N), hepatocyte degeneration (G), sinusoids expanding (SW), and necrosis into hepatic tissue (O) (H & E- stain, 40X).

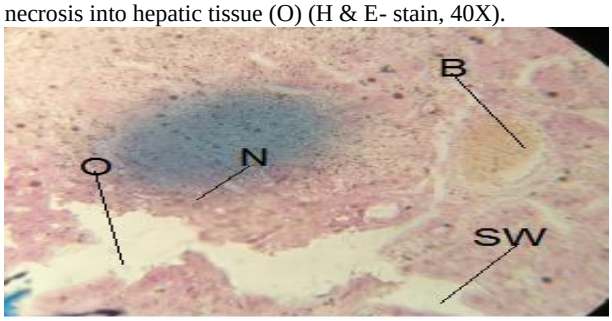

Figure 7. A Cross-section of liver tissue from a rat fetus from a dosed mother with spasmine:Hepatocyte necrosis (N), sinusoids broadening (SW), necrosis into hepatic tissue (O), and congestion into central vein (B) (H & E- stain, 40X).

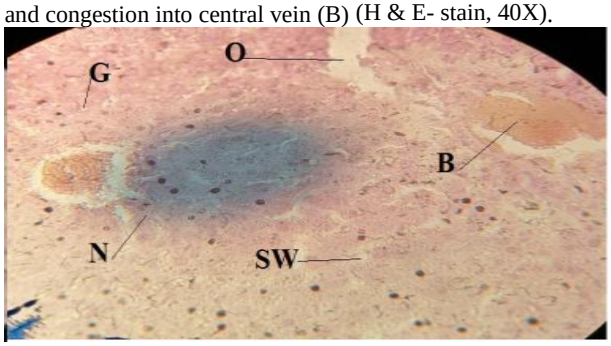

Figure 8. A Cross-section of liver tissue from a rat fetus from a dosed mother with spasmine :Hepatocyte necrosis (N), sinusoids broadening (SW), necrosis into hepatic tissue (O), and congestion into central vein (B) (H & E- stain, 40X).

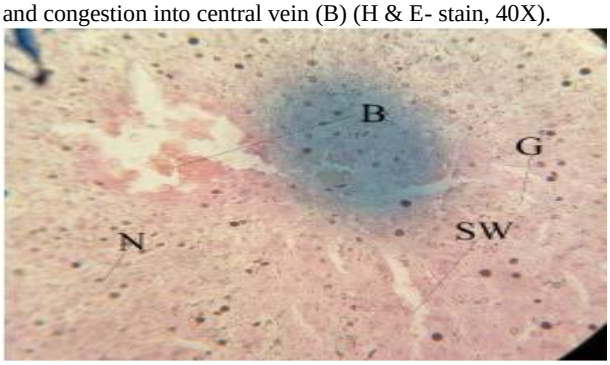

Figure 9. A Cross-section of liver tissue from a rat fetus from a dosed mother with spasmine::hepatocyte necrosis (N), hepatocyte degeneration (G), sinusoids expanding (SW), and congestion into the central vein (B) (H & E -stain, 40X).

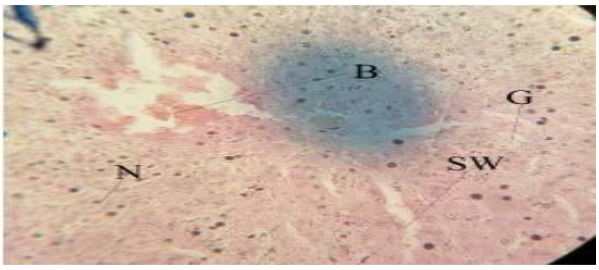

Figure 10. A Cross-section of liver tissue from a rat fetus from a dosed mother with spasmine: Hepatocyte necrosis (N), hepatocyte degeneration (G), sinusoids expanding (SW), necrosis into hepatic tissue (O), and inflammatory cell infiltration (F) (H & E- stain, 40X).

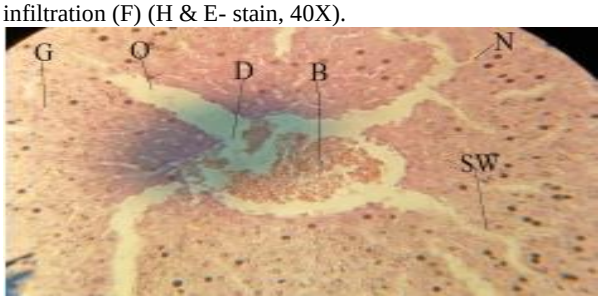

Figure 11. A Cross-section of liver tissue from a rat fetus from a dosed mother with spasmine: destruction of central vein wall (D), (N), hepatocyte degeneration (G), sinusoids hepatocyte necrosis widening (SW), necrosis into the hepatic tissue (O), and congestion into the central vein (B) (H & E -stain, 40X).

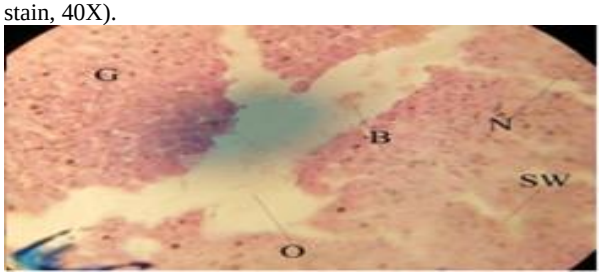

Figure 12 . A Cross-section of liver tissue from from a dosed pregnant rat from dosed with spasmine: hepatocyte necrosis (N), hepatocyte degeneration (G), sinusoids expanding (SW), necrosis into hepatic tissue (O), and bleeding (B) (H & E-stain, 40X).

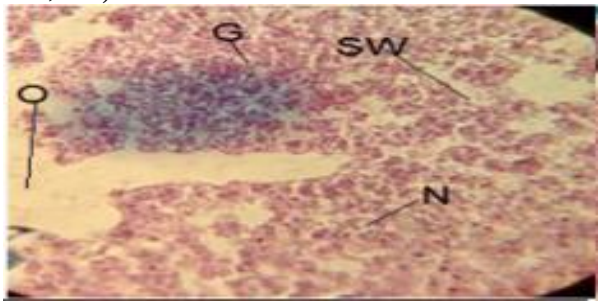

Figure 13. A Cross-section of liver tissue from from a dosed pregnant rat from dosed with spasmine :loss of the overall structure of the hepatic tissue.Necrosis into hepatic tissue (O), hepatocyte necrosis (N), hepatocyte degeneration (G), and sinusoids expanding (SW) (H & E -stain, 40x).

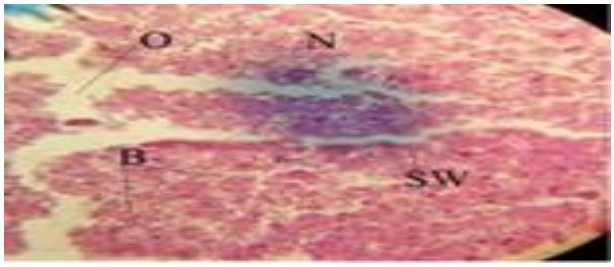

Figure 14. A Cross-section of liver tissue from from a dosed pregnant rat from dosed with spasmine: A breakdown in the fundamental architecture of the liver's tissue: Hepatocyte necrosis (N), sinusoids broadening (SW), necrosis into hepatic tissue (O), and bleeding into hepatic tissue (B) (H & E -stain, 40x).

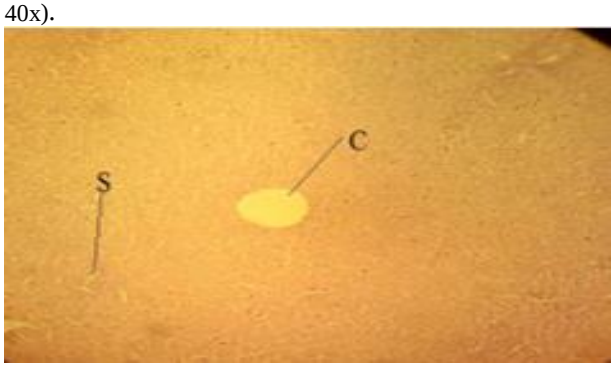

Figure 15 . A Cross-section of liver tissue of a rat fetus from a control group: Normal structure of hepatic tissue, showing sinusoids (S), central vein (C) (H & E -stain, 10x).

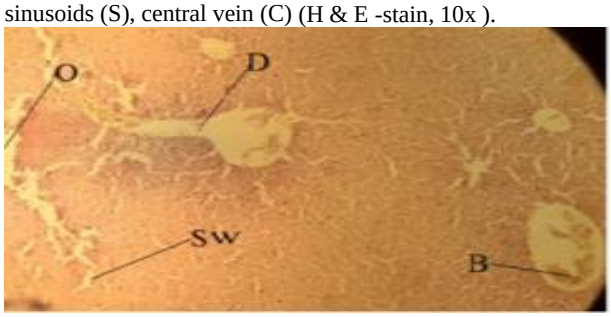

Figure 16. A Cross-section of liver tissue from from a dosed pregnant rat from dosed with spasmine :Destruction of the wall of the central vein (D), sinusoids widding (Sw), necrosis in hepatic tissue (O), and congestion in the central vein (B) (H & E -stain, 10x).

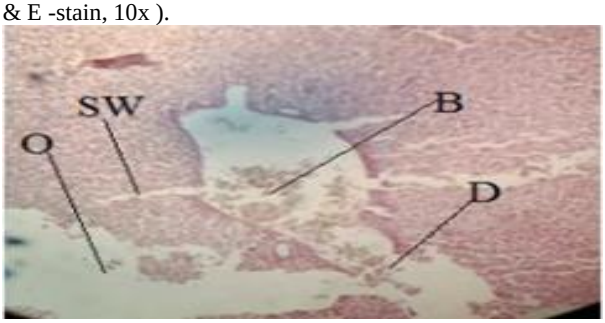

Figure 17. A Cross-section of liver tissue from from a dosed pregnant rat from dosed with spasmine: Inflammatory cell infiltration (F), necrosis in hepatic tissue (O), expansion of the central vein (E) (H & E -stain, 10x).

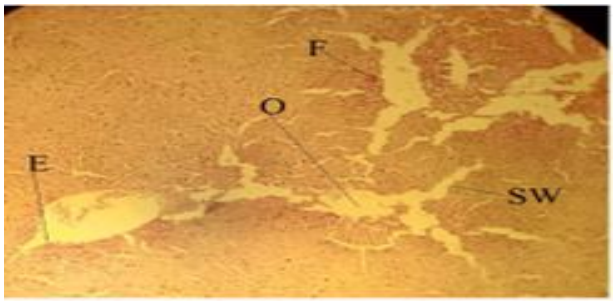

Figure 18. A Cross-section of liver tissue from from a dosed pregnant rat from dosed with spasmine :Congestion in the central vein (B) as a result of necrosis in the hepatic tissue (O) and destruction of the central vein wall (D) (H & E- stain, 10x).

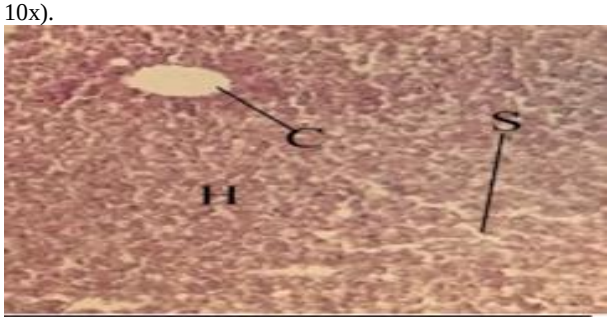

Figure 19. A Cross-section of liver tissue of a rat fetus from a control group: (H), central vein (C), sinuses (S), and hepatic cells (H) are all visible in this cross slice of pregnant rat liver from control group (H & E -stain, 40X).

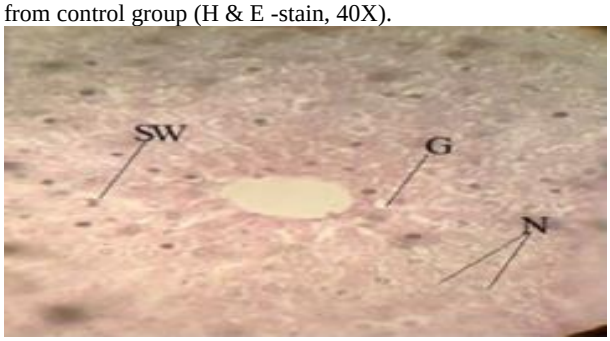

Figure 20. A Cross-section of liver tissue from from a dosed pregnant rat from dosed with spasmine: Hepatocyte necrosis (N), hepatocyte degeneration (G), and sinusoids broadening (SW) (H & E -stain, 40X).

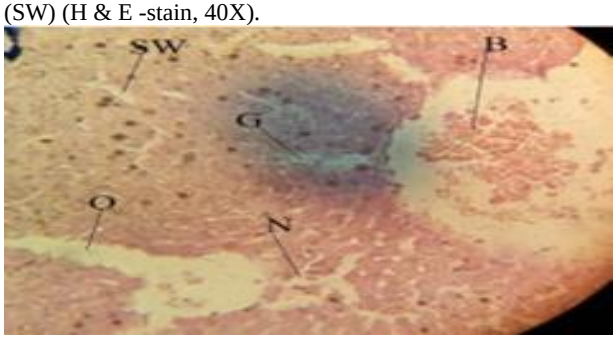

Figure 21. A Cross-section of liver tissue from from a dosed pregnant rat from dosed with spasmine :hepatocyte necrosis (N), destruction of central vein (D), sinusoids expanding (SW), and congestion into the central vein (B) (H & E -stain, 40X).

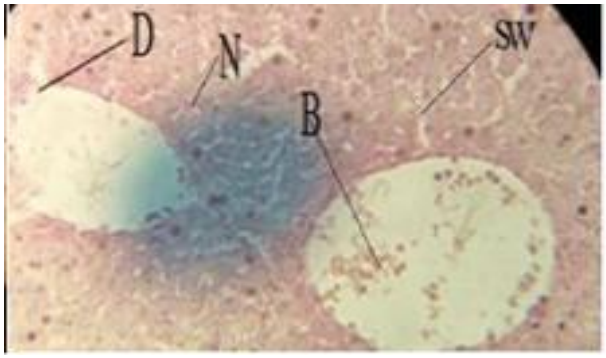

Figure 22. A Cross-section of liver tissue from from a dosed pregnant rat from dosed with spasmine:Necrosis into hepatic tissue (O), congestion in the central vein (B), Hepatocyte necrosis (N), sinusoids widening (SW), hepatocyte necrosis (N), and sinusoids widening (SW) (H & E -stain, 40X).

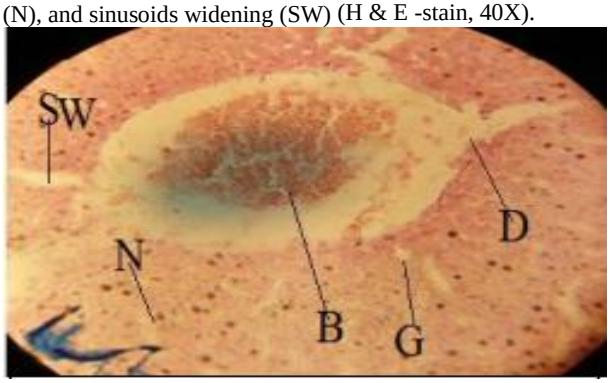

Figure 23. A Cross-section of liver tissue from from a dosed pregnant rat from dosed with spasmine: destruction of the wall of the central vein (D),Necrosis of hepatocytes (N), necrosis of hepatic tissue (O), and congestion in the central vein (B) (H & E -stain, 40X).

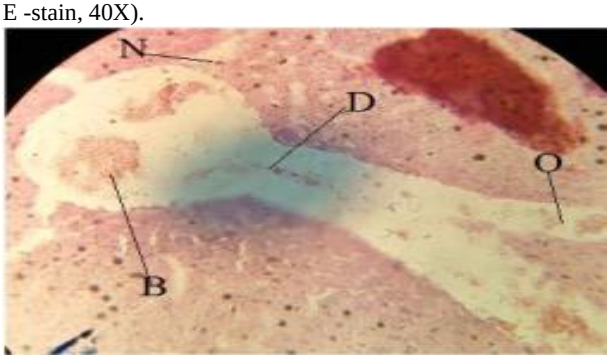

Figure 24.A Cross-section of liver tissue from from a dosed pregnant rat from dosed with spasmine:Abnormalities hepatocyte necrosis (N), hepatocyte degeneration (G), sinusoids broadening (SW), and congestion into the central vein (B) (H & E -stain, 40X).

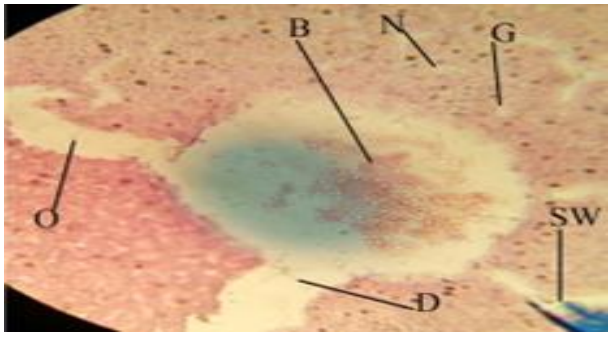

Figure 25. A Cross-section of liver tissue from from a dosed pregnant rat from dosed with spasmine :Expansion and destruction of the central vein wall (D), hepatocyte necrosis (N), hepatocyte degeneration (G), necrosis into hepatic tissue (O), sinusoids expanding (SW), and congestion into hepatic vessles (B) ,Expansion and destruction of the central vein wall (D)(H & E -stain, 40X).

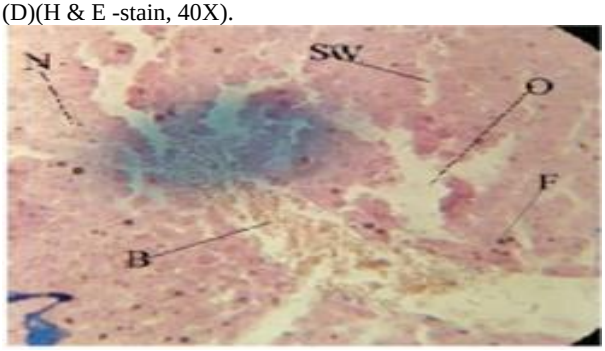

Figure 26. A Cross-section of liver tissue from from a dosed pregnant rat from dosed with spasmine :Hepatocyte necrosis (N), necrosis into hepatic tissue (O), sinusoids expanding (SW), congestion into hepatic vessle (B) (B), and inflammatory cell infiltration (F))(H & E -stain, 40X).

4. REFERENCES

1. Umpierrez,E.; Chung,H.; Chung,H. ; Iversen,L.; Lim,W. and Lee,JOURNAL OF Terminology and Information on Drugs. UNODC.ISBN,(2016), 921-978.
2. Abdulhady,S.S. and Ibrahim, K. M HPreparation and evaluation of mebeverine hydrochloride asmucoadhesivebuccal tablet for local anesthesia. TROPICAL JOURNAL. PHARMACOLOGY RESEARCH. 16 (8) ,(2017), 1805-1812.
3. Ford, J. A. Non-medical Prescription drug Use and Delinquency: An analysis with a national sample. DRUGS.38(2) ,(2008),493-516.
4. Stankovic , I. N.and Colak,D. Prenatal Drugs and Their Effects on the Developing Brain: Insights From Three-Dimensional Human Organoids.FRONTIERS. NEUROSEIENCE. (2022), https://doi.org/10.3389/ fnins. 2022.848648.
5. Champer ,C.H . and Scialli ,A.R. Teratogenesis and Environmental Exposur ,in : Creasy and ResniksMatemal-Fetal medicine by Resnik, R,; Greene, M. F ,;Lams ,J.D,; Lockwood , Ch .J.; Moore Th. R., seven edition . Elsevier Saunders ,Philadelphia. (2014) ,
6. Annahazi, A.; Roka, R.;Rosztoczy, A. and Wittmann, T.Role of antispasmodics in the treatment of irritable bowel syndrome. WORLD JOURNAL

GASTROENTEROLOGY. 20 (20), (2014),6031–6043.
7. Daniluk ,J.; Malecka-Wojciesko ,E.; Skrzydlo-Radomanska ,B. and Rydzewska ,G.The Efficacy of Mebeverine in the Treatment of Irritable Bowel Syndrome—A Systematic Review. JOURNAL CLINICAL MEDICINE. 11, (2022), 1044.
8. Ensslin, H.K. ; Maurer, H.H. .; Gouzoulis, E. ; Hermle, L. and Kovar. K.A. Metabolism of racemic 3,4-methylenedioxyethylamphetamine in humans, isolation, identification, quantification, and synthesis of renal metabolites. Drug Metabolism and Disposition.24, (1996) ,813-820.
9. Abdel-Hamid ,S.M.; Abdel-Hady, S.E.; El-Shamy, A.H. and El-Dessouky ,H.F.A novel formulation for mebeverine hydrochloride. Drug Development and Industrial Pharmacy . 33, (2007), 1078-1089.
10. Hatami, K.; Kazemi-Motlagh, A.H.; Ajdarkosh, H.; Zargaran, A.; Karimi, M.; Shamshiri, A.R.; Ghadir, M.R. Comparing the Efficacy of Cumin Sofouf With Mebeverine on Irritable Bowel Syndrome Severity and Quality of Life: A Double-blind Randomized Clinical Trial. Crescent .JOURNAL MEDICINE BIOLOGY SEIENCE. 7, (2020),186–194.
11. Gilbody, J.S.; Fletcher, C.P.; Hughes, I.W.; Kidman, S.P. Comparison of two different formulations of mebeverine hydrochloride in irritable bowel syndrome. INRTNATIONAL JOURNAL CLINICAL PRACTIE. 54, (2000),461–464.
12. Rahman, M. Z,; ahmed , D. S.; Mujib , B. S.; Mahmuduzzaman, M. and Rahman, M A. Comparative safety and efficacy of trimebutine versus mebeverine in the treatment of irritable bowel syndrome. MYMENSINGH MEDICAL JOURNAL. 23(1),(2014), 105-113.
13. Elliott ,S. and Burgess ,V.Investigative implications of the instability and metabolism of mebeverine. JOURNAL OF ANATOMICAL TOXICOLOGY. 30,(2006) ,91-97.
14. Hafez,E.S. Reproductive and breeding technique for laboratory animals.Lead Febiger,Philadelphia,U.S.A , (1970),305-313.
15. Suvarna,S.K.;Lyaton,C. and Bancroft,J.D.Bancrofts theory and practice of histological technique.7ed .Elsevier.Limited . , China.Xiv, (2013), 604.
16. Morgan,G.A.;LeechN.A.;Gloecner,G.W.and Barrett, K.C.SPSS for introductory statistic:use a introduction .2nd ed.Lawrenz Erlbaum association publishers Mahwash,New Jersey. London.(2010),
17. Plmieri, C.and Conger, R.Teratogenic Potential of the newer antiepilepticdrugs. CNS DRUGS. 16(11), (2002), 755-764 .
18. Ozsurekci,Y. and Aykac,K.Oxidative stress related diseases in newborns. JOURNAL OF OXIDATIVE .MEDCINE CELL LONGEVITY, (2016),9.
19. Amiri,M.Oxidative stress and free radicals in liver and kidney diseases ;an updated short-review. JOURNAL OF NEPHROPATHALOGY. 3(7/3),(2018),127-131.
20. Freeman, B.A. and Crapo, J. D.Free Radicals and Tissue Injury. Laboratory .Investigation. 47(5), (1982), 412-426.
21. Haroun, H.S. Terdtogenicity and teratogenic factors. Mo. JOURNAL ANATOMY AND PHSYSIOLOGY.3(1), (2017),1-8 .
22. Al-Naemi, R.S.; Ab. Dullah, Q.H. and Ibrahim, S.A. Impactof oxidative stress on pregnancy outcome in albino rats. IRAQI JOURNAL OF VERTERNARY SEIENNCE .26(2), (2012), 93-99.
23. Elshama, S.; Abdalla,M.E. and Mohamed, A.M.Role of natural antioxidant treatment of toxicity. JOURNAL OF TOXICOLOGICAL ANALYSIS. 1(1), (2018),3.

Arabic Abstract

أجريت الدراسة لتحديد دور عقار السبازمين في بعض المعايير الوزنية و النسجية لأكباد إناث الجرذان الحوامل وأجنتها في اليوم التاسع عشر من الحمل. أجريت الدراسة في كلية التربية للبنات في جامعة الكوفة للمدة من 1 كانون الثاني 2022 ولغاية 15 حزيران 2022. وبعد الحصول على 8 من الجرذان الحوامل تم تجريع 4 منهم بجرعة من المحلول الفسيولوجي وقد مثلت هذه المجموعة السيطرة (G1) بينما 4 من إناث الجرذان الحوامل جرعت عقار السبازمين بجرعة (0.48 ملغم/كغم/وزن الجسم) (G2) لمدة 19 يوماً، وكانت الجرذان الحوامل في المجموعة السيطرة بعمر (12) أسبوع ووزن (231) غرام بينما كانت الحيوانات الحوامل في المجموعة المعاملة بعقار السبازمين بعمر (11) اسبوع ووزن (230) جرام.

سجلت نتائج الدراسة انخفاضاً معنوياً ($P < 0.05$) في أوزان الكبد لكل من الحيوانات الحامل وأجنتها في مجاميع الجرذان المعالجة بعقار السبازمين ، كما أظهرت النتائج أن معاملة الجرذان بعقار السبازمين حتى اليوم التاسع عشر من الحمل أدى إلى تغيرات مرضية وغير طبيعية في أنسجة الكبد مثل تلف جدار الوريد المركزي، نخر خلايا الكبد، توسع الجيبانيات، تنخر الأنسجة الكبدية وارتشاح الخلايا الالتهابية في الجرذان الحوامل وأجنتها مقارنة بالجرذان الحوامل واجنتها في مجموعات السيطرة أثناء الحمل في اليوم التاسع عشر.

الاستنتاج: إن العلاج بعقار التشنج أدى إلى انخفاض وزن الحوامل وكبد الأجنة كما أحدث تغيرات نسجية مرضية مختلفة في بنية أكباد الجرذان الحوامل وأجنتها خلال اليوم التاسع عشر من الحمل.

0096477699201 65
https://journals.uokerbala.edu.iq
Iraq - Holy Karbala